The role of nitric oxide synthases in the pathophysiology of chronic obstructive pulmonary disease

Inaugural Dissertation
Submitted to the
Faculty of Medicine
in partial fulfilment of the requirements
for the PhD Degree
of the Faculty of Veterinary Medicine and Medicine
of the Justus Liebig University Giessen

by

Nirmal Parajuli
of
Bhojpur, Nepal

Giessen 2009

From the Medical Clinic II, Excellence Cluster of Cardio-Pulmonary System,
University of Giessen Lung Centre

Chairman: Werner Seeger, Prof., M.D.

of the Faculty of Medicine of the Justus Liebig University Giessen

First Supervisor and Committee Member: Prof. Dr. Norbert Weißmann
Second Supervisor and Committee Member: Prof. Dr. Paul T. Schumacker

Committee Members: Prof. Dr. Martin Diener
PD Dr. Christian Mühlfeld

Date of Doctoral Defence: 9th December, 2009

LIST OF FIGURES

LIST OF TABLES

LIST OF ABBREVIATION

·OH	Hydroxyl radical
ATS	American thoracic society
BTS	British thoracic society
COPD	Chronic obstructive pulmonary disease
eNOS	Endothelial nitric oxide synthase
ERS	European respiratory society
FEV_1	Forced expiratory volume per second
FVC	Forced vital capacity
GOLD	Global initiative for chronic obstructive lung disease
H_2O_2	Hydrogen peroxide
HAT	Histone acetylases
HE	Haematoxylin and eosin
IB	Inhaled bronchodilator
ICS	Inhaled corticosteroides
iNOS	Inducible nitric oxide syntheses
L-NIL	N6-(1-Iminoethyl)-L-lysine.dihydrochloride
$NADP^+$	Nicotinamide adenine dinucleotide phosphate
NO	Nitric oxide
PBS	Phosphate buffered saline
RNS	Reactive nitrogen species
ROS	Reactive oxygen species
SC	Systemic corticosteroids
T	Theophylin
WHO	World health organization

1. INTRODUCTION

1.1 Definitions

Chronic obstructive pulmonary disease (COPD) is a slowly progressive disease condition characterized by poorly reversible airflow limitation that is associated with an abnormal inflammatory response in the lung. The inflammation is chronic and occurs both in the large and small airways, resulting in a heterogeneous disease phenotype with morphological changes in three regions of the lungs: central airways (chronic bronchitis), peripheral airways (small airway disease), and the lung parenchyma (emphysema)[1]. Spirometric definition of the disease emphasizes the degree of air flow obstruction with a forced expiratory volume per second (FEV_1) of <70% and ratio of FEV_1/ forced vital capacity (FVC) of < 0.7 [1].

The etymology of COPD started with the Greek word emphysema, meaning “to blow into”, “air-containing” or “inflated”. COPD was described as “voluminous lungs” by Bonet in 1679 and as “turgid lungs particularly from air” described by Morgagni in 1769 [2, 3]. Later, the first description of emphysema with enlarged lung airspaces in the human was furnished by Ruysh in 1721, followed by Matthew Baillie in 1807, who not only clearly recognized and illustrated emphysema, but also pointed out its essentially destructive character. In the early 1800s, Laennec made contributions to the basic description of the pathologic changes in COPD by distinguishing interstitial emphysema. It was further described with enlarged airspaces to the clinical syndrome of emphysema and its association with chronic bronchitis and bronchiectasis[2, 3]. The foundation of the pathologic anatomy of pulmonary emphysema was laid by J. Gough in 1952, who described centrilobular emphysema and panlobular emphysema[4]. A comprehensive microscopic description of emphysema was provided by Mc Lean, who demonstrated the relationship between the tissue destruction and inflammatory alterations to the bronchioles and the vasculature. Later a Ciba Guest Symposium in 1959 defined emphysema in anatomical terms as “a condition of the lung characterized by increase beyond the normal of airspaces, distal to the terminal bronchiole, either from dilatation or from destruction of their walls”[5].

Subsequent definitions of COPD have been associated with physiological functions, rather than the original definition which was confined only to tissue destruction. However, these definitions were also restricted to the alveolar compartment and its associated structures of the respiratory system. Chronologically the definition of COPD arose as follows:

In 1995, the ERS guideline[6] definened COPD as "… a disorder characterized by reduced maximum expiratory flow, and slow forced emptying of the lungs, features which do not change markedly over several months. Most of the airflow limitation is slowly progressive and irreversible. The airflow limitation is due to varying combinations of airway diseases and emphysema; the relative contribution of two processes is difficult to define in vivo. Emphysema is defined anatomically; chronic bronchitis is defined clinically..." After this, in 1995, ATS guidelines[7] defined COPD as "…..a disease characterized by the presence of airflow obstruction due to chronic bronchitis or emphysema; the airflow obstruction is generally progressive, may be accompanied by airway hyperreactivity, and may be partially reversible". Further "COPD may include a significant reversible component and some patients with asthma may go on to develop irreversible airflow obstruction indistinguishable from COPD." The BTS guidelines[8] defined COPD in 1997 as "….a general term which covers many previously used clinical labels that are now recognized as being different aspects of the same problem. Diagnostic labels encompassed by COPD include chronic bronchitis, emphysema, chronic obstructive airway diseases, chronic airflow limitation and some case of chronic asthma. COPD is a chronic, slowly progressive disorder characterised by airways obstruction (FEV_1 <80% predicted and FEV_1/ FVC ratio <70%) which does not change markedly over several months. The impairment of lung function is largely fixed but is partially reversible by bronchodilator (or other) therapy. Most cases are caused by tobacco smoking. COPD causes significantly more mortality and morbidity than do other causes of airflow limitation in adults". The Gold guidelines[9] defined COPD in 2003 as "…. a disease state characterized by airflow limitation that is not fully reversible. The airflow limitation is usually both progressive and associated with an abnormal inflammatory response of the lungs to noxious particles or gases".

However, none of the above definitions addressed the issue of vascular and systemic involvement in COPD. Further, the ATS/ ERS standards[10] in 2004 acknowledged the systemic importance of COPD by defining "…a preventable and treatable diseases state characterized by airflow limitation that is not fully reversible. The airflow limitation is usually progressive and is associated with an abnormal inflammatory response of the lungs to noxious particles or gases, primarily caused by cigarette smoking. Although COPD affects the lungs, it also produces significant systemic consequences".

The definition of COPD remains incomplete because of its broad association with vascular disease and many morbid/ co-morbid conditions. A short comparision of the spirometric definition of COPD is given in **Table 1**.

Table 1 Comparision of spirometric definition of COPD including classification of disease severity based on FEV_1

	ATS	ERS	BTS	GOLD[1]	ATS/ERS[1]
Definition	FEV_1/VC <0.75	FEV_1/VC<88 pp[2] FEV_1/VC<89 pp3	FEV_1/VC<0.70 FEV1<80 pp	FEV_1/VC<0.70	FEV1/VC≤0.70
Severity at risk	–	–	–	normal spirometry[5]	FEV_1/VC<0.70 FEV_1≥80 pp[6]
Mild	>50 pp	≥70 pp	60-90 pp	≥80pp	≥80 pp
Moderate	35-49 pp	50-69 pp	40-59 pp	50≤and<80 pp	50-80 pp
Severe	<35 pp	<50 pp	<40 pp	30≤and<50 pp	30-50 pp
Very severe	-	-	-	<30 pp	<30 pp

[1]refer to value after bronchodilatation
[2]in men and [3]women
[4] based on percent predicted (pp) of FEV_1 according to all guidelines
[5] and reported respiratory symptoms
[6] patient who smoke and have exposed to pollulant, cough, or dyspnea

1.2 Epidemiology

The World Health Organization (WHO) estimated that COPD is predicted to be the third leading cause of death worldwide by 2020. Accordingly, the age adjusted death rate of COPD is increasing tremendously after causing considerable disability with COPD patients

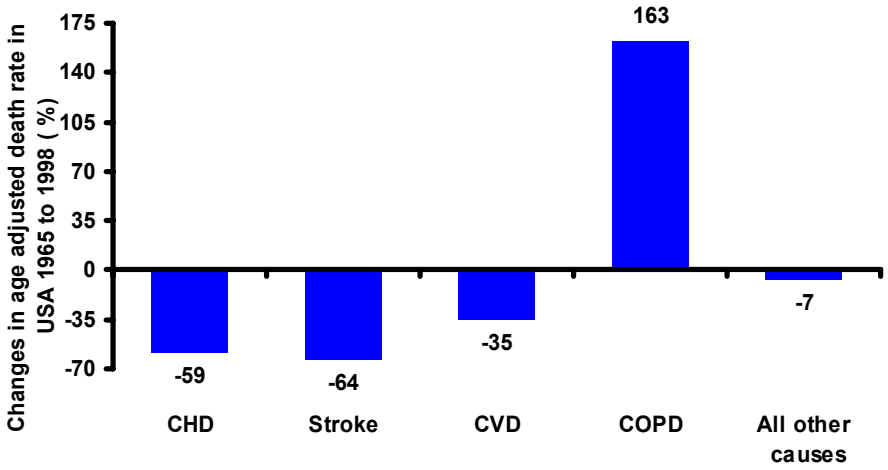

COPD = Chronic obstructive pulmonary diseases
CHD = Coronary heart diseases
CVD = Cerebrovascular diseases **Adapted from: www.copdgold.com**

Figure 1. Changes in age-adjusted death rate in the USA, from 1965 to 1998 (%)

whereas mortality from cardiovascular disease, cancer and other diseases has declined over the past 30 years by new innovative treatments [11] (**Fig. 1**).

1.3 Risk factors

COPD arises from an interaction between environmental exposure and host factors, which probably play a major role and account for much of the heterogeneity in susceptibility to smoke and other risk factors. The human lung from infancy through to old age can be subjected to deleterious oxidative events as a consequence of inhaling environmental pollutants or irritants since the lungs are continuously exposed to relatively high oxygen tensions[12].

Table 2 Different environmental and host risk factors for COPD

Environmental factors	Host factors
Smoking: active, passive and maternal smoking	Polyunsaturated fatty acid metabolism, infection
Air pollution	α1-antitrypsin deficiency
Occupation	Genetics, Family history
Socioeconomic status/ poverty	Age
Nutrition	Airway hyperresponsivenes,
oxidants	Low birthweight

Symptoms of COPD include breathlessness on exertion, cough, irregular sputum production, infective exacerbations, fatigue and its complications include cor pulmonale, anemia, pneumothorax and respiratory failure[6, 11, 13]. Genes regulating proteases/antiproteases, antioxidant factors, mucociliary clearance and inflammatory mediators are amongst important factors of the disease [14-16].

1.4 Pathology

1.4.1 Chronic bronchitis

The presence of chronic cough and sputum production for at least three months of two consecutive years is termed chronic bronchitis. The chronically inflamed bronchial epithelium with hypertrophy of the mucus glands and increased goblet cells are indicative of chronic bronchitis. Further, the cilia are destroyed and the efficiency of the mucociliary escalator is impaired. Mucus viscosity and mucus production are increased. Pooling of the mucus leads to increased susceptibility to infection. Repeated infections and inflammation cause irreversible damage of the airways structure due to narrowing and distortion of the peripheral airways[17, 18].

1.4.2 Emphysema

Emphysema is characterised by abnormal dilatation of the terminal air spaces distal to the terminal bronchioles, with destruction of their wall and loss of lung elasticity. The distribution of the abnormal air spaces in panacinar emphysema results in distension and destruction of the whole acinus, particularly in the lower half of the lungs whereas the centriacinar emphysema involves damage around the respiratory bronchioles affecting the upper lobes and upper parts of the lower lobes of the lung[19]. Destruction of the lung parenchyma results in floppy lungs and loss of the alveoli, which can result in a collapse of the small airways and air trapping with hyperinflation of the lungs. Hyperinflation flattens the diaphragm results in less effective contraction, reduced alveolar efficiency and further air trapping. Over time this leads to severe airflow obstruction, resulting in insufficient expiration to allow the lungs to deflate fully prior to the next inspiration[20].

1.4.3 Systemic effects

A low body mass index and loss of lean muscle mass are common in COPD patients with severe emphysema and chronic bronchitis, as in “pink puffers”. Weight loss is a poor prognostic sign and a low body mass index increases the risk of death from COPD having emphysema. However, patients with severe chronic bronchitis with less emphysema are overweight as like seen in the so-called “blue bloater” [21].

1.4.4 Pulmonary vascular changes

An increase in arterial muscle media thickness as well as intimal fibrosis in the muscular arteries, and a progressive muscularization of the small arterioles has been found in COPD. A progressive increase in the numbers of smaller muscularized arteries, percentage of the medial thickness, and percentage of intimal thickness of muscularized arteries has been shown to be associated with COPD patient[20, 22].

1.5 Functional changes

Many pulmonary function abnormalities are occuring in COPD, but a persistent reduction in maximal forced expiratory flow is the defining physiological feature. Increased airway resistance, increased residual volume, increased compliance, increased residual volume/total lung capacity ratio, decreased inspiratory capacity, maldistribution of ventilation, and ventilation-perfusion mismatching are the typical functional changes observed[23, 24].

1.6 Cigarette smoke

Cigarette smoke is a complex mixture containing up to 4,700 chemicals with 1,017 molecules per puff as well as high concentrations of free radicals and other oxidants. Nitric oxide is one of the major oxidants present in cigarette smoke, at concentrations of 500–1,000 ppm[25]. The tar phase of cigarette smoke contains stable radicals, including the semiquinone radical, which can react with oxygen to produce O_2·-, ·OH and H_2O_2 [26]. Inhaling cigarette smoke produces an abnormal or enhanced inflammatory response that leads to pathological changes in the lungs of all smokers including the severe COPD patients.

The respiratory epithelium is a major target for oxidative injury from oxidants generated either exogenously from cigarette smoke/air pollutants or endogenously from phagocytes/other cell types. Thus, the lung's efficient enzymatic and non-enzymatic antioxidant systems are very important in the protection of the airways against exogenous and endogenous oxidants. If an imbalance of oxidants and antioxidants e.g., the excess of oxidants and/or a depletion of antioxidants, oxidative stress occurs[27, 28]. Oxidative stress from reactive oxygen species and reactive nitrogen species (ROS and RNS, respectively) has been thought to play a major role in the pathogenetic mechanisms of COPD[28].

Oxygen is a key molecule involved in the process of energy fixation. The total oxygen consumption in the respiratory chain undergoes tetravalent reduction to produce water by a cytochrome oxidase (cytochrome-C: oxygen oxidoreductase) (O_2+4e−+4H→2H_2O) of the IV complex in the mitochondrial electron transport chain. Tetravalent reduction of oxygen can result in the production of ROS with at least one unpaired electron and nonradical oxidants. The addition of one electron to oxygen produces superoxide (O_2·-), a second electron produces hydrogen peroxide (H_2O_2) and a third electron forms the very reactive hydroxyl radical (·-OH) and the addition of a fourth electron generates water[29]. These ROS can react with other molecules such as proteins, lipids and DNA. Other oxidants include the alkoxyl (RO·), peroxyl (RO_2·) and hydroperoxyl free radicals, singlet oxygen and hypochlorous acid (HOCl). The ·OH is the most reactive of all the radicals and reacts immediately with organic molecules at its site of production[30].

Nitric oxide (NO·) is produced endogenously, from its amino acid substrate L-arginine, by nitric oxide synthases[28]. The inducible form of NOS is calcium-independent, and generates NO· in large amounts over long periods of time[31].

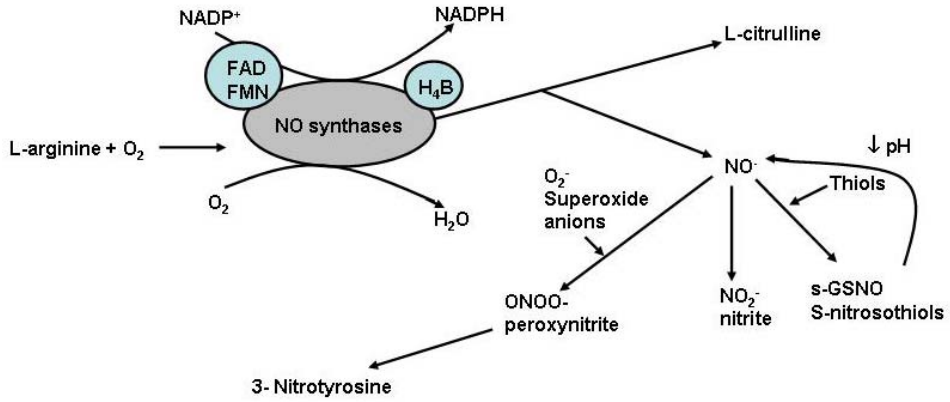

Figure 2. Synthesis of nitric oxide (NO·-) and NO·- related products.

$NADP^+$ Nicotinamide adenine dinucleotide phosphate, NADPH: reduced $NADP^+$, FAD: Falvin adenine dinucleotide, FMN: Flavin mononucleotide, s-GNO; s-nitrosglutathione

The NO_2- is a major end-product of NO and the reaction of NO· with O_2·- forms the potent oxidant peroxynitrite (ONOO-). The ONOO- can react with and cause nitration of various compounds. The amino acid tyrosine is particularly susceptible to nitration, forming 3-nitrotyrosine, which has been used as a marker for the generation of RNS *in vivo*. NO· contains an odd number of electrons, making it a radical, and is highly reactive in nature. The reaction of NO· with O_2·- results in the formation of ONOO- and secondarily can result in NO_2^- generation. NO_2- is also a substrate for myeloperoxidases (MPO) and the eosinophil peroxidase (EPO), which catalyzes peroxidase-mediated oxidation of biological targets[32]. NO· also reacts with compounds containing thiol groups, resulting in the formation of S-nitrosothiols (SNO). SNOs such as S-nitroso-l-glutathione may inhibit enzymes such as glutathione (GSH) peroxidase (GPx), GSH reductase (GR), glutathione-S-transferase (GST) and glutamate cysteine ligase (GCL). These enzymes rapidly respond to oxidative stress by converting SNOs into nitrate. NO· also reacts rapidly with free radicals to form RNS[25] (**Fig. 2**).

The oxidants from cigarette smoke can (i) damage lipids, nucleic acids and proteins, (ii) deplete antioxidants such as GSH; enhance the respiratory burst in phagocytic cells, (iii) inactivate protease inhibitors such as α_1-antitrypsin (α_1-AT); enhance molecular mechanisms involved in pro-inflammatory gene expression, (iv) decrease binding affinity and translocation of steroid receptors, (v) increase apoptosis, and (vi) impair skeletal muscle function[28].

1.7 Pathogenesis

1.7.1 Inflammation

Cigarette-smoke exposure induces an inflammatory response in the lung which involves different structural and inflammatory cells and a large array of inflammatory mediators. The interaction of these complex steps eventually leads to airway remodeling as well as obstruction and emphysema. Inflammatory cells[27, 33, 34], including neutrophils and alveolar macrophages from the lungs of smokers are more activated and release increased amounts of ROS, such as O_2·- and H_2O_2, which further increases the oxidative burden produced directly by inhaling cigarette smoke[35, 36]. The generation of oxidants in the lungs of smokers is enhanced by the presence of increased amounts of free iron in the airspaces[37]. Free iron in the ferrous form can generate the ·OH radical in a Fenton reaction.

Lung epithelial cells are other possible sources of ROS. Type II alveolar epithelial cells have been shown to release both H_2O_2 and O_2·- in similar quantities to alveolar macrophages. ROS released from type II epithelial cells are able, in the presence of MPO, to inactivate α1-antitrypsin *in vitro*[38]. ROS can also be generated intracellularly as a by-product of normal metabolism. Mitochondrial respiration is one of the possible sources of free radicals, resulting from electrons leaking from the electron transport chain on to oxygen to form O_2·- . Morever, xanthine dehydrogenase has also been shown to be increased in bronchoalveolar lavage fluid from COPD patients compared with normal subjects, and is associated with increased O_2·- and uric acid production[39, 40]. A substantial amount of O_2·- is also produced by membrane oxidases and the NADPH oxidase system. In addition, NO· is generated by the action of inducible form of NOS found in the respiratory epithelium, endothelial cells and activated macrophages[41, 42].

It is likely that genetic and epigenetic factors are also involved in determining the progression of the inflammatory cascade, as supported by studies in animal models with mouse strains. Mouse strains resistant to cigarette smoke-induced emphysema have a genetic response to smoke exposure that decreases the expression of multiple inflammatory genes and increases the expression of anti-inflammatory genes, which effectively prevents inflammation and likely emphysema. Genetically different susceptible strains react in an opposite manner increasing the expression of inflammatory genes both of the innate and adaptive immunity[43]. Both ROS

and RNS can perpetuate inflammation. To depict this important inflammatory immune response, their free radical footprints are listed in **Table 3.**

Table 3 Free radicals and their foot prints in chronic obstructive pulmonary disease

Marker	Change
Carbon monoxide[44]	Increase
8-isoprostanes[45, 46]	Increase
Ethane[45, 46]	Increase
Nitrotyrosine[47]	Increase
Alpha 1 proteinase inhibitor activity[48]	Decrease
Hydrogen Peroxide[49]	Increase
Nitric oxide[50]	Increase

The progressive airflow limitation in COPD is caused by the remodeling and narrowing of small airways as well as by the destruction of the lung parenchyma and the airways due to emphysema. There is a specific pattern of inflammation in the airways and lung parenchyma, with increased numbers of macrophages, T-lymphocytes, a predominance of CD8 (cytotoxic) T-cells, and, in more severe disease stages, B-lymphocytes; with increased numbers of neutrophils in the airway lumen[51]. The inflammatory response in COPD involves both innate and adaptive immune responses. Multiple inflammatory mediators are increased in COPD, and are derived from inflammatory and structural cells of the airways and lungs[52]. The molecular basis of this amplification of inflammation may be partly determined by genetically. For many years, it was assumed that the inflammatory reaction in the lungs of smokers consisted of neutrophils and macrophages and that neutrophil elastases and macrophage proteinases were responsible for the lung destruction in COPD. This concept has recently been changed to include more complicated inflammatory process. In this regard, the infiltration of T-cells into the lung has been demonstrated in COPD patients. Further analysis of the immune cell profiles in the alveoli and small airways of COPD patients has revealed an increase in all of the cell types, including macrophages, T-lymphocytes, B-lymphocytes and neutrophils[53, 54].

1.7.2 Protease–antiprotease imbalance

There is an increased protease burden in the lungs of patients suffering from COPD as a result of the influx and activation of inflammatory leukocytes which release proteases. The deficiency of antiproteases such as α_1-antitrypsin is the result of inactivation by oxidants which creates a protease-antiprotease imbalance in the lungs. Inactivation of α_1-antitrypsin (α_1-AT) by oxidants occurs at a critical methionine residue in its active site. This can be caused by oxidants from cigarette smoke or oxidants released from inflammatory leukocytes,

resulting in a marked reduction in the inhibitory capacity of α_1-AT *in vitro*[55, 56]. In addition, secretion of proteases by lung epithelial cells leads by itself to an increase in the release of ROS,[57] creating a protease-antiprotease imbalance in lung.

1.7.3 Oxidative stress

The oxidant burden in the lungs is enhanced in smokers by the increased numbers of neutrophils and macrophages in the alveolar space[58]. Oxidative stress may reach the circulation during cigarette smoking, which could decrease the deformability of neutrophils, increasing their sequestration in the pulmonary microcirculation[59, 60]. Thus, cigarette smoking increases neutrophil sequestration in the pulmonary microcirculation, at least in part, by decreasing neutrophil deformability. Once neutrophils are sequestered, components of cigarette smoke can alter neutrophil adhesion to the endothelium by upregulating CD18 integrins[61, 62] and ultimately by upregulating the NADPH oxidase H_2O_2 – generating system[63,61]. These sequestered neutrophils may subsequently respond to chemotactic components in cigarette smoke and become more adhesive to pulmonary vascular endothelial cells.

Studies using animal models of smoke exposure[64] have demonstrated increased neutrophil sequestration in the pulmonary microcirculation *in situ*, associated with an upregulation of adhesion molecules on the surface of these cells[63]. Activation of neutrophils sequestered in the pulmonary microvasculature[65] could also induce the release of reactive oxygen intermediates and proteases within a microenvironment, with limited access for free radical scavengers and antiproteases. Thus, destruction of the alveolar wall as it occurs in emphysema might be the result of a proteolytic insult derived from the intravascular space.

The influx of inflammatory cells into the lungs may perpetuate inflammatory mechanisms through the regulation of cytokine secretion. Patients with COPD inhibit increased levels of interleukin (IL)-6, IL-1β, tumour necrosis factor (TNF)-α and IL-8 in airway secretions[66,67,68]. Oxidative stress may also be a mechanism for enhancing airspace inflammation and is a characteristic feature of COPD[11]. Oxidative stress can result in the release of chemotactic factors such as IL-8 from airway epithelial cells[69], and epithelial cells from COPD patients release more IL-8 than do those of smokers or healthy individuals[68]. Lipid peroxidation products such as 8-isoprostane can also act as signalling molecules and cause the release of inflammatory mediators such as IL-8 from lung cells[70]. The lipid peroxidation product

4-hydroxy-2-nonenal can cause the upregulation of TGF-β[71] and can up regulate antioxidant enzyme gene expression[72]. Oxidative stress has a fundamental role in enhancing inflammation through the upregulation of redox-sensitive transcription factors, such as nuclear factor (NF)-kB and activating protein (AP)-1 and also by activation of the extracellular signal related kinase, Jun N-terminal kinase and the p38 mitogen-activated protein kinase pathways[73, 74].

Oxidative stress activates histone acetyltransferase (HAT) activity in epithelial cells[75]. Histone acetylation occurs following cigarette-smoke exposure of epithelial cells and is prevented by antioxidant therapy with N-acetylcysteine (NAC)[76]. Furthermore, in animal models of cigarette-smoke exposure, increased levels of acetylated histone and decreased histone deacetylase (HDAC) activity have been reported in lung cells. Both of these events can enhance gene expression[77]. HDAC activity in alveolar macrophages obtained from cigarette smokers is downregulated, which can enhance gene expression[76]. This event may be due to nitration of HDAC2 by ONOO- [78]. Recent studies have suggested that acetylated histone residues, specifically histone H4, are present to a greater extent in lung tissue in smokers and in smoking COPD patients. This is associated with a decrease in $HDAC_2$, specifically in smoking COPD patients and in patients with severe COPD[79]. Thus, oxidative along with nitrosative stress has fundamental effects on the molecular mechanisms regulating inflammation in COPD.

1.7.4 Apoptosis

The loss of alveolar endothelial cells and epithelial cells by apoptosis may be an initial event in the development of emphysema[80]. Apoptosis occurs to a greater extent in endothelial cells in emphysematous lungs than in nonsmoker lungs[81]. Airway lymphocytes and stimulated peripheral blood leukocytes from patients with COPD also exhibit apoptosis. The process of endothelial apoptosis is thought to be regulated by vascular endothelial growth factor receptor-2 (VEGF-R2). Downregulation of VEGF-R2 has been shown to produce emphysema in animal models and reduced expression of VEGF-R2 is evident in emphysematous human lungs[82]. Studies have also reported that the "apoptosis/emphysema" induced by VEGF inhibition in animal models is associated with increased markers of oxidative stress and is prevented by antioxidants, suggesting oxidative stress is involved in this process.

1.7.5 Systemic oxidative stress

After smoking, nitrite, nitrate and cysteine levels in peripheral blood decrease. In some studies, no difference has been observed in the production of reactive oxygen intermediates from peripheral blood neutrophils following smoke exposure. The antioxidant capacity of the blood also fell immediately after smoke exposure and the concentration of plasma lipid products increased. It is now recognized that COPD is not only a disease which affects the lungs, but has important systemic consequences, such as cachexia and effects on skeletal muscle function. This increasing evidence suggests that similar mechanisms involving oxidative stress and inflammation in the lung may also be responsible for many of the systemic effects of COPD[83].

Peripheral blood neutrophils from COPD patients have been shown to release more ROS. Products of lipid peroxidation are also increased in the plasma in smokers and patients with COPD. Increased levels of nitrotyrosine have been reported in the plasma of COPD patients as a marker of systemic oxidative stress. Patients with COPD often display weight loss, which correlates inversely with the occurrence of exacerbations. Inducible NOS expression is increased in the skeletal muscle in response to inflammatory cytokines, and is dependent on NF-kB activation[84]. Furthermore, oxidative stress may result in the apoptosis of muscle cells, which has also been described in skeletal muscle cells in patients with COPD who have lost weight and may contribute to oxidative stress-dependant muscle atrophy[85, 86]. Both local and systemic oxidative stresses are involved in many of the pathogenic processes in COPD patient as well as in the systemic phenomena such as skeletal muscle dysfunction.

1.7.6 Nitrosative stress

Nitric oxide (NO) and related compounds are produced by a wide variety of residential and inflammatory cells like eosinophils, neutrophils, monocytes, macrophages in the respiratory system. The NO is generated via a five electron oxidation of the terminal guanidium nitrogen on the amino acid L-arginine and this reaction is catalyzed by NOS, which exist in three different forms like constitutive NOS (cNOS): NOS3 or endothelial NOS (eNOS), NOS1 or neuronal NOS (nNOS). These cNOS is expressed in neuronal, epithelial and endothelial cells whereas NOS2 or inducible NOS (iNOS) is mainly expressed in macrophages, epithelial, endothelial and vascular smooth muscle cells. The iNOS isoform is upregulated by proinflammatory cytokines like TNF-α, INF-Υ and IL-β and releases NO in large amounts for longer periods of time[87]. The ROS, NO and RNS are essential for many physiological

reactions and for host defense. However, if exposure to airway pollutants, infections, inflammatory reactions, or decreased levels of antioxidants, as well as enhanced levels of ROS and RNS may ultimately cause deleterious effects in the airways[87,88,89, 90].

Recently, exhaled NO has been partitioned into central and peripheral portions of lung, with reduced NO in the bronchial fraction, but increased NO in the peripheral fraction, which includes the lung parenchyma and small airways[32, 38]. The increased peripheral NO in COPD patients may reflect increased expression of inducible NO synthase in epithelial cells and macrophages of patients with COPD[91, 92]. This unstable peroxynitrite is degraded to nitrate that is increased in exhaled breath condensate of COPD patients[93]. Peroxynitrite can modify tyrosine residues, thiols and heme groups[87] in the lung, and macrophages of COPD patients[92,78]. Morever, peroxynitrite increases airway hyper-responsiveness, respiratory epithelial damage and eosinophil activation[94] along with inactivation of surfactants, inhibition of protein phosphorylation that associated with different signal transduction pathway[87]. Peroxynitrite also able to activate matrix metalloproteinase (MMP)[95] to inactivate α_1-antiproteinase[96] and to enhance the production of the potent neutrophil chemoattractant interleukin-8 (IL-8)[97]. All of these factors perpetuate inflammatory processes in the lung through nitrosative stress. Further, peroxynitrite can alter its protein which may result in cell death by mitochondrial damage, DNA strand breakage and structural/functional modification of proteins. Such modified proteins are recognized as antigens by the adaptive immune system which can thus elicit an autoimmune T-cell response.

1.7.7 Hypoxia

Progressive airflow limitation and destruction of the alveolar capillary network may lead to decreased oxygen transport and alveolar hypoxia in COPD. Vascular endothelial growth factor (VEGF) receptor blockade signaling caused emphysema in rodents with decrease VEGF and VEGF receptor expression in emphysematous lungs[98, 99]. Recent evidence has demonstrated that cigarette smoke impairs hypoxia inducible factor-1α (HIF-1α) expression in ischemic limbs of mice, causing decreased revascularization. Moreover, protein translator regulator (RTP-801) or “regulated in development and DNA damage-1” (Redd-1), a negative regulator of mammalian target of rapamycin (mTOR) signaling and hypoxia-responsive gene products are induced by cigarette smoke. Knockdown of the RTP801 gene in mice resulted in significant resistant to cigarette smoke-induced inflammation and emphysema[98, 99]. About 60% of patients with COPD suffer from mild pulmonary hypertension and the pulmonary

hypertension in COPD can not fully be explained by hypoxia alone, as it occurs in nonhypoxic patients as well[100]. A direct toxic effect of cigarette smoke on the pulmonary vasculature has been suggested to act in concert with a potential hypoxic effect observed in COPD. Further, the progression of tissue destruction and loss of pulmonary vasculature may mismatch perfusion ventilation to the gradual increase in alveolar and tissue hypoxia[98]. Thus, It is still not clear that the direct and indirect involvement of hypoxia for the pathogenesis of COPD.

1.8 Animal models

COPD is a complex disease involving several biomolecular, histological, and molecular abnormalities. A systematic approach to understand these aspects is essential to have in-depth knowledge of this disease. To date, three major experimental approaches have been adopted to study COPD. COPD was either induced by inhalation of cigarette smoke or by noxious stimuli, tracheal instillation of tissue-degrading enzymes to induce emphysema-like lesions, or gene-modifications leading to a COPD-like phenotype[19, 20].

A number of animal models have been reported that exhibit at least one of the features of the complicated pathology of COPD, such as chronic bronchitis[101] and emphysema [20, 102, 103]. In these models, airspace enlargement has been demonstrated after chronic exposure to mainstream smoke, and also in shorter exposures to high concentrations of smoke. Ideally, such models need to represent the various patterns of alveolar wall destruction that have been reported in humans, as well as host factors that parallel the etiology of the pathological condition. Animal models with genetic predisposition (e.g., an inherent α_1-AT deficiency or increased sensitivity to oxidative stress) to develop emphysema are probably the most relevant, in mimicking the susceptible human population [104, 105]. The application of genetic engineering strategies in mice offers a great potential to dissect the pathogenetic pathways of emphysema.

Examining the role of inflammation and excessive proteolysis in pulmonary tissue destruction in COPD are some of the major focuses of recent research[106]. Evidence was provided that the alveolar epithelial cell apoptosis causes emphysema in C57Bl/6J mice. Inflammation, proteolysis, oxidative stress, apoptosis, or cell homeostasis in general are interrelated mechanisms that contribute to cigarette smoke-induced emphysema[106, 107]. Tobacco smoke has

been routinely used as a noxious stimulant to induce COPD in a wide variety of animals. In addition to rabbits, mice, dogs, and rats, guinea pigs have been shown to be very susceptible species. Within a few months of exposure to active tobacco smoke, guinea pigs develop COPD-like lesions and emphysema-like airspace enlargement[106, 108].

Thus, the manifestation of COPD is thought to occur by triggering of inflammatory pathways with the influx of leukocytes and cytokines due to chronic irritation by smoke. This inflammatory cellular influx and cytokines can induce cellular local ROS and RNS generation by activating NADPH oxidases (leukocytes and mitochondria) and nitric oxide synthases. In addition, alveolar and tissue hypoxia may be responsible for the disease manifestation due to NF-kB and xanthine/xanthine oxidase activation (Fig. 3)[83].

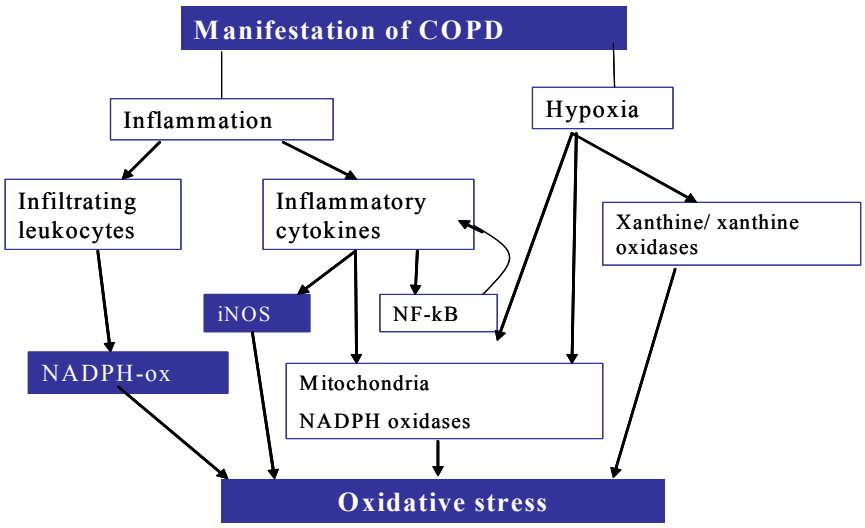

source: Langen,R.C., Korn,S.H., & Wouters,E.F. ROS in the local and systemic pathogenesis of COPD. Free Radic. Biol. Med. 35, 226-235 (2003). (modified)

Figure 3. ROS in the local and systemic pathogenesis of COPD

Thus, the prevailing pathological concept of the development of COPD consists of a sequence of airway inflammation, followed by chronic bronchitis, airway remodeling and lastly pulmonary emphysema[11, 109]. However, recent pathological concepts view COPD as a systemic disease involving skeletal muscle wasting, diaphragmatic dysfunction and systemic inflammation[17]. Furthermore, the pulmonary hypertension noted in COPD patients was thought to occur as a consequence of hypoxic association.

However, there is a growing body of evidence suggests that cigarette smoke has a direct impact on the pulmonary vasculature, indicating that *cor pulmonale* and pulmonary

hypertension are not necessarily secondary to hypoxia and airway remodeling in COPD patients[110-112]. Thus, the disease progression in COPD is not clear yet and experiments are lacking to identify the relationship of pulmonary hypertension to COPD from a physiology as well molecular and cellular biology stand point. Further, it is not clearly understood if the progression of the disease is triggered by a change either in alveolar or the vascular compartments of the lung. Against this background, the current dogma that COPD is first and foremost an airway disease was challenged by showing that vascular changes induced by cigarette smoke inhalation that may cause alveolar destruction[110, 112]. However, no investigation identified the time course of the development of vascular pathology in COPD in relation to the development of lung emphysema. Moreover, the roles of NO synthases and oxidative stress in vascular alterations in COPD have not been deciphered yet.

2. AIMS OF STUDY

Against this background, the overall goal of this thesis was to investigate the mechanisms for the development of lung emphysema and to characterize the possible involvement of vascular pathobiology and endothelial dysfunction in a smoke-induced mouse model of COPD. In particular, this thesis aimed:

1. To examine the structural and functional alveolar changes in chronic tobacco smoke exposed mice.
2. To evaluate vascular changes, hemodynamics and vasoreactivity in chronic tobacco smoke exposed mice.
3. To compare the time course of a possible vascular phenotype with the development of lung emphysema in tobacco-smoke exposed mice.
4. To decipher the role of eNOS and iNOS in the observed changes.

The overall working-hypothesis of this thesis was to challenge the current dogma that COPD is primarily an airway disease and to develop on this hypothesis a therapeutic compound to treat COPD as with its direction.

3. MATERIALS

3.1 Solutions and substances

- Sodium hydroxide 1N (1mol/l) Merck, Darmstadt, Germany
- Chlorhidric acid 1N (1mol/l) Merck, Darmstadt, Germany
- Isoflurane Forene® Abbott, Wiesbach, Germany
- Atropinsulfate 0.5 mg/ ml Braun, Melsungen, Germany
- Medetomidinhydrochloride 1 mg/ ml Domitor®, Pfizer, Karlsruhe, Germany
- Atipamezolhydrochloride 5 mg/ ml Antisedan® Pfizer, Karlsruhe, Germany
- Heparine Liquemin N 25000® Roche, Basel, Swiss
- Ketamin hydrochloride 100 mg/ ml Ketamin® Pharmacia, Erlangen, Germany
- Oncotic agent HAES® Fresenius Kabi, Bad Homburg, Germany
- Lidocainhydrochloride 2% Xylocain® Astra Zeneca, Wedel, Germany
- Physiological Saline solution For washing and weting Baxter S.A., München, Germany
- Ventilation gas, 50% O_2, 50%N_2, Air Liquid, Siegen, Germany

3.2 Consumables

- Single use syringes 1ml, 2ml, 5ml, 10ml Inject Luer® Braun, Melsungen, Germany
- Needle 26G (0.9mm x 25mm) BD Microlance 3® Becton Dickinson, Heidelberg, Germany
- Medical adhesive bands Durapore® 3M St. Paul, MN, USA
- Cannula for vein catheter support 22G and 20G Vasocan Braunüle® Braun, Melsungen, Germany
- Gauze 5 x 4 cm Purzellin® Lohmann und Rauscher, Rengsdorf, Germany
- Single use gloves Transaflex® Ansell Surbiton, Surrey, UK
- Gauze balls size 6 Fuhrman Verrbandstoffe GmbH, Much, Germany
- Perfusor-tubing 150 cm Original-Perfusor®-tubing Braun, Melsungen, Germany
- Combi-Stopper Intermedica GmbH, Kliein-Winternheim, Germany
- Stopcock for infusion therapy and pressure monotoring Discofix®-Braun, Melsungen, Germany
- Napkins Tork, Mannheim, Germany
- Threads Nr. 12 Coats GmbH, Kenzingen, Germany
- Surgical threads non-absorbable Size 5-0 ETHIBOND EXCEL® Ethicon GmbH, Norderstedt, Germany

- Surgical threads with needle size 5-0, 6-0 and 7-0 ProleneTM, Ethicon GmbH, Norderstedt, Germany
- Surgical instruments Martin Medizintechnik, Tuttlingen, Germany
- Heating pad Thermo-Lux® Witte und Suttor, Murrhardt, Germany
- Tracheal cannula from BD Microlance 15 or 20G shortened to 1.5cm Becton Dickinson, Heidelberg, Germany

3.3 Systems and machines for animal experiments

- System for isolated ventilated and perfused mouse lung experiments Hugo Sachs Electronics, Harvard apparatus GmbH, March-Hugstetten, Germany
- Ventilator for mice SAR830A/P Ventilator IITH Inc. Life Science Woodland Hills, California, USA
- PET-Tubes with different diameters Tygon® Saint-Gobain Performance Plastics Charny, France
- Blood analyzer ABL 330 Radiometer, Copenhagen, Denmark
- Polyethylene cannula for systemic arterial pressure measurement in mice, Fine Science Tools GmbH, Heidelberg, Germany
- Silicone catheter for right heart chateterization custom-made instrument for venous catheter insertion with hemostatic ventil 5F Intradyn® Braun, Melsungen, Germany
- Computer and monitor transducer Combitrans monitoring met mod. II for arterial blood pressure measurement Braun, Melsungen, Germany

3.4 Histology

- Parafilm American National Can Menasha, Wisconsin, USA
- Urine pots with covers, Leica Microsystems, Nussloch, Germany
- 100ml Automated microtom RM 2165, Leica Microsystems, Nussloch, Germany
- Flattening table HI 1220 Leica Microsystems, Nussloch, Germany
- Flattening bath for paraffin sections HI 1210 Leica Microsystems, Nussloch, Germany
- Tissue embedding machine EG 1140H Leica Microsystems, Nussloch, Germany
- Cooling plate EG 1150C Leica Microsystems, Nussloch, Germany
- Tissue processing automated machine TP 1050 Leica Microsystems, Nussloch, Germany
- Stereo light microscope DMLA Leica Microsystems, Nussloch, Germany
- Digital Camera Microscope DC 300F Leica Microsystems Nussloch,Germany
- Ethanol 70%, 95%, 99.6% Fischer, Saarbrücken, Germany

- Isopropanol (99.8%) Fluka Chemie, Buchs, Swiss
- Methanol, reinst Fluka Chemie, Buchs, Swiss
- Formaldehyd alcohol free =37% Roth, Karlsruhe, Germany
- Resorcin Fuchsin Chroma, Münster, Germany
- Kernechtrot Aluminiumsulfat Chroma, Münster, Germany
- Roti-Histol (Xylolersatz) Roth, Karlsruhe, Germany
- Xylol Roth, Karlsruhe, Germany
- Hydrogen peroxide 30% pro analysi Merck, Darmstadt, Germany
- Universal-embedding cassettes / cover slips 24x36mm, Menzel, Germany
- Leica Microsystems, Nussloch, Germany
- Histological glass slides Superfrost Plus® R. Langenbrinck, Emmendingen, Germany
- Microtom blades S35 Feather, pfm - Produkte für die Medizin AG, Köln, Germany
- Paraffin embedding medium Paraplast Plus® Sigma Aldrich, Steinheim, Germany
- Pikric acid Fluka Chemie, Buchs, Swiss
- Mounting medium Pertex® Medite GmbH, Burgdorf, Germany
- Natriumchlorid pro analysi Roth, Karlsruhe, Germany
- Di-Natriumhydrogenphosphat Dihydrat, pro analysis Merck, Darmstadt, Germany
- Kaliumdihydrogenphosphat pro analysi Merck, Darmstadt, Germany
- Trypsin Digest All 2® Zytomed, Berlin, Germany
- Avidin-Biotin-Blocking Kit Vector/ Linaris, Wertheim-Bettingen, Germany
- Normal Horse Serum, Alexis Biochemicals, Grünberg, Germany
- Normal Goat Serum, Alexis Biochemicals, Grünberg, Germany
- Normal Rabbit Serum, Alexis Biochemicals, Grünberg, Germany
- Vectastain Elite ABC Kits anti-mouse anti-rabbt, anti-goat, Vector/ Linaris, Wertheim-Bettingen, Germany
- Vector VIP Substrat Kit, Vector/ Linaris, Wertheim-Bettingen, Germany
- DAB Substrat Kit, Vector/ Linaris, Wertheim-Bettingen, Germany
- Methylgreen Counterstain, Vector/ Linaris, Wertheim-Bettingen, Germany
- Silicon, Sigma-Aldrich Biochemie GmbH, Steinheim, Germany
- Acetone, Sigma-Aldrich Biochemie GmbH, Steinheim, Germany
- Nitric oxide synthase inhibitor (L-NIL), Sigma-Aldrich Biochemie GmbH, Steinheim, Germany
- Laser capture micro dissection, Leica Microsystems, Nussloch, Germany

3.5 Antibodies

- Anti-alpha-smooth muscle Actin; Clone 1A4 monoclonal, mouse antihuman dilution 1:1000 Sigma Aldrich, Steinheim, Germany
- Anti-von Willebrand factor polyclonal, rabbit anti-human dilution 1:1000 Dako Cytomation, Hamburg, Germany
- Rabbit polyclonal nitrotyrosine antibody, Sigma Aldrich, Steinheim, Germany
- Rabbit polyclonal iNOS Antibody, Santa cruz biotechnology, Heidelberg Germany
- Rabbit Polyclonal eNOS antibody, Biotrend chemikalien GmbH, Koln, Germany

3.6 Systems and software for morphometry

- Computer Q 550 IW Leica Microsystems Nussloch, Germany
- Software Q Win V3 Leica Microsystems Nussloch, Germany
- Makro for Muscularization degree, wall thickness, septum (alveolar morphometry) Leica Microsystems, Nussloch, Germany

3.7 Smoke generating system

- Smoke generator, Custom-made, Tübingen, Germany
- Vacuum pump for smoke generator, Custom-made, Tübingen,Germany
- Pump for removing smoke, TSE, Tübingen, Germany
- Smoke chamber, TSE, Tübingen, Germany
- Millipore filter Millipore, Schwalbach, Germany
- Cigarette, University of Kentucky, Lexington, USA
- Computer program for monitoring smoke, TSE, Tübingen, Germany

4. METHODS

4.1 Animals

Adult WT C57Bl/6J and iNOS$^{-/-}$ with eNOS$^{-/-}$ (B6.129P2-Nos2tm1Lau/J with B6.129P2-Nos3tm1Unc/J) mice, 20–22 g were obtained from Charles River Laboratories, Sulzfeld, Germany. Animals were housed under controlled conditions of equal day light cycle of 12 hours with food and water supply *ad libitum*. Animals were randomly allocated to smoke exposed and unexposed groups of 6 mice each, with parallel groups for: (i) alveolar morphometry, (ii) vascular morphometry including right ventricular and systemic arterial blood pressure measurements, (iii) protein and mRNA analysis, (iv) lung function tests, and (v) vasoreactivity. All experiments were approved by the governmental ethics committee for animal welfare (Regierungspräsidium Giessen, Germany).

4.2 Experimental design and tobacco smoke exposure

WT, eNOS$^{-/-}$, and iNOS$^{-/-}$ mice were exposed to the mainstream smoke of 3R4F cigarettes; (University of Kentucky, Lexington, KY, USA) at a concentration of 140 mg particulate matter/m^3 for 6 h/day, 5 days/week for up to 8 months. After assessing the time course of COPD development in WT mice and in the knockout mice, WT animals were exposed to smoke with parallel treatment with the iNOS inhibitor L-NIL at a concentration known to be highly iNOS selective (600 μg/ml in drinking water, Biotium, USA) in a separate set of experiments. To assure age-matched controls, respective control groups were kept under identical conditions as smoke-exposed mice but without smoke exposure. The age of the control mice had no significant effect on any of the parameters measured in this study and given respective control group as 0 months of smoke exposure.

Experimental plan / time table of analysis

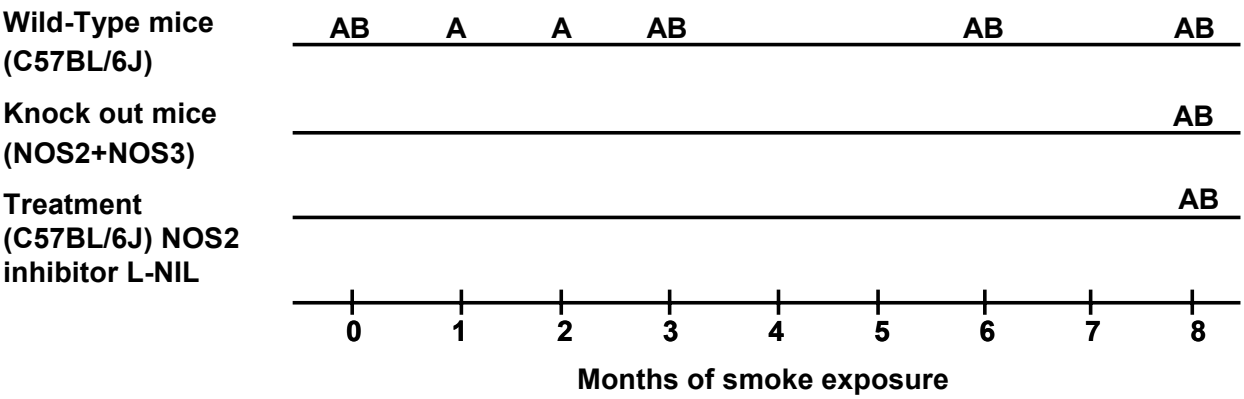

A: Alveolar morphometry, vascular morphometry, right heart hypertrophy, hemodynamics

AB: Alveolar morphometry, vascular morphometry, right heart hypertrophy, hemodynamics, lung function test, isolated perfused mouse lung experiment, real time PCR, Western blot, different target staining by immunohistochemistry and immunofluorescence, *in-situ* hybridization

4.3 Mice preparation

Mice after smoke exposure were anesthetized by intraperitoneal injection with ketamine/xylazine (20µl ketamine/20µl xylazine/40µl NaCl) and sacrificed for morphometrical investigation. During sacrifice, mice were given first incision in longitudinal ventral area from trachea to abdomen, diaphragm was opened and tracheal area was cleaned.

For alveolar morphometry, lungs were fixed in chest by infusion of 4.5% formaldehyde solution at 22 cm H_2O of inflating pressure via the trachea. For vascular morphometry, lungs were first flushed free of blood with the saline via the pulmonary artery after making opening through incision in left ventricle and then fixed by passing zamboni fixative solution at 22 cm H_2O pressure. During fixation, tracheal pressure of 12 cm H_2O was maintained. For both alveolar and vascular morphometry, lungs were isolated from the chest cavity after 20 minutes and allowed to immerse overnight in respective fixative solution. Thus fixed lungs were transferred to 0.1 M phosphate buffered saline the following day.

After this, the lung lobes were individually placed in histological cassettes and dehydrated in an automated dehydration station and than embedded in paraffin blocks. Staining was done on 3µm lung sections for alveolar/vascular-luminal morphometry and number of alveoli: number of vessels. Similar study was also carried out with human COPD patient lungs too.

4.3.1 Alveolar morphometry

The mean linear intercept, mean air space and mean septal wall thickness were measured from paraffin sections of each lung's lobe after staining with hematoxylin and eosin (HE)[113]. The detailed protocol is given in **Appendix I**. This HE stained lung sections were scanned to build mosaics picture and each mosaics were investigated microscopically by using a Qwin macro program from Leica. Bronchi, airways and vessels were excluded in measurement. Maximum 50-100 smaller mosaics areas were investigated in blinded fashion from each lung's lobe.

4.3.2 Vascular morphometry

The degree of muscularization in small pulmonary arteries was investigated in mouse lung paraffin sections after staining for smooth muscle and endothelial cells using specific marker α-actin and Willebrand factor (vWf) antibodies respectively. The detailed protocol is given in **Appendix II**.

Morphometric quantification was carried out microscopically using a Qwin macro program from Leica[114, 115]. This program automatically recognized α-actin stained colour and categorized vessel into fully muscularized (>70% vessel circumference), partially muscularized (5%-70% vessels circumference) and nonmuscularized (<5% vessels circumference). One hundred pulmonary artieries (85 vessels for 20-70 micrometer diameter vessels, 10 vessels for 70-150 micrometer vessels and 5 vessels for more than 150 micrometer vessels) were analyzed from each lung lobe in a blinded fashion. The degree of muscularization is given as percentage of total vessel count.

4.3.3 Lumen morphometry

The lumen areas of pulmonary arteries were investigated in elastica Van Gieson stained parrafin lung section. The detail staining protocols are given detail in **Appendix III**. This staining was used to differentiate between elastic fibers (purple black staining), the cell nucleus (dark brown staining), the collagenous fibers (red staining) and the muscle fiber and cytoplasm (yellow staining).

Morphometrical quantification was carried out microscopically using a Qwin macro program from leica[115, 116]. From each stained section, 85 vessel (20-70 micrometer diameter), 10 vessels (70-150 micrometer diameter) and 5 vessels (more than 150 micrometer diameter) were measured. The specific mosaic picture automatically differentiated the external diameter of vessel (tunica externa), internal diameter of vessel (intimal layer) and calculated the vascular lumen area. All vascular lumen areas were averaged after categorization to different vessel size as given above.

4.3.4 Ratio of the number of alveoli / number of vessels

For counting the total number of vessel and alveoli, above stained lung sections for vascular morphometry (α-actin and vWf) were analyzed by using a Qwin macro program from leica to create 32 number of smaller mosaic picture under magnification of X10 in a blinded fashion. Each mosaic was marked with definite scale for measuring area. All alveoli and vessels number were counted averaged and the ratio of alveolai/vessels was calculated.

4.4 Isolated perfused mouse lung experiment

For measurement of vasoreactivity and lung functional parameters, an isolated perfused mouse lung setup was used. Isolated mouse lung perfusion was performed in a water-jacketed

chamber (type 839, Hugo Sachs Elektronik, March-Hugstetten, Germany). Deeply anesthetized and anticoagulated animals were intubated via a tracheostoma and ventilated with room air (positive pressure ventilation 250 µl tidal volume, 90 breaths/min and 2 cm H_2O positive end-expiratory pressure). A midsternal thoracotomy was followed by an insertion of catheters into the pulmonary artery. Lungs were perfused with Krebs–Henseleit buffer (120 mM NaCl, 4.3 mM KCl, 1.1 mM KH_2PO_4, 2.4 mM $CaCl_2$, 1.3 mM $MgCl_2$, and 13.32 mM glucose as well as 5% (w/v) hydroxyethylamylopectin as an oncotic agent; $NaHCO_3$ was adjusted to result in a constant pH of 7.37– 7.40) at a flow rate of 2 ml / min using a peristaltic pump (ISM834A V2.10, Ismatec, Glattbrugg, Switzerland). In parallel to perfusion, the ventilation was changed from room air to a pre-mixed normoxic gas (21% O_2, 5.3% CO_2, balanced with N_2). After rinsing the lungs with ~20 ml buffer, the perfusion circuit was closed for recirculation and the left arterial pressure was set at 2.0 mmHg. Meanwhile, the flow was slowly increased from 0.2 to 2 ml / min and the entire system was heated to 37°C. The pressure in the pulmonary artery and in the left ventricle was registered via catheters.

The artificial thorax was closed and the lungs were ventilated with negative pressure of -2 cm H_2O and -12 cm H_2O, respectively. The end-expiratory pressure was kept constant at -2 cm H_2O. The tidal volume, pulmonary resistance and dynamic lung compliance were calculated using the HSE Pulmodyn program (Hugo Sachs Elektronik, March Hugstetten, Germany)[117].

After assessment of the lung function, the lungs were ventilated with positive pressure at a tidal volume of 250 µl and an end-expiratory pressure of 2 cm H_2O. For evaluation of vasoreactivity, a hypoxic ventilation with a gas mixture containing 1% O_2, 5.3% CO_2, balanced with N_2 was used. Two 10-min periods of hypoxic ventilation (1% O_2) were alternated with 15 min normoxic periods. This was followed by application of increased doses of phenylepinephrine (0.1, 1, 10, 100 µM) into the buffer fluid. Each dosage increase was performed after pulmonary artery pressure reached a constant value. After application of the highest phenylepinephrine concentration, the response to inhaled NO (10, 100 ppm) and intravascularly infused acetylcholine (1, 10 µM) was determined.

4.5 In vivo hemodynamic measurements

Mice were anaesthetized with ketamine (6 mg/100 g, intraperitoneally) and xylazine (1mg/100g, intraperitoneally) and were anticoagulated with heparin (1000 U/Kg). The trachea was cannulated, and the lungs were ventilated with room air at a tidal volume of 0.2 ml and at

a rate of 120 breaths per minute maintained at a physiological temperature throughout the experiment. Systemic arterial pressure was determined by catheterization of the carotid artery. For measurement of right ventricular systolic pressure (RVSP) a PE-10 tube was inserted into the right ventricle via the right vena jugularis. The changes in the carotid arterial with the right ventricular pressure were monitored continuously and the mice were maintained in homeothermic condition[114].

4.6 Heart ratios

All hearts from mice of different group were isolated and dissected for right ventricular weight (RV) and left ventricle plus septum weight (LV+ septum). After sectioning, they were dried for 1 week at room temperature. The right to left ventricle plus septum weight ratio was calculated[114].

4.7 Localization of eNOS, iNOS, and nitrotyrosine

Localization of eNOS and iNOS was investigated in lung sections from cryopreserved tissue by immunostaining[118]. Lung sections (10 μm) were fixed in ice-cold acetone/methanol solution (1:1) and blocked with 3% (w/v) bovine serum albumin (BSA) in phosphate buffered saline (PBS) for 1 hour followed by an overnight incubation with an 1:50 dilution of anti-eNOS (BD Biosciences, Heidelberg, Germany) or 1:100 dilution of anti-iNOS (Abcam, Cambridge, UK) antibody, diluted in PBS with 3% (w/v) BSA. Indirect immunofluorescence was obtained after incubation for 90 min with a 1:500 dilution of Alexa Fluor® 555 conjugated anti-rabbit antibody (Invitrogen, Karlsruhe, Germany) in BSA. Nuclear counterstaining was performed with Hoechst-33258 (1:10000 dilution in PBS; Invitrogen, Karlsruhe, Germany) for 10 min.

Nitrotyrosine was detected in paraffin-embedded lung sections of both mouse and human lung tissue using a rabbit anti-nitrotyrosine antibody (Sigma, Munich, Germany). The expression of nitrotyrosine was assessed on 3 μm, paraffin-embedded lung sections in animal and human lung tissue samples. After heating at 61°C, lung sections were deparaffinized in xylene and rehydrated. The endogenous peroxidase activity was quenched with 3% (v/v) H_2O_2 in methanol. For staining, a 1:250 dilution of antinitrotyrosine antibody (rabbit anti-nitrotyrosine; Sigma, Munich, Germany) was used. Subsequently the immune complexes were visualized with a peroxidase-conjugated secondary antibody (Vector labs, LINARIS,

Wertheim-Bettingen, Germany). An additional methyl green counterstaining of the sections was performed.

4.8 Non-isotopic in situ hybridization (NISH) combined with immunofluorescence on mouse lung sections

Localization of mRNA by non-isotopic *in situ* hybridization was determined in cryostat lung sections[118]. The generation of single-stranded digoxigenin (DIG)-labelled riboprobes for non-isotopic *in situ* hybridization was done by the *in vitro* transcription method. For the generation of the probes, the template was amplified by nested PCR out of cDNA from lung homogenate using the following primers:

NISH iNOS (F) 5′-GCCCCTGGAAGTTTCTCTTC-3′

NISH iNOS (R) 5′-ACCACTCGTACTTGGGATGC-3′

NISH iNOS (F) T3 5′-AATTAACCCTCACTAAAGGTTCCAGAATCCCTGGACAAG-3′

NISH iNOS (R) T7 5′-TAATACGACTCACTATAGGTGCTGAAACATTTCCTGTGC-3′

NISH eNOS (F) 5′-AAGTGGGCAGCATCACCTAC-3′

NISH eNOS (R) 5′-GTCCAGATCCATGCACACAG-3′

NISH eNOS (F) T3 5′-AATTAACCCTCACTAAAGGCTTCAGGAAGTGGAGGCTGA-3′

NISH eNOS (R) T7 5′-TAATACGACTCACTATAGGAGTAACAGGGGCAGCACATC-3′

In brief, 1μg of the purified PCR-amplified template containing T3 and T7 RNA polymerase promoter sequences was mixed with 2 μl digoxigenin-11-uridine triphosphate (Roche, Mannheim, Germany), 4 μl of 5x transcription buffer (Promega, Mannheim, Germany), 1 μl of RNasin (Peqlab, Erlangen, Germany) and 2 μl of T3 or T7 Phage polymerase (Promega, Mannheim, Germany) in a total reaction volume of 20 μl. The reaction mixture was incubated at 37°C for 2 h. The RNA probes were purified with a PCR purification kit (Qiagen, Hilden, Germany). The non-isotopic *in situ* hybridization was performed on 8 μm thick Tissue-Tek®-embedded (Sakura Finetek, Staufen, Germany) mouse lung cryostat sections.

4.9 Laser-assisted microdissection

Microdissection was performed to isolate pulmonary arterial vessels from cryostat lung sections[118, 119]. In brief, cryosections (10μm) of Tissue-Tek®-embedded (Sakura Finetek, Staufen, Germany) lung tissue were mounted on membrane-coated glass slides. After hemalaun staining for 45 s, mouse lung sections were subsequently immersed in water, 70%, 96% and stored in 100% ethanol until use. Human lung cryosections were stained with

hematoxylin for 10 s, washed with water, stained with eosin (1:5) for 20 s and subsequently immersed in water, 70%, 96% and stored in 100% ethanol until use.

Intrapulmonary arteries with a diameter 50–150 μm were selected and microdissected under optical control using the Laser Microbeam System (P.A.L.M., Bernried, Germany). Afterwards, the microdissected vessels were catapulated to an inverted Eppendorf tube lid filled with 25 μl of mineral oil. After collection, the vessels were spun down in 300 μl of RNA lysis buffer, vortexed and directly frozen to store in liquid nitrogen until analysis.

4.10 RNA isolation, pre-amplification, cDNA synthesis and real-time polymerase chain reaction

RNA from laser-microdissected or homogenized mouse and human lung tissue was isolated by RNeasy Micro and Mini kits, respectively (Qiagen, Hilden, Germany). The isolated RNA was pre-amplified and relative quantification of the eNOS, iNOS subunits was done using the iQ SYBR Green Supermix (BIO-RAD, Munich, Germany). Total messenger RNA was extracted from frozen human lung tissue and microdissected vessels by using an RNeasy Mini or Micro Kit (Qiagen, Hilden, Germany) according to the manufacturer's instructions. The isolated RNA was subsequently pre-amplified with a modified Quick Amp Labelling Kit (Agilent, Böblingen, Germany). PCR with reverse transcription was performed with 1 μg of RNA each, using the iScript cDNA Synthesis Kit (BIO-RAD, Munich, Germany). The condition for the reverse transcription was as follows: 1 cycle at 25°C for 5 min; 1 cycle at 42°C for 30 min; 1 cycle at 85°C for 5 min.

Real-time PCR was performed with the iQ SYBR Green Supermix according to the manufacturer's instructions (BIO-RAD, Munich, Germany). In brief, a 25 μl mixture was used containing 12.5 μl iQ SYBR Green Supermix, 0.5 μl forward and reverse primer, 9.5 μl sterile water and 2 μl of the 1:5 diluted complementary DNA template. A negative control (non-template control) was performed in each run. The real time PCR was performed with a Mx3000P (Stratagene, Heidelberg, Germany) under the following conditions: 1 cycle at 95°C for 10 min, then 40 cycles at 95°C for 10 s, 59°C for 10 s, 72°C for 10 s, followed by a dissociation curve. The intron-spanning primers were designed by using sequence information from the NCBI database. The Ct values were normalized to the endogenous control (Porphobilinogen deaminase, PBGD).

PBGD mouse (F) 5′-GGGAACCAGCTCTCTGAGGA-3′

PBGD mouse (R) 5′-GAATTCCTGCAGCTCATCCA-3′

iNOS mouse (F) 5′-TGATGTGCTGCCTCTGGCT-3′

iNOS mouse (R) 5′-AATCTCGGTGCCCATGTACC-3′

eNOS mouse (F) 5′-ACACAAGGCTGGAGGAGCTG-3′

eNOS mouse (R) 5′-TGGCATCTTCTCCCACACAG-3′

PBGD human (F) 5′-CCCACGCGAATCACTCTCAT-3′

PBGD human (R) 5′-TGTCTGGTAACGGCAATGCG-3′

iNOS human (F) 5′-ATGAGGAGCAGGTCGAGGAC-3′

iNOS human (R) 5′-CTGACATCTCCAGGCTGCTG-3′

eNOS human (F) 5′-ACCTCGTCCCTGTGGAAAGA-3′

eNOS human (R) 5′-CCTGGCCTTCTGCTCATTCT-3′

4.11 Western blots

For the quantification of eNOS, iNOS and nitrotyrosine in mouse and human lung tissue, the polyclonal antibodies anti-eNOS (BD Biosciences, Heidelberg, Germany), or antiiNOS (Abcam, Cambridge, UK) and anti-nitrotyrosine (Abcam, Cambridge, UK) raised in rabbits were used. Frozen mouse and human lung tissue samples were homogenized in RIPA buffer, containing 1 mM sodium vanadate, 0.1 mM phenylmethylsulphonyl fluoride (PMSF), 40 µl/ml protease-inhibitor mix complete (Roche, Mannheim, Germany) and 30 µl/ml β-mercaptoethanol. Subsequently the samples were centrifuged for 10 min at 8000 g. The supernatant (containing 4x LDS loading buffer) was heated at 99°C for 10 min and equal amounts of protein were loaded on an 8% SDS polyacrylamide gel. The proteins were transferred to a polyvinylidene fluoride membrane (Pall Corporation, Dreieich, Germany) by the semi dry-blotting method. The membrane was washed for 5 min with wash buffer (20 mM Tris-Cl, pH 7.5, 150 mM NaCl, 0.1% (v/v) Tween 20) and subsequently blocked in 6% (w/v) non-fat dry milk powder dissolved in wash buffer at room temperature.

Incubation with a diluted primary antibody (iNOS_ab3523 1:2000, Nitrotyrosine_ab7048 1:1000, both Abcam, Cambridge, UK; eNOS`610298 1:1000, BD Biosciences, Heidelberg, Germany; β-actin_A5316 1:30000, Sigma-Aldrich, Munich, Germany) was performed at 4°C overnight. After washing several times with wash buffer, a horseradish peroxidase-conjugated secondary antibody (anti-rabbit_W401B and anti-mouse_W402B respectively, Promega, Mannheim, Germany) was applied for 1 h at room temperature. After washing the membrane,

visualization was carried out using the enhanced chemiluminescence kit (ECL, Amersham, Braunschweig, Germany) and X-ray photo film (Kodak, Stuttgart, Germany).

4.12 Patient characteristics

Human lung tissues were obtained from transplanted COPD patients (Gold stage IV) and donor controls. The studies were approved by the Ethics Committee of the Justus-Liebig-University, School of Medicine (AZ 31/93). The human lung tissue was snap-frozen directly after explantation for mRNA and protein extraction or fixed in 4.5% paraformaldehyde or Tissue-Tek® (Sakura Finetek, Staufen, Germany), respectively for histology and laser assisted microdissection. Patients' characteristics details are given in Table 4.

Table 4 Patient characteristics

Patient	FEV1/FVC	Diagnosis	Age (yr)	Sex	Pack/ years	Treatment
1 COPD	49.3%	COPD	53	m	39	IB / T/ SC
2 COPD	45.0%	COPD	48	m	31	IB / ICS
3 COPD	30.6%	COPD	58	m	88	IB / ICS / T
4 COPD	39.7%	COPD	58	m	70	IB / SC /T
5 COPD	62.9%	COPD	59	m	5	IB/ ICS
1 Donor		Normal	24	m		
2 Donor		Normal	52	f		
3 Donor		Normal	61	f		
4 Donor		Normal	26	m		
5 Donor		Normal	29	m		

4.13 Statistical analyses

All data are expressed as means ± SEM. Comparison of multiple groups was performed by analysis of variance (ANOVA) with the Student–Newman–Keuls post-test. For comparison of two groups a Student's *t*-test was performed. *P* value below 0.05 was considered as statistical significant for all analysis.

5. RESULTS

5.1 Lung emphysema development in wild-type mice exposed to tobacco smoke

Exposure of wild-type (WT) mice to cigarette smoke for up to 8 months resulted in development of lung emphysema starting after 6 months, as evident from an increase in the mean linear intercept, an increase in the airspace and a decrease in the septal wall thickness. The lung emphysema was more pronounced after 8 months of tobacco exposure. There was no difference in the mean linear intercept, air space, and septal wall thickness between the non smoke exposed age matched controls (0 months) (**Fig. 4 a–d**).

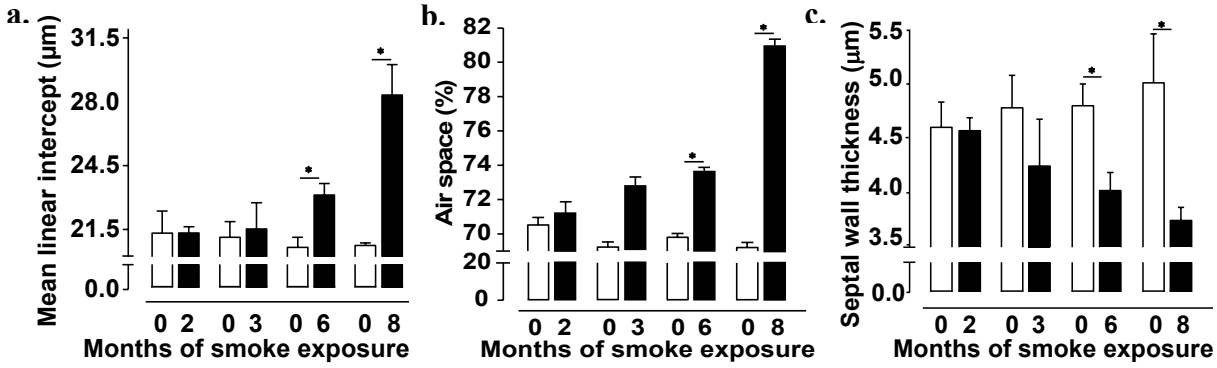

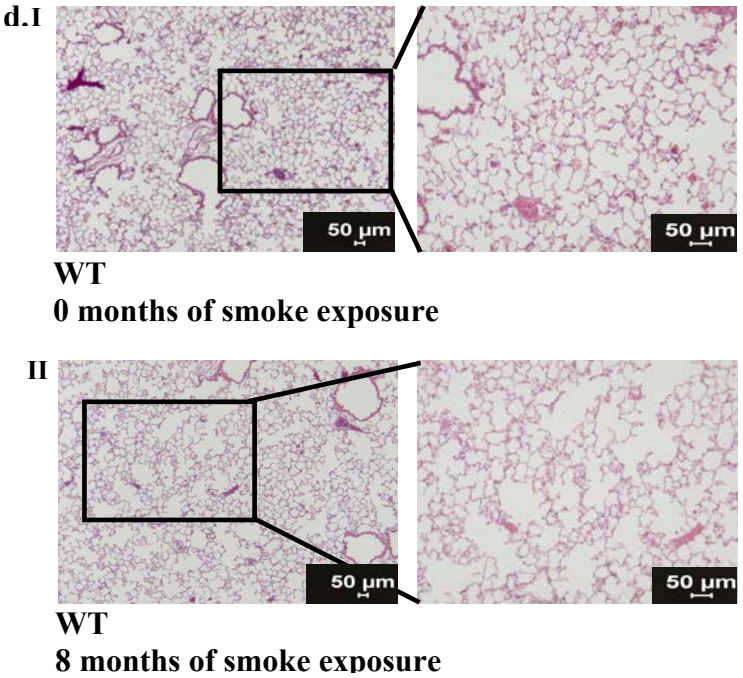

Figure 4. Comparison of the time course for the development of emphysema during 8 months of smoke exposure in wild-type (WT) mice.

(**a**) mean linear intercept, (**b**) air space and (**c**) septal wall thickness, quantified from lung sections stained with hematoxylin & eosin (HE), (**d**) representative histology from lung sections satined with HE (I, II). Data are given for n = 6 lungs each in the time course of tobacco smoke exposure for up to 8 months. ∗significant differences (P<0.05) compared with respective unexposed controls (0 months of exposure).

5.2 Lung functional changes in wild-type mice exposed to tobacco smoke

The late onset of lung emphysema development was mirrored by the development of lung functional changes. This lung functional data showed increased dynamic lung compliance, increase dynamic lung tidal volume and decreased lung airway resistance after 8 months of tobacco smoke exposure. There was no difference in the dynamic lung compliance, increase dynamic lung tidal volume and decreased lung airway resistance between the non smoke exposed age matched controls (0 months) (**Fig. 5 a-c**).

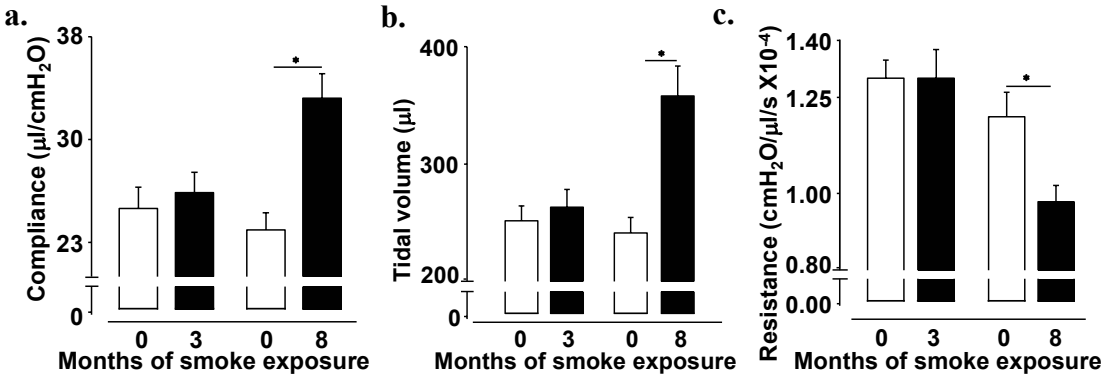

Figure 5. Lung compliance, tidal volume and airway resistance during the course of smoke exposure for 8 months in wild-type (WT) mice.

Lung functional parameters determined in isolated, artificially ventilated and perfused mouse lungs under negative pressure ventilation. (**a**) lung compliance, (**b**) tidal volume and (**c**) airway resistance in WT mice. ∗significant differences (P<0.05) compared with respective unexposed controls (0 months of exposure).

5.3 Pulmonary hypertension development in wild-type mice exposed to tobacco smoke

5.3.1 Hemodynamics, heart ratio and number of alveoli / number of vessels

Most interestingly, tobacco smoke exposure caused development of pulmonary hypertension, which preceded the development of lung emphysema. This was shown by an increase in right ventricular systolic pressure and increase in the ratio of the absolute numbers of alveoli: number of vessels within 3 months, followed by right heart hypertrophy after 6 months of tobacco smoke exposure. There was no difference in the right ventricular systolic pressure, the ratio of the absolute numbers of alveoli: number of vessels (**Fig. 6a, b)** and the heart ratio (**Table 5**) between the non smoke exposed age matched controls (0 months).

In contrast to the increased right ventricular pressure, mean systemic artery pressure was significantly and consistently decreased after 3 months of smoke exposure in WT mice. There was no difference in the right ventricular pressure, mean systemic artery pressure between the non smoke exposed age matched controls (0 months) (**Fig. 6c**).

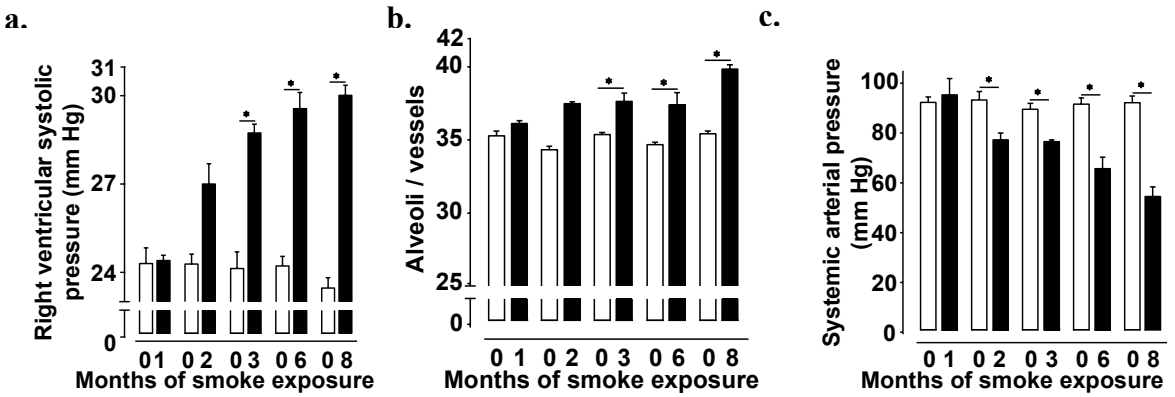

Figure 6. Comparison of the time course of the development of pulmonary hypertension during 8 months of smoke exposure in wild-type (WT) mice.

(**a**) right ventricular systolic pressure quantified by right heart catheterization in anesthetized animals. (**b**) ratio of the number of alveoli to the number of vessels per area quantified from lung sections co-stained against α-smooth muscle actin and von Willebrand factor. (**c**) systemic arterial pressure in WT mice. Data are given for n = 6 lungs each in the time course of tobacco smoke exposure for up to 8 months. ∗significant differences (P<0.05) compared with respective unexposed controls (0 months of exposure).

The weight of left ventricle plus septum remained same till 8 months of smoke exposure and only the right ventricular weight was increased after 6 months of smoke exposure as shown in **Table 5**.

Table 5 Comparision of the mass of the right ventricle (RV), the left ventricle+septum (LV+S) and thew ratio of RV/(LV+S) during 8 months of smoke exposure in WT mice.

Group	RV (g) ± SEM		LV+ S (g) ± SEM		RV/(LV+S) ± SEM	
Months of smoke exposure	Non smoke	Smoke	Non smoke	Smoke	Non smoke	Smoke
1 month	0.0051 ±0.0002	0.0055 ±0.0002	0.0210 ±0.0008	0.0236 ±0.0004	0.2400 ±0.0035	0.2300 ±0.0052
2 months	0.0057 ±0.0003	0.0058 ±0.0004	0.0232 ±0.0014	0.0230 ±0.0011	0.2400 ±0.0045	0.2500 ±0.0063
3 months	0.0052 ±0.0002	0.0056 ±0.0002	0.0210 ±0.0003	0.0224 ±0.0009	0.2500 ±0.0075	0.2500 ±0.0045
6 months	0.0051 ±0.0002	0.0063 ±0.0003∗	0.0202 ±0.0006	0.0208 ±0.0010	0.2500 ±0.0041	0.3000 ±0.0046∗
8 months	0.0052 ±0.0001	0.0064 ±0.0002∗	0.0206 ±0.0003	0.0206 ±0.00091	0.2500 ±0.0036	0.3100 ±0.0132∗

∗significant difference (P<0.05) compared with respective months age-matched non-smoke exposed controls.

5.3.2 Degree of muscularization and vascular lumen area

Pulmonary hypertension was accompanied by an increase in the degree of muscularization of lung resistance pulmonary arteries (of diameter 20–70 μm) and a reduction in mean vascular lumen area after 3 months of smoke exposure. There was no difference in the degree of muscularization and narrowing of vascular lumen between the non smoke exposed ages matched controls (0 months) (**Fig.7a–c**).

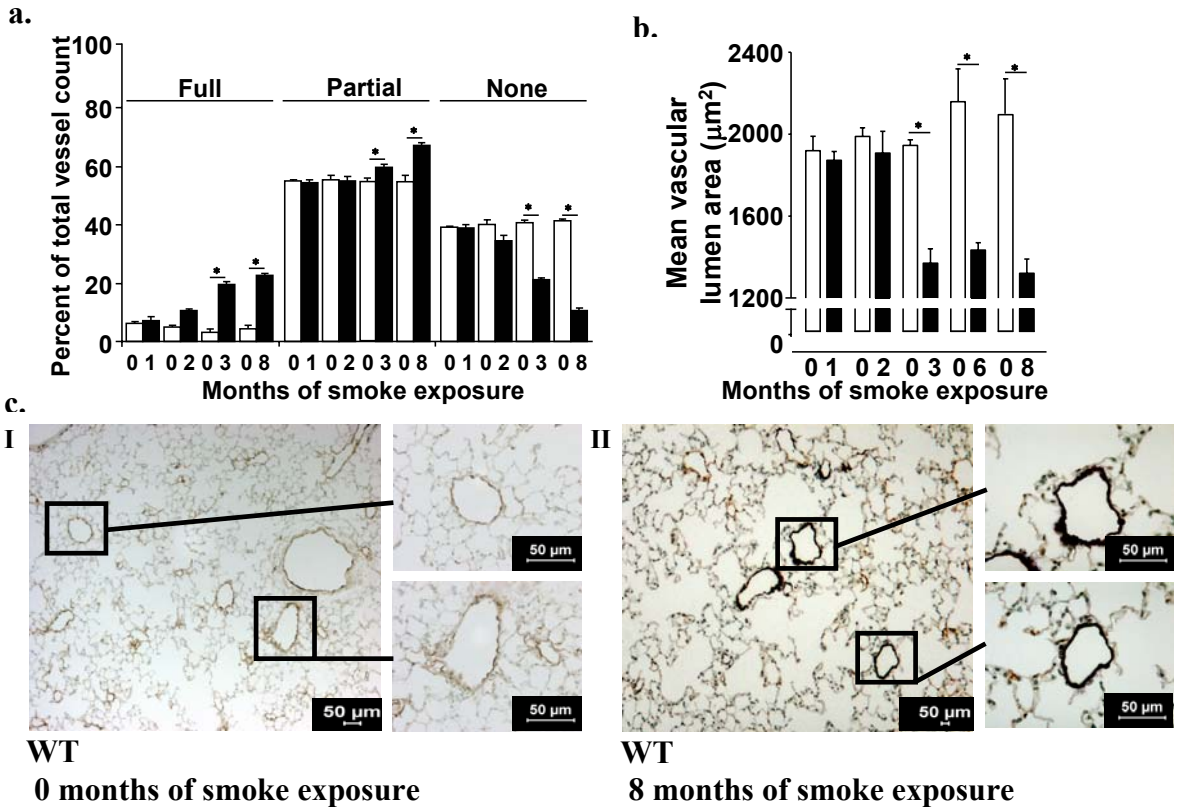

Figure 7. Degree of muscularization and narrowing of vascular lumen during 8 months of smoke exposure in wild-type (WT) mice.

(**a**) degree of muscularization of small pulmonary arteries (diameter 20–70 µm). Data are given as percentage of total vessel count for fully muscularized (Full), partially muscularized (Partial) and non-muscularized (None) vessels from lung sections costained against α-smooth muscle actin and von Willebrand factor. (**b**) mean vascular lumen area (µm^2) of small pulmonary arterial vessels (diameter 20–70µm) from van Gieson stained lung section. (**c**) representative histology from lung sections stained antibodies against α-smooth muscle actin and von Willebrand factor (**I, II**). Data are given for n = 6 lungs each in the time course of tobacco smoke exposure for up to 8 months. ∗significant differences (P<0.05) compared with respective unexposed controls (0 months of exposure).

A similar increase in the degree of muscularization and narrowing of vascular lumen was found in larger pulmonary arteries. There was no difference in the degree of muscularization and narrowing of vascular lumen between the non smoke exposed ages matched controls (0 months) (of diameter 71–150 µm, and those >150 µm, **Fig. 8a-d**).

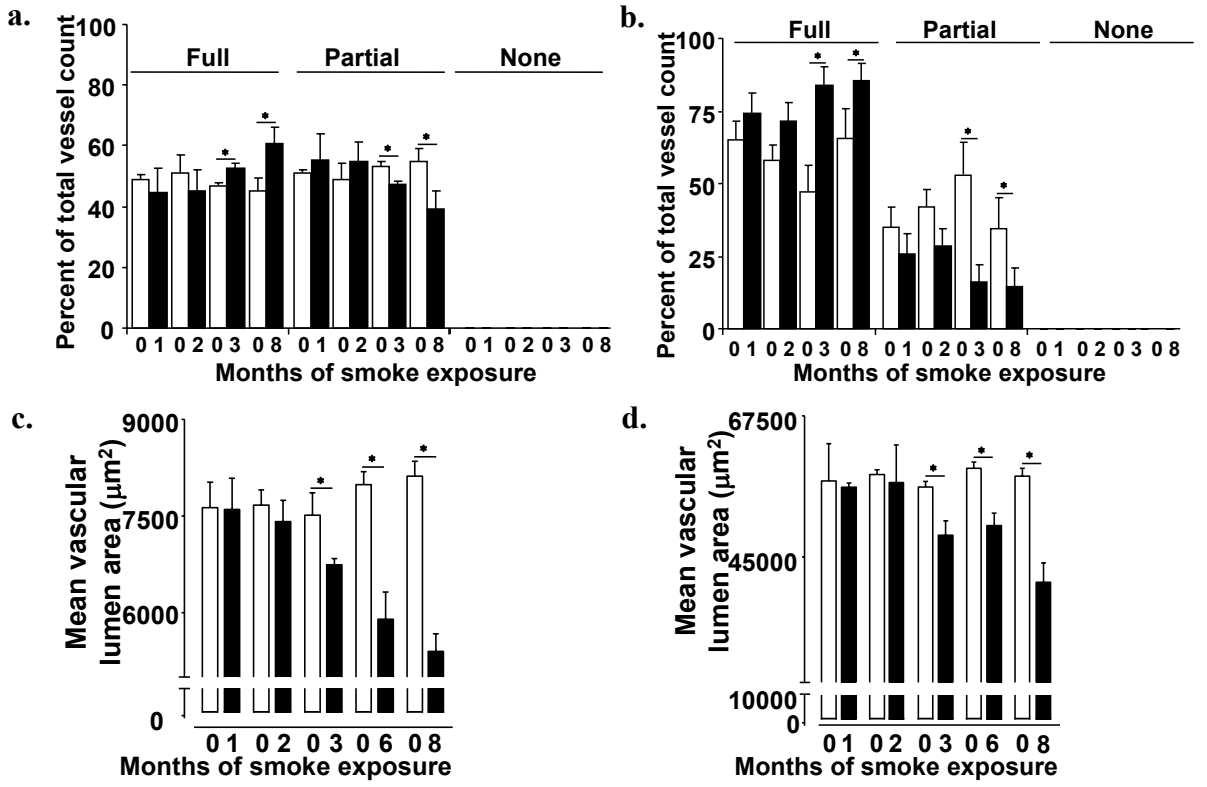

Figure 8. Degree of muscularization and narrowing of vascular lumen in pulmonary arterial vessels during 8 months of smoke exposure in wild-type (WT) mice with COPD.

(**a**) development of the increase in the degree of muscularization of pulmonary arterial vessels (diameter 70–150 µm). (**b**) development of the increase in the degree of muscularization of pulmonary arterial vessels (diameter >150 µm). (**c**) development of the decrease in the mean vascular lumen area (µm^2) of pulmonary arterial vessels (diameter 70–150 µm). (**d**) development of the decrease in the mean vascular lumen area (µm^2) of pulmonary arterial vessels (diameter >150 µm). Data are given for n = 6 lungs each in the time course of tobacco smoke exposure for up to 8 months. ∗significant differences (P<0.05) compared with respective unexposed controls (0 months of exposure).

5.4 Regulation of iNOS and eNOS expression in the pulmonary vasculature of wild-type mice after exposure to tobacco smoke

5.4.1 Localization of iNOS and eNOS in mRNA and protein level

As the regulation of NOS is thought to contribute to the development of COPD, eNOS and iNOS expression was focussed during the course of tobacco smoke exposure. Immunofluorescence staining suggested that iNOS protein expression was prominently upregulated in the pulmonary vasculature in smoke-exposed mice (**Fig. 9a I**). *In situ* hybridization mirrored these results, showing upregulation of iNOS messenger RNA in the pulmonary vasculature, with some additional reactivity found in bronchi (**Fig. 9b I**).

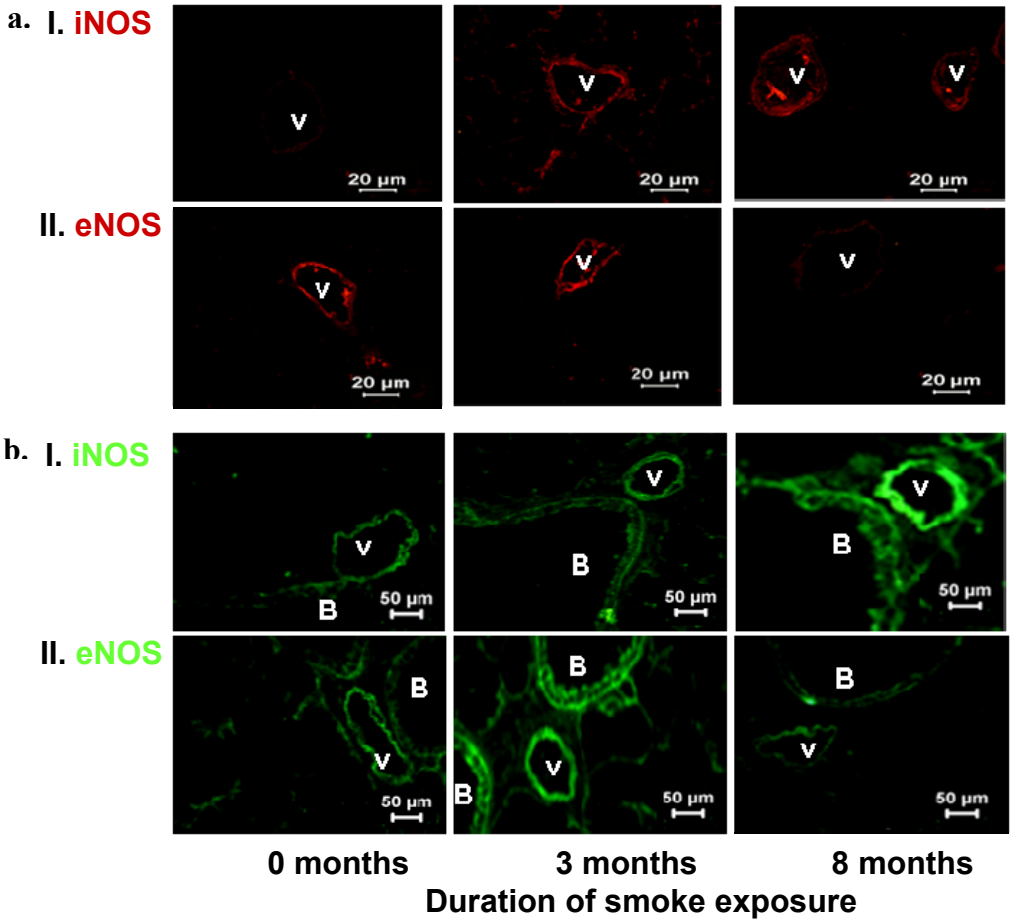

Figure 9. Localization of the inducible nitric oxide synthase (iNOS) and endothelial nitric oxide synthase (eNOS) in wild-type (WT) mouse lungs.

(a) immunostaining (I, II, red) and (b) non-isotopic in situ hybridization (I, II, green) for iNOS and eNOS in WT mouse lung sections. Data are given for 3 and 8 months of smoke exposure as well as for unexposed controls. V = vessel, B = bronchus. **(In situ hybridization kindly provided by Michael Seimetz)**

In contrast to iNOS, immunofluorescence staining suggested a downregulation of eNOS in the pulmonary vasculature, again backed up by *in situ* hybridization, with some transient upregulation within the first 3 months of smoke exposure (**Fig. 9a, b**). Non-vascular areas that were positive for iNOS and eNOS may represent bronchial smooth muscle cells and alveolar cells.

5.4.2 Expression of iNOS and eNOS on mRNA and protein level

Further these results were confirmed by quantitative PCR analysis of microdissected pulmonary vessels (50–100 µm) and by Western blotting from homogenized lung tissue showing the upregulation of iNOS after 3 months of smoke exposure on the mRNA and protein level (**Fig. 10 a, b**). By contrast eNOS was transiently upregulated in mRNA but was downregulated after 8 months of tobacco smoke exposure in protein level (**Fig. 11 a, b**).

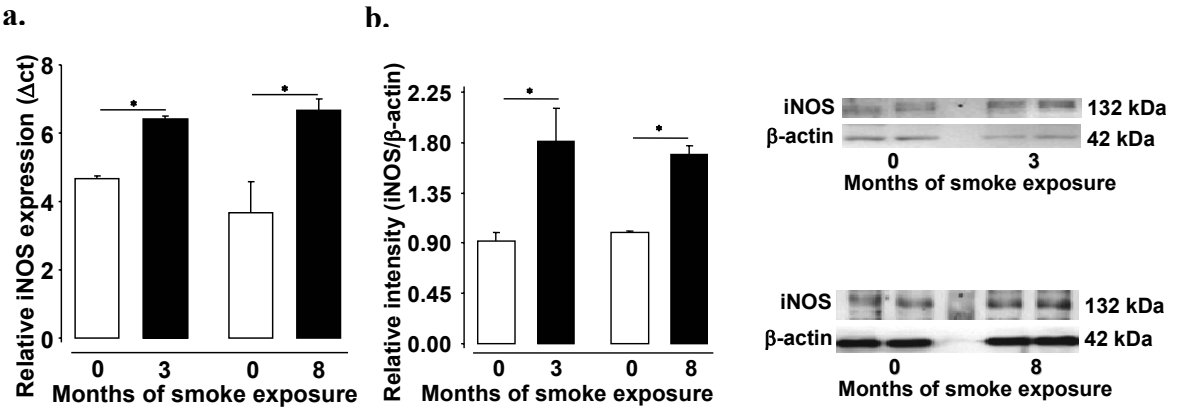

Figure 10. Relative quantification of the inducible nitric oxide synthase (iNOS) in wild-type (WT) mouse lungs.

(**a**) quantitative RT-PCR analysis for iNOS mRNA of laser-microdissected small pulmonary arteries (diameter 50–100 μm). iNOS values were related to porphobilinogen deaminase (PBGD) mRNA levels. Data are from duplicate measurements of n = 20 vessels from n = 3 lungs each. (**b**) Western blot analysis of iNOS from lung homogenate, normalized to β-actin. The full blot is shown on the right and densitometry is given on the left. Values are derived from duplicate measurements of n = 3 individual lungs each. Data are given for 3 and 8 months of smoke exposure as well as for unexposed controls (0 months). *significant difference (P<0.05) compared with respective 0 month of smoke exposure.

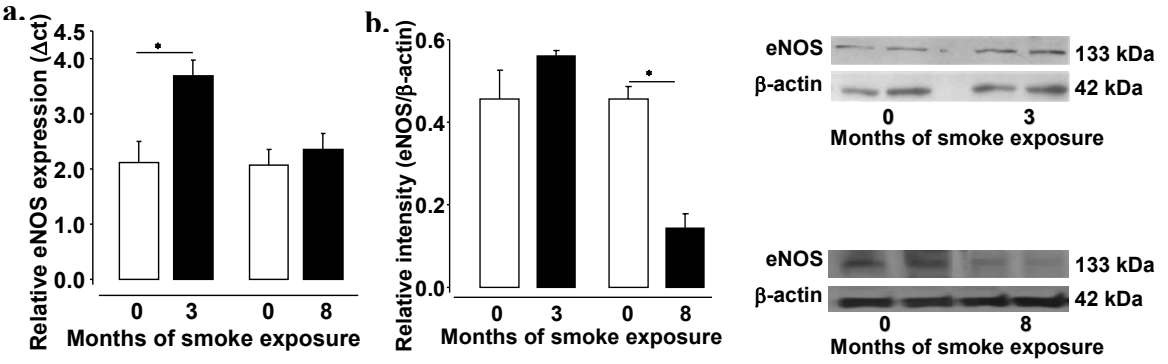

Figure 11. Relative quantification of the endothelial nitric oxide synthase (eNOS) in wild-type (WT) mouse lungs.

(**a**) quantitative RT-PCR analysis for eNOS mRNA of laser-microdissected small pulmonary arteries (diameter 50–100 μm). eNOS values were related to PBGD mRNA levels. Data are from duplicate measurements of n = 20 vessels from n = 3 lungs each. (**b**) Western blot analysis of eNOS from lung homogenate, normalized to β-actin. The full blot is shown on the right and densitometry is given on the left. Values are derived from duplicate measurements of n = 3 individual lungs each. Data are given for 3 and 8 months of smoke exposure as well as for unexposed controls (0 months). *significant difference (P<0.05) compared with respective 0 month of smoke exposure.

5.5 iNOS but not in eNOS deficient mice are completely protected from lung emphysema development upon tobacco smoke exposure

The development of emphysema after 8 months of tobacco smoke exposure in iNOS$^{-/-}$, eNOS$^{-/-}$ and WT mice was compared. The iNOS deficient mice were completely protected against the development of emphysema as evident from quantification of increased mean linear intercept, increased air space, decreased septal wall thickness; where as the eNOS$^{-/-}$ were susceptible to emphysema like smoke exposed WT mice (**Fig. 12a-d**).

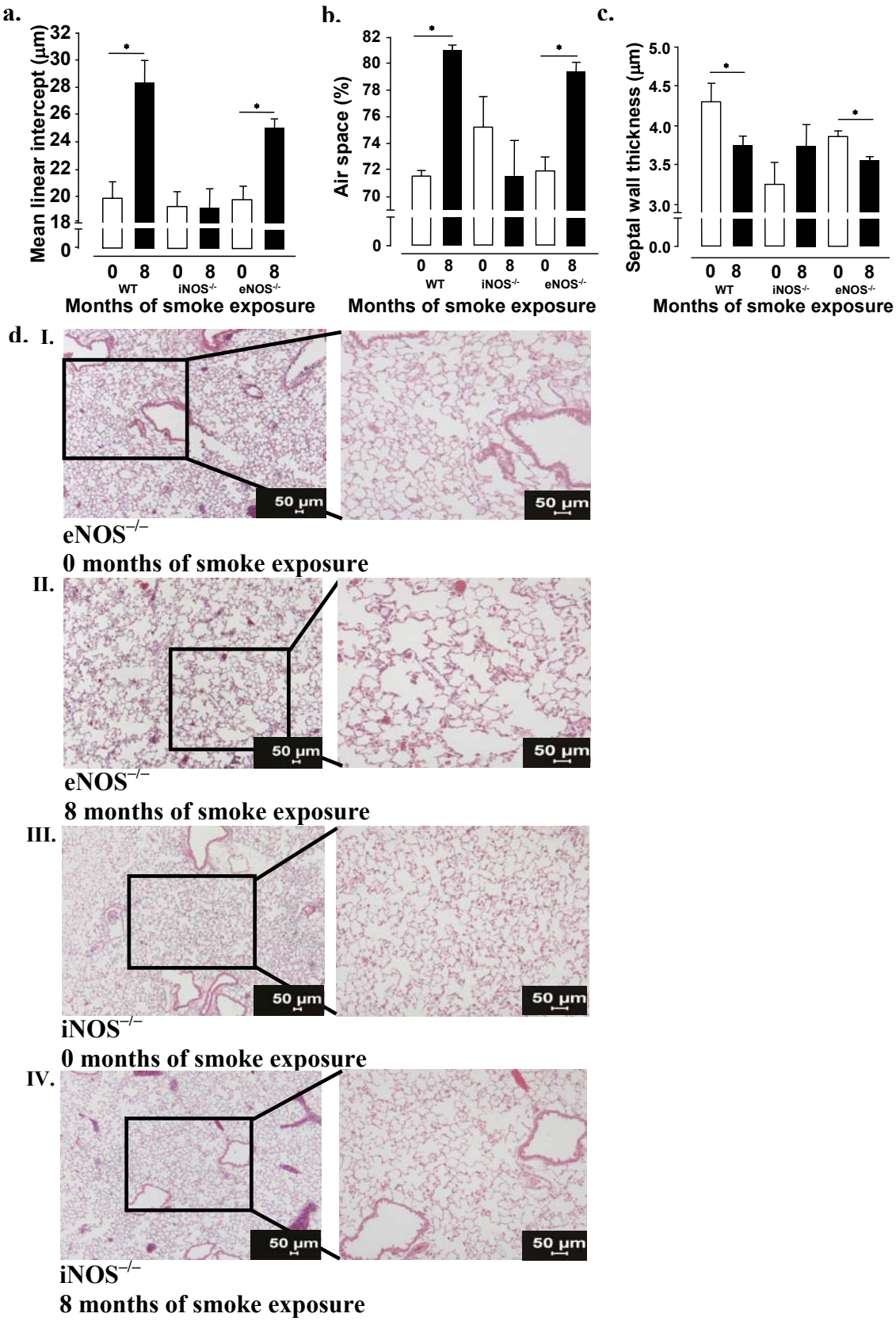

Figure 12. Comparison of the development of emphysema after 8 months of smoke exposure in wild-type (WT) mice and in mice lacking the inducible nitric oxide synthase (iNOS$^{-/-}$) or endothelial nitric oxide synthase (eNOS$^{-/-}$).

(**a**) mean linear intercept, (**b**) air space, (**c**) septal wall thickness quantified from lung sections stained with hematoxylin & eosin (HE). (**d**) representative histology from lung sections stained with HE in eNOS$^{-/-}$ (**I, II**) and iNOS$^{-/-}$ (**III, IV**) mice Data are given for n = 6 lungs each. *significant difference (P<0.05) compared with the respective unexposed control (0 months).

5.6 iNOS but not in eNOS deficient mice are completely protected from lung functional changes upon tobacco smoke exposure

The development of functional alterations in iNOS$^{-/-}$, eNOS$^{-/-}$ and WT mice after 8 months of tobacco smoke exposure were compared. The functional alteration in eNOS-deficient mice were similar to those seen in smoke exposed WT controls as indicated by increased lung compliance, increased tidal volume and decreased airway resistance. However, iNOS$^{-/-}$ mice showed resistant to these functional parameters upon smoke exposure (**Fig. 13 a-c**).

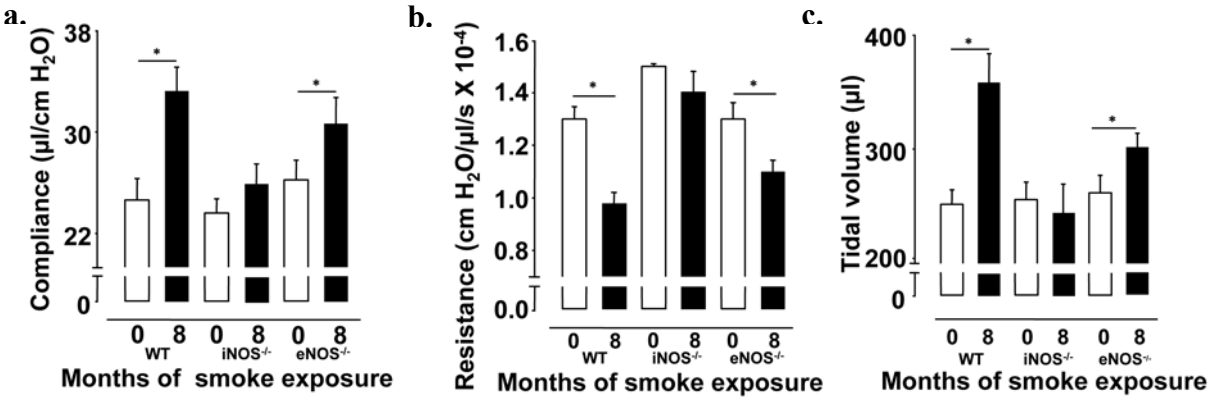

Figure 13. Lung compliance, tidal volume, airway resistance during the course of smoke exposure for 8 months in wild-type (WT) mice and in mice lacking the inducible nitric oxide synthase (iNOS$^{-/-}$) or endothelial nitric oxide synthase (eNOS$^{-/-}$).

Lung functional parameters determined in isolated artificially ventilated and perfused mouse lungs under negative pressure ventilation. (**a**) lung compliance, (**b**) tidal volume, and (**c**) airway resistance compared with unexposed controls (0 months). *significant difference (P<0.05) compared with the unexposed controls.

5.7 iNOS but not in eNOS deficient mice are completely protected from pulmonary hypertension development upon tobacco smoke exposure

The development of pulmonary hypertension after 8 months of tobacco smoke exposure in iNOS$^{-/-}$, eNOS$^{-/-}$ and WT mice was compared.

5.7.1 Hemodynamics, heart ratio and number of alveoli / number of vessels

As similar to the functional parameter, iNOS deficient mice were completely protected against the development of pulmonary hypertension as evident from the right ventricular systolic pressure, right ventricular hypertrophy and the ratio of number of alveoli / number of vessels where as the eNOS$^{-/-}$ mice were susceptible to development of pulmonary hypertension upon smoke exposure (**Fig. 14a, b, Table 6**). In addition, the decrease in systemic aterial pressure seen in WT mice did not occur in the iNOS- deficient mice, but occur in eNOS$^{-/-}$ mice (**Fig. 14c**).

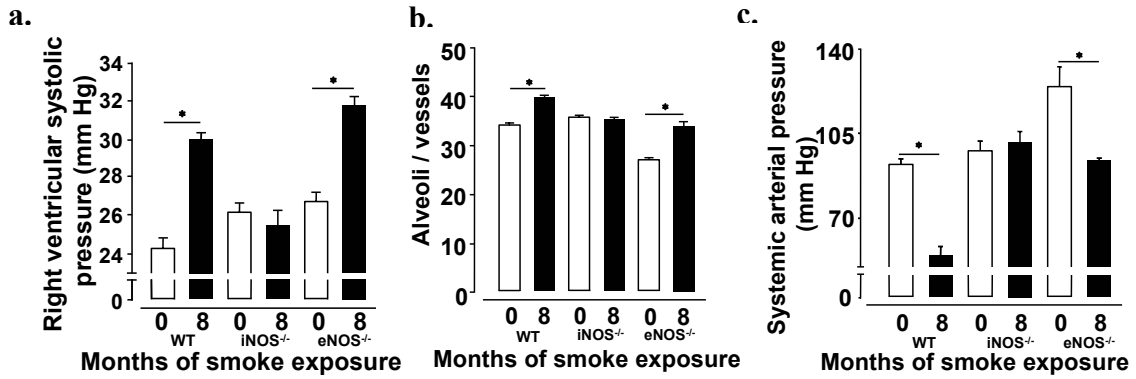

Figure 14. Comparison of development of the pulmonary hypertension after 8 months of smoke exposure in wild-type (WT) mice and in mice lacking the inducible nitric oxide synthase (iNOS$^{-/-}$) or endothelial nitric oxide synthase (eNOS$^{-/-}$).

(**a**) right ventricular systolic pressure quantified by right heart catheterization in anesthetized animals. (**b**) ratio of number of alveoli to the number of vessels per area quantified from lung sections co-stained against α-smooth muscle actin and von Willebrand factor and (**c**) Systemic arterial pressure. Data are given for n = 6 lungs each. *significant difference (P<0.05) compared with the respective unexposed control (0 months).

Table 6 Comparision of the mass of the right ventricle (RV), the left ventricle+septum (LV+S) and the ratio of RV/(LV+S) during 8 months of smoke exposure in wild-type (WT) mice and in mice lacking the inducible nitric oxide synthase (iNOS$^{-/-}$) or endothelial nitric oxide synthase (eNOS$^{-/-}$).

	RV (g) ± SEM		LV+S (g) ± SEM		RV/(LV+S) ± SEM	
Months of smoke exposure	**Non smoke**	**Smoke**	**Non smoke**	**Smoke**	**Non smoke**	**Smoke**
8 months (WT)	0.0062 ±0.0002	0.0080 ±0.0001*	0.0253 ±0.0003	0.0260 ±0.0004	0.2400 ±0.0071	0.3000 ±0.0072*
8 months (eNOS$^{-/-}$)	0.0056 ±0.0001	0.0076 ±0.0004*	0.0238 ±0.0004	0.0238 ±0.0014	0.2400 ±0.0044	0.3200 ±0.0059*
8 months (iNOS$^{-/-}$)	0.0055 ±0.0001	0.0057 ±0.0002	0.0227 ±0.0009	0.0231 ±0.0005	0.2400 ±0.0043	0.2400 ±0.0063

*significant difference (p<0.05) compared with respective months of untreated smoke exposure group.

Further, iNOS deficient mice are completely protected from right heart hypertrophy as evident from the quantification of right ventricle weight, RV/LV+ septum ratio whereas eNOS$^{-/-}$ mice were susceptible to right heart hypertrophy to the same degree as WT mice. The weight of LV+ Septum did not change in iNOS$^{-/-}$ and eNOS$^{-/-}$ mice like WT mice upon smoke exposure (**Table 5**).

5.7.2 Degree of muscullariazation and vascular lumen area

Pulmonary hypertension was accompanied by an increase in the degree of muscularization of lung resistance pulmonary arteries (diameter 20–70 μm) and a reduction in the mean vascular lumen area. This increase was completely absent in iNOS$^{-/-}$ mice but not in eNOS$^{-/-}$ mice upon smoke exposure. In the latter, the increase in the degree of muscularization as well as the reduction of the vascular lumen area was identified to the change observed in WT mice after 8 months of smoke exposure (**Fig. 15a–c**).

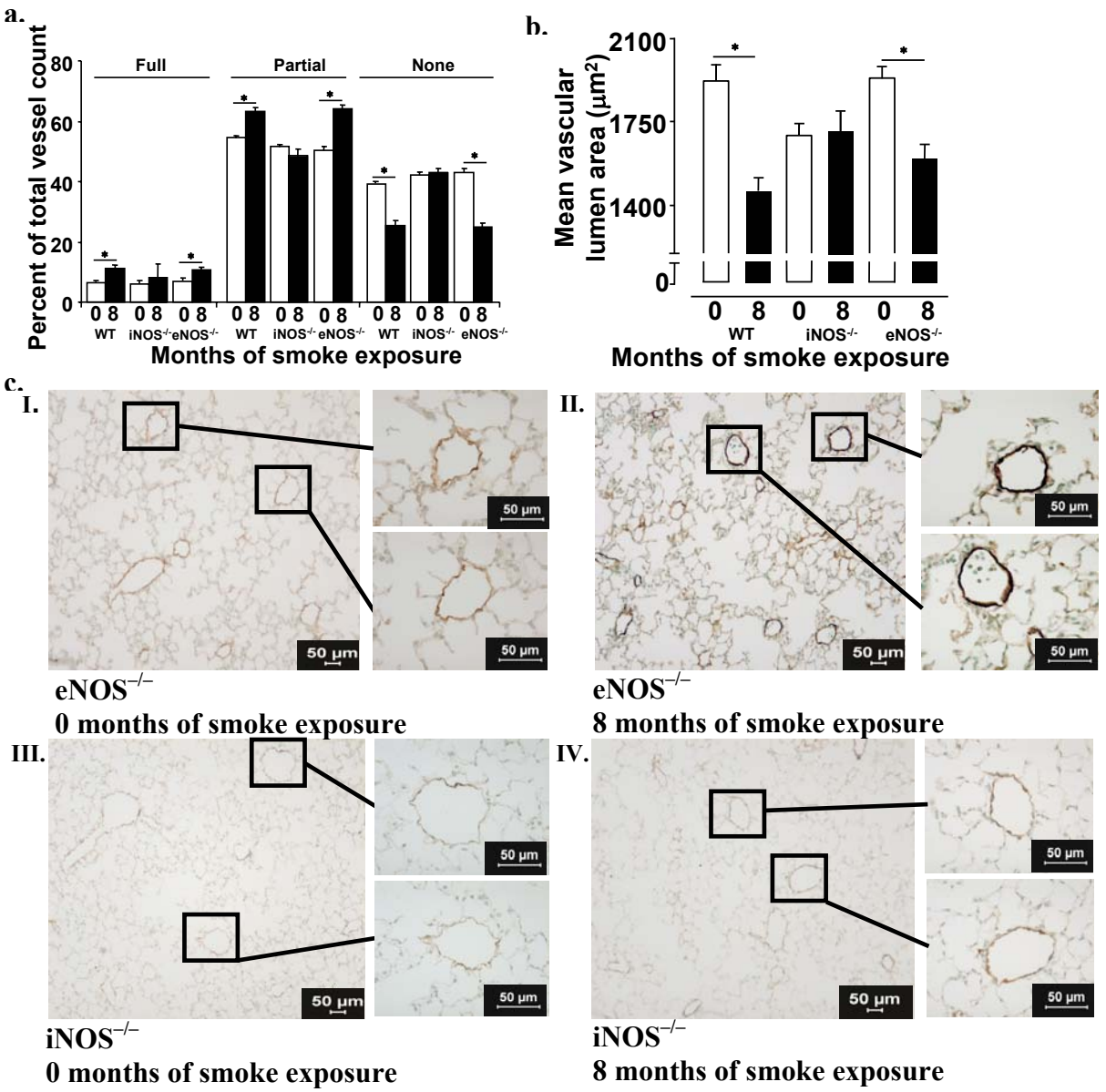

Figure 15. Degree of muscularization and vascular lumen area after 8 months of smoke exposure in wild-type (WT) mice and in mice lacking the inducible nitric oxide synthase (iNOS$^{-/-}$) or the endothelial nitric oxide synthase (eNOS$^{-/-}$).

(**a**) degree of muscularization of small pulmonary arteries (diameter 20–70 μm). Data are given as percentage of total vessel count for fully muscularized (Full), partially muscularized (Partial), and non-muscularized (None) vessels from lung sections costained against α-smooth muscle actin and von Willebrand factor. (**b**) mean vascular lumen area (μm^2) of small pulmonary arterial vessels (diameter 20–70 μm) from elastica van Gieson-stained lung sections. (**c**) representative histology from lung sections from eNOS$^{-/-}$ mice (**I, II**) and iNOS$^{-/-}$ mice (**III, IV**) stained with antibodies against α-smooth muscle actin and von Willebrand factor. Data are given for n = 6 lungs each. *significant difference (P<0.05) compared with the respective unexposed controls (0 months).

A similar increase in the degree of muscularization and narrowing of the vascular lumen as for the small vessels (diameter 20–70 μm) was found in larger pulmonary arteries (diameter 71–150 μm, and >150 μm) in eNOS$^{-/-}$ and WT mice, but not in mice deficient for the iNOS (**Fig. 16 a-d**).

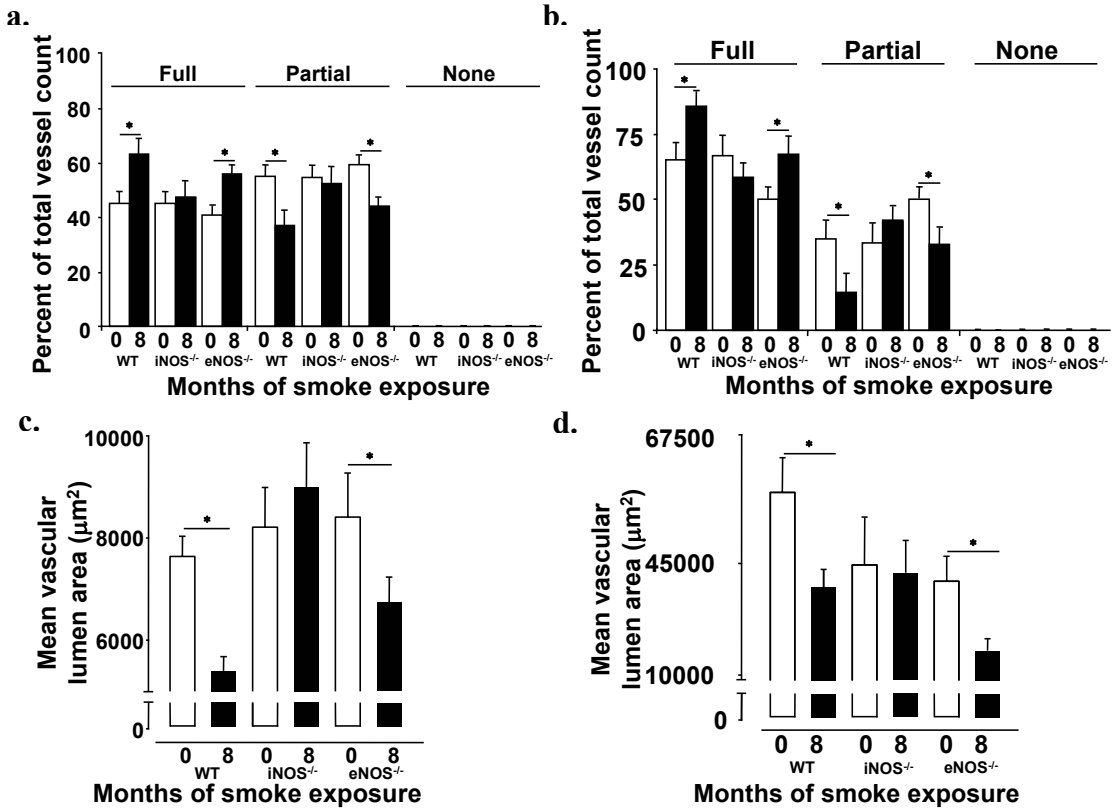

Figure 16. Degree of muscularization and vascular lumen area after 8 months of smoke exposure in wild-type (WT) mice and in mice lacking the inducible nitric oxide synthase (iNOS$^{-/-}$) or the endothelial nitric oxide synthase (eNOS$^{-/-}$).

(a) degree of muscularization of pulmonary arterial vessels (diameter 70–150 µm). (b) degree of muscularization of pulmonary arterial vessels (diameter >150 µm). (c) mean vascular lumen area (µm2) of pulmonary arterial vessels (diameter 70–150 µm). (d) mean vascular lumen area (µm2) of pulmonary arterial vessels (diameter >150 µm). *significant difference ($P<0.05$) compared with the unexposed controls.

5.7.3 Vasoreactivity measurement

Further investigations using isolated, perfused and ventilated lungs revealed pulmonary vascular dysfunction in WT mice after 8 months of exposure to tobacco smoke, represented by an increased vasoreactivity to hypoxic ventilation and phenylephrine application, as well as reduced vasorelaxation to acetylcholine and inhaled NO. These alterations were completely prevented in the smoke-exposed iNOS$^{-/-}$ mice (**Fig. 17 a, b)**.

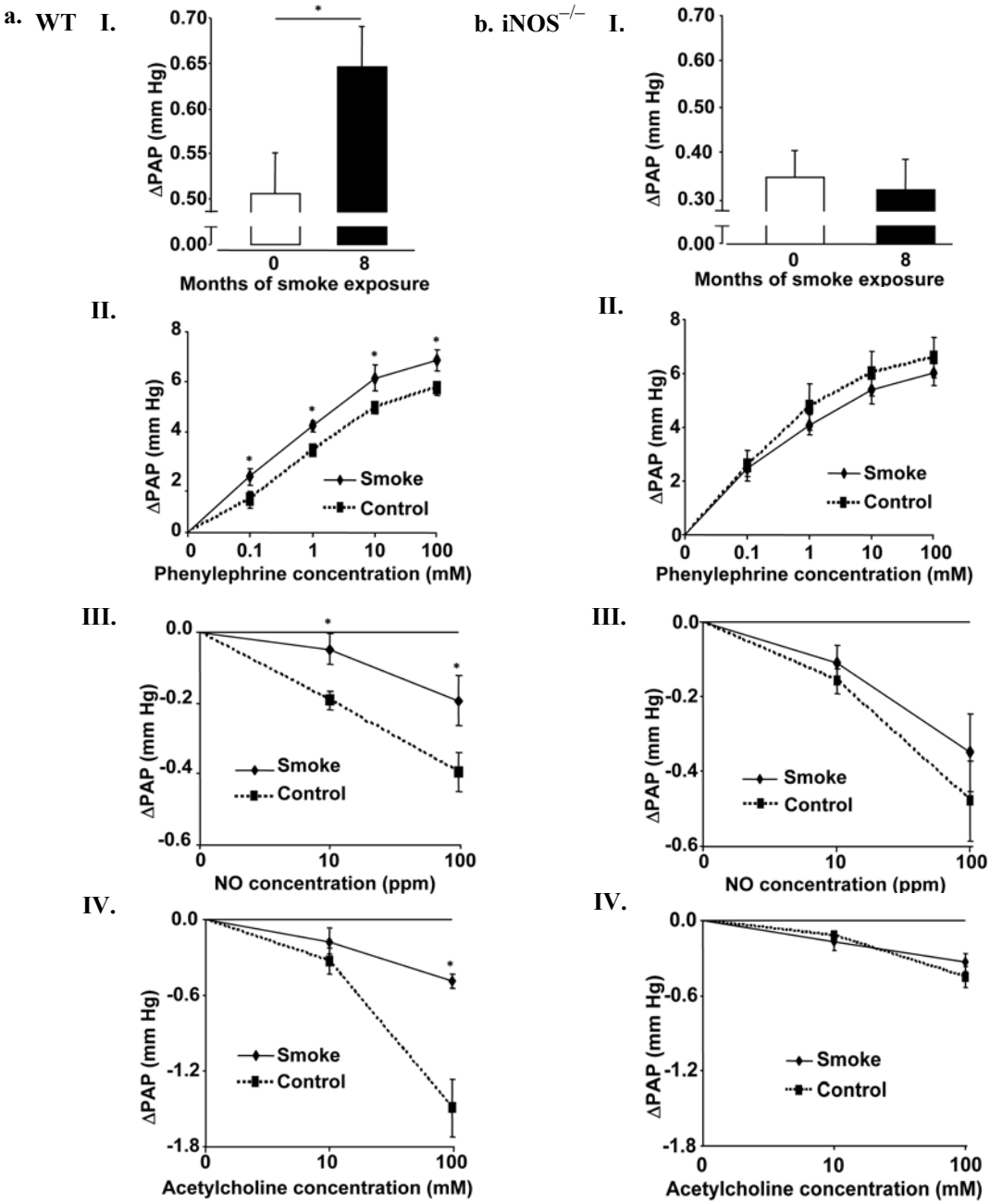

Figure 17. Vasoreactivity to acute alveolar hypoxia, phenylephrine, acetylcholine and inhaled NO in WT and iNOS$^{-/-}$ mice after 8 months of smoke exposure compared with unexposed controls.

Data were derived from isolated perfused and ventilated lung experiments. (**a**) WT mice. (**b**) iNOS$^{-/-}$ mice. (**I**) strength of hypoxic pulmonary vasoconstriction induced by the reduction of O_2 concentration in the inspired gas from 21 to 1%. (**II**) vasoconstrictor response to increasing doses of phenylephrine. (**III**) Vasodilation in response to increasing doses of acetylcholine. (**IV**) Vasodilation in response to increasing doses of inhaled nitric oxide. Data are derived from n = 5–6 animals per group. *significant difference (P<0.05) compared with the respective unexposed control. Error bars are not shown when falling into symbol.

5.8 Treatment of WT mice with the iNOS inhibitor L-NIL protected against the development of emphysema upon tobacco smoke exposure

Treatment of WT mice with the iNOS-specific inhibitor L-NIL by oral application in the drinking water (600µg/ml) resulted in a complete protection against the development of lung emphysema as evident from alveolar morphometry which showed decrease mean linear intercept, decrease air space and increase septal wall thickness after 8 months of tobacco smoke exposure as seen in WT mice but not in L-NIL treated mice (**Fig. 18a–d**).

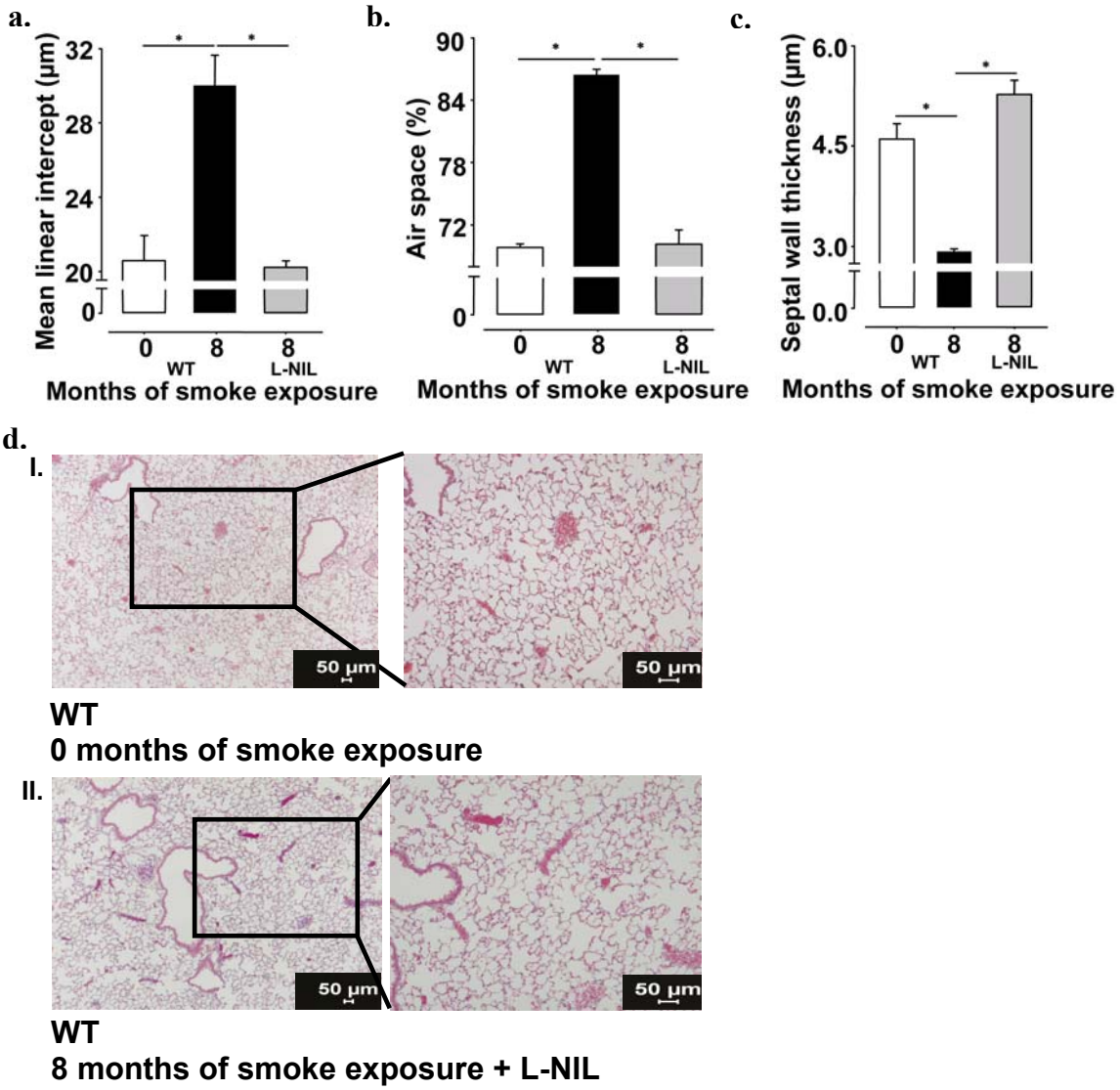

Figure 18. Comparison of the development of emphysema after 8 months of smoke exposure in L-NIL-treated wild-type (WT) mice

Alveolar morphometry given as (**a**) mean linear intercept, (**b**) air space, (**c**) septal wall thickness quantified from lung sections stained with hematoxylin & eosin (HE). (**d**) representative histology from lung sections stained using HE (**I, II**) comparing L-NIL-treated mice with untreated mice following 8 months of smoke exposure. Data are for n = 6 lungs each. *significant difference compared with untreated mice after 8 months of smoke exposure.

5.9 Treatment of WT mice with the iNOS inhibitor L-NIL protected against the development of lung functional changes upon tobacco smoke exposure

Above structural findings were mirrored by determination of lung functional parameters. These investigations showed decreased lung compliance, decreased tidal volume and increased airway resistance in L–NIL treated mice compared to WT mice after 8 months of tobacco smoke exposure as seen in WT mice (**Fig. 19 a-c**). The values for the L–NIL treated mice were in same range as those observed in non-exposed control mice.

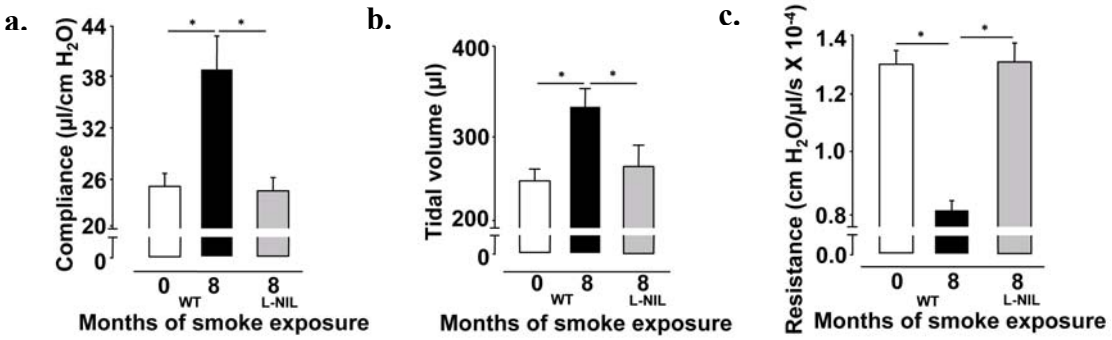

Figure 19. Lung compliance, tidal volume, airway resistance and systemic arterial pressure during the course of smoke exposure for 8 months comparing L-NIL-treated with untreated mice.

Lung functional parameters determined in isolated artificially ventilated and perfused mouse lungs under negative pressure ventilation. (a) lung compliance (b) tidal volume and (c) airway resistance. *significant difference ($P<0.05$) compared with 8 months of smoke exposure.

5.10 Treatment of WT mice with the iNOS inhibitor L-NIL protected against the development of pulmonary hypertension upon tobacco smoke exposure

5.10.1 Hemodynamics, heart ratio and number of alveoli / number of vessels

The treatment of WT mice with the iNOS-specific inhibitor L-NIL furthmore resulted in complete protection from the development of pulmonary hypertension, as evident from decrease right ventricular systolic pressure and decrease number of alveoli: number of vessels compared to non-treated smoke exposed mice. In addition, the decrease in systemic aterial pressure seen in WT mice was not seen after the treatment with the iNOS-specific inhibitor L-NIL L-NIL treatment resulted in a complete prevention of the change induced by tobacco smoke in WT mice, as L-NIL treated mice showed similar values after smoke exposure as unexposed control mice (**Fig. 20 a–c).**

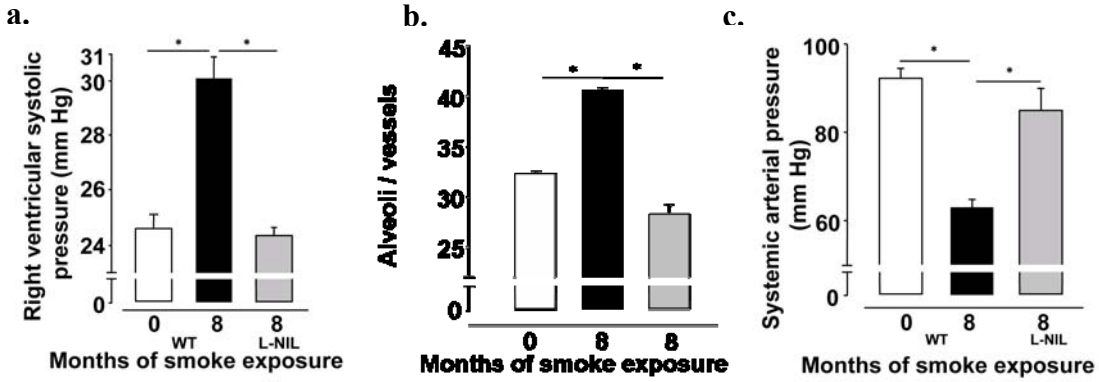

Figure 20. Comparison of development of the pulmonary hypertension during the course of smoke exposure for 8 months comparing L-NIL-treated with untreated mice.

(a) right ventricular systolic pressure (b) ratio of number of alveoli to the number of vessels and (c) Systemic arterial pressure compared Data are given for n = 6 lungs each. *significant difference (P<0.05) compared with the respective exposed control (8 months).

Furthermore, the L-NIL treated mice were completely protected from right heart hypertrophy as evident from the quantification of right ventricle weight and the RV/LV+Septum ratio after 8 months of tobacco smoke exposure. The weight of LV+Septum did not change in both treated and untreated mice (**Table 7**).

Table 7 Comparision of the mass of the right ventricle (RV), the left ventricle + septum (LV+ S) and the ratio of RV/(LV+S) during the course of smoke exposure for 8 months comparing L-NIL treated with untreated mice with untreated mice.

Group	(RV) (g) ± SEM		LV+ S (g) ± SEM		RV / (LV+S) ± SEM	
Months of smoke exposure	Non smoke	Smoke	Non smoke	Smoke	Non smoke	Smoke
8 months (WT)	0.0052 ±0.0001	0.0067 ±0.0002*	0.02100 ±0.0003	0.0216 ±0.0009	0.2500 ±0.0075	0.3100 ±0.0032*
8 months (L-NIL treated)		0.0059 ±0.0002*		0.0242 ±0.0010		0.2400 ±0.0048*

*significant difference (*P*<0.05) compared with smoke exposed controls.

5.10.2 Degree of muscullariazation and vascular lumen area

The treatment of WT mice with the iNOS-specific inhibitor L-NIL also protected from the increased degree of muscularization of small pulmonary arteries (20–70 μm) after 8 months of smoke exposure (**Fig 21 a-c**).

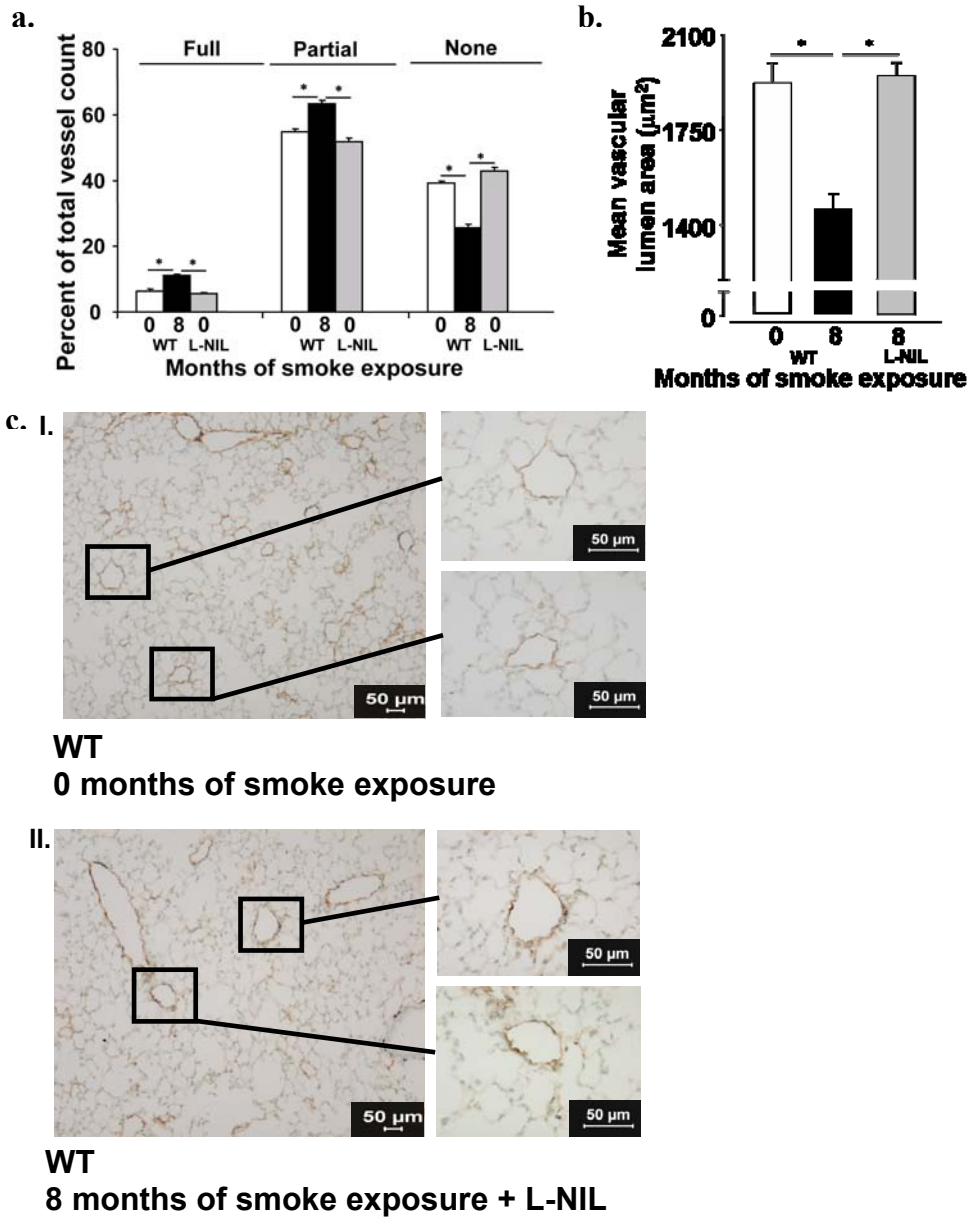

Figure 21. Degree of muscularization and vascular lumen area of pulmonary vessels during the course of smoke exposure for 8 months comparing L-NIL-treated with untreated mice.

(**a**) degree of muscularization of small pulmonary arteries (diameter 20–70 µm) as percent of total vessel count for fully muscularized (Full), partially muscularized (Partial), and non-muscularized (None) vessels. (**b**) mean vascular lumen area (μm^2) of small pulmonary arterial vessels (diameter 20–70 µm). (**c**) representative histology from lung sections stained using antibodies against α-smooth muscle actin and von Willebrand factor (I, II), comparing L-NIL-treated mice with untreated mice after 8 months of smoke exposure. Data are from n = 6 lungs each. *significant difference compared with untreated mice after 8 months of smoke exposure.

In addition, the treatment with L-NIL also protected from an increase in the degree of muscularization and a narrowing of vascular lumen in the categories of a vessel diameter of 70–150 µm and >150 µm **(Fig. 22 a-d).**

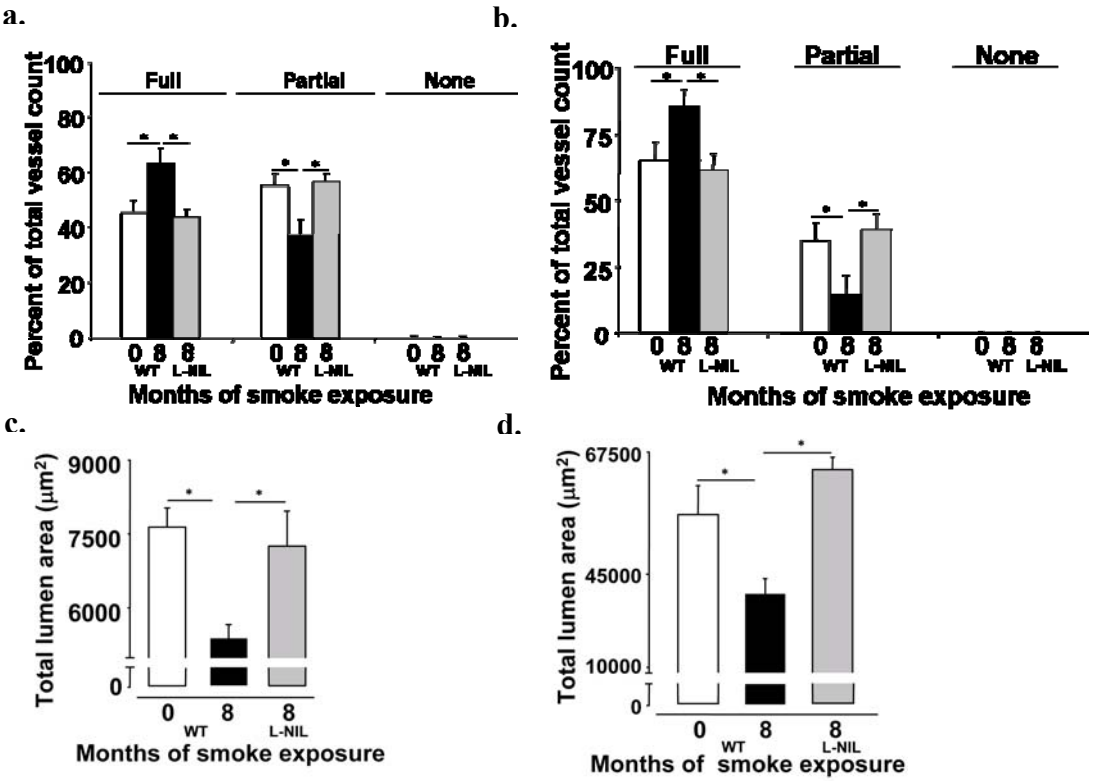

Figure 22. Degree of muscularization and vascular lumen area of pulmonary vessels during the course of smoke exposure for 8 months comparing L-NIL-treated with untreated mice.

(a) degree of muscularization of pulmonary arterial vessels (diameter 70–150 μm). (b) degree of muscularization of pulmonary arterial vessels (diameter >150 μm). (c) mean vascular lumen area (μm^2) of pulmonary arterial vessels (diameter 70–150 μm). (d) mean vascular lumen area (μm^2) of pulmonary arterial (vessels diameter >150 μm). Data are for n = 6 lungs each. *significant difference ($P<0.05$) compared with the 8months exposed mice.

5.11 Comparison of the degree of emphysema between human COPD and in the mouse model of tobacco smoke induced emphysema

When comparing lung tissue from healthy human donors to that from GOLD stage IV patients with a history of smoking (**Table 4**), increased mean linear intercept and air space as well as a decrease septal wall thickness was found. These changes were similar to those found when compared to non-smoke exposed WT mice exposed to 8 months of tobacco smoke (**Fig. 23 a-d**).

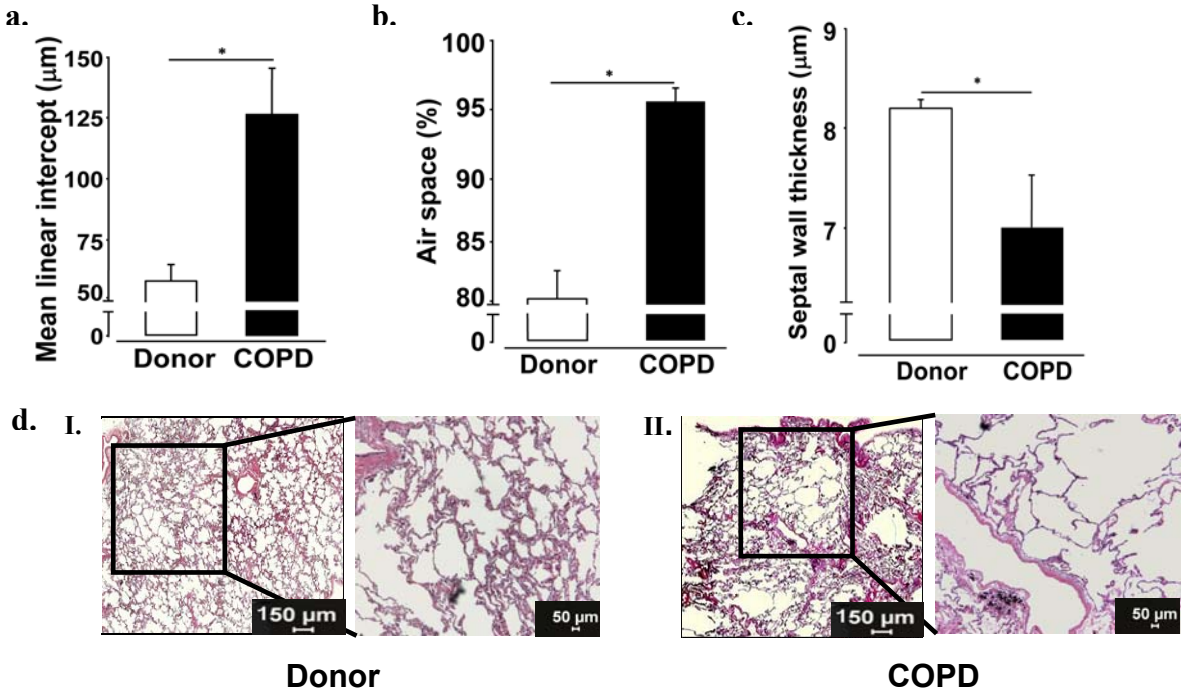

Figure 23. Alterations in the alveolar structure in lungs from human patients with severe chronic obstructive pulmonary disease (COPD) and healthy donors.

Alveolar morphometry given as (**a**) mean linear intercept, (**b**) air space, (**c**) septal wall thickness quantified from lung sections stained with hematoxylin & eosin (HE), (**d**) Representative histology from lung sections stained with HE (**I, II**).

5.12 Comparison of vascular alteration in human COPD with the mouse model of tobacco smoke induced COPD

As in smoke-exposed mice, an increase in the ratio of the number of alveoli to the number

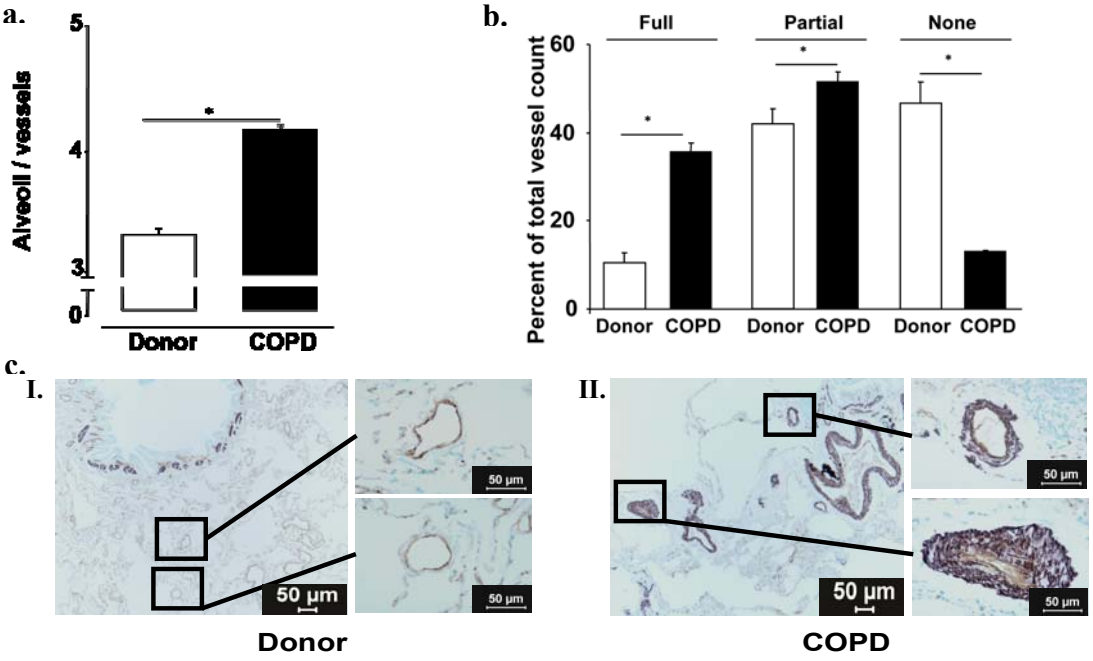

Figure 24. Alterations in vascular structure in lungs from human patients with severe chronic obstructive pulmonary disease (COPD) and healthy donors.

(**a**) degree of muscularization of small pulmonary arteries (diameter 20–70 µm). (**b**) ratio of number of alveoli to number of vessels per area quantified from lung sections stained against α-smooth muscle actin and von Willebrand factor. (**c**) representative histology from lung sections stained with antibodies against α-smooth muscle actin and von Willebrand factor (**I, II**).

vessels and the degree of muscularization were found in the human lung from COPD patients with a smoke history (**Fig. 24 a-c**).

Similarly, the degree of muscularization in larger pulmonary arterial vessel (diameter 70-150 μm and >150 μm) was increased in lung from human COPD patients compared to donor (**Fig. 25a, b**).

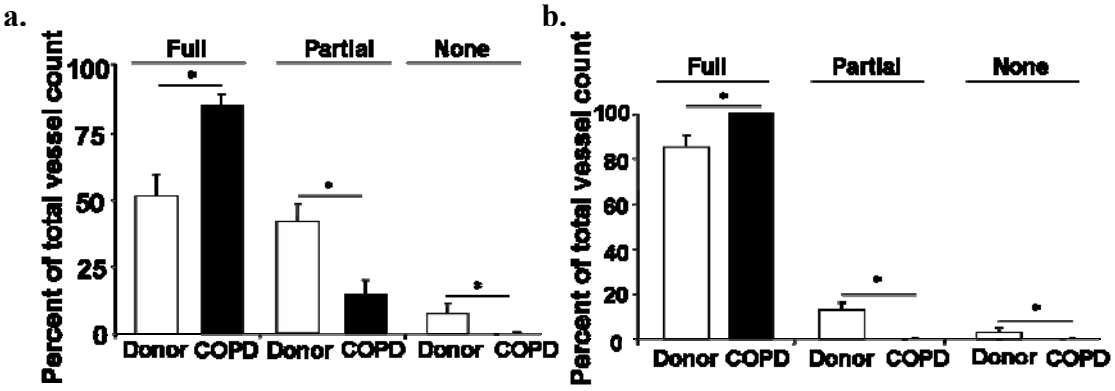

Figure 25. Degree of muscularization of pulmonary arterial vessels (diameters 71–150 μm, >150 μm) in lungs from human patients with COPD compared to healthy donor control lungs.

Degree of muscularization in pulmonary arterial vessels (**a**) diameter 71–150 μm (**b**) diameter >150 μm from lungs of human patients with COPD compared with healthy donor controls. *significant difference (P<0.05) compared with healthy donor controls.

5.13 Comparison of iNOS and eNOS protein localization in lung sections from human COPD and from the mouse model of tobacco smoke induced COPD

As in smoke exposed WT and non-exposed control mice, localization and expression of iNOS and eNOS showed similar pattern like upregulation of iNOS and downregulation of eNOS in pulmonary vasculature in the COPD and donor controls human lungs (**Fig. 26 I, II**).

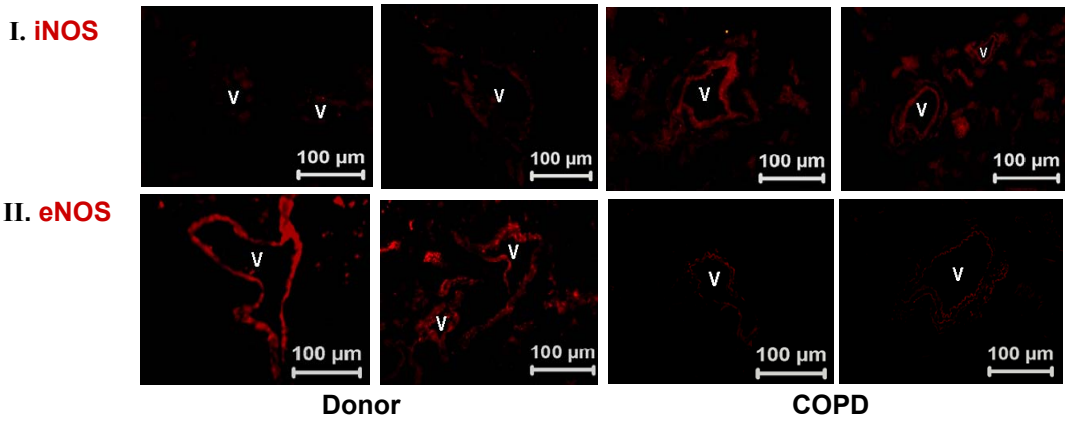

Figure 26. Localization of inducible nitric oxide synthase (iNOS) and endothelial nitric oxide synthase (eNOS) in lungs from human patients with severe chronic obstructive pulmonary disease (COPD) and from healthy donors.

iNOS (**I**) and eNOS (**II**) immunostaining in GOLD stage IV COPD lungs and in healthy donor controls.

The iNOS and eNOS localization were seen specific to pulmonary vasculature however they are also expressed in alveolar compartment like alveolar epithelium, smoth muscle cell, bronchi. In human COPD lungs when compare to healthy donor controls, a similar regulation was seen in WT smoke exposed mice after 8 months compare to non–smoke exposed controls.

5.14 Comparison of iNOS and eNOS mRNA and protein expression in the pulmonary vasculature of lung from human COPD and lung from in the mouse model after tobacco exposure

Immunostaining for iNOS and eNOS was mirrored by a upregulation of iNOS on the mRNA and protein level and a downregulation of eNOS on the protein level as seen in WT smoke exposed mouse (**Fig. 27a, b**). In human COPD lungs when compare to healthy donor controls, a similar regulation was seen in WT smoke exposed mice after 8 months compare to non–smoke exposed controls.

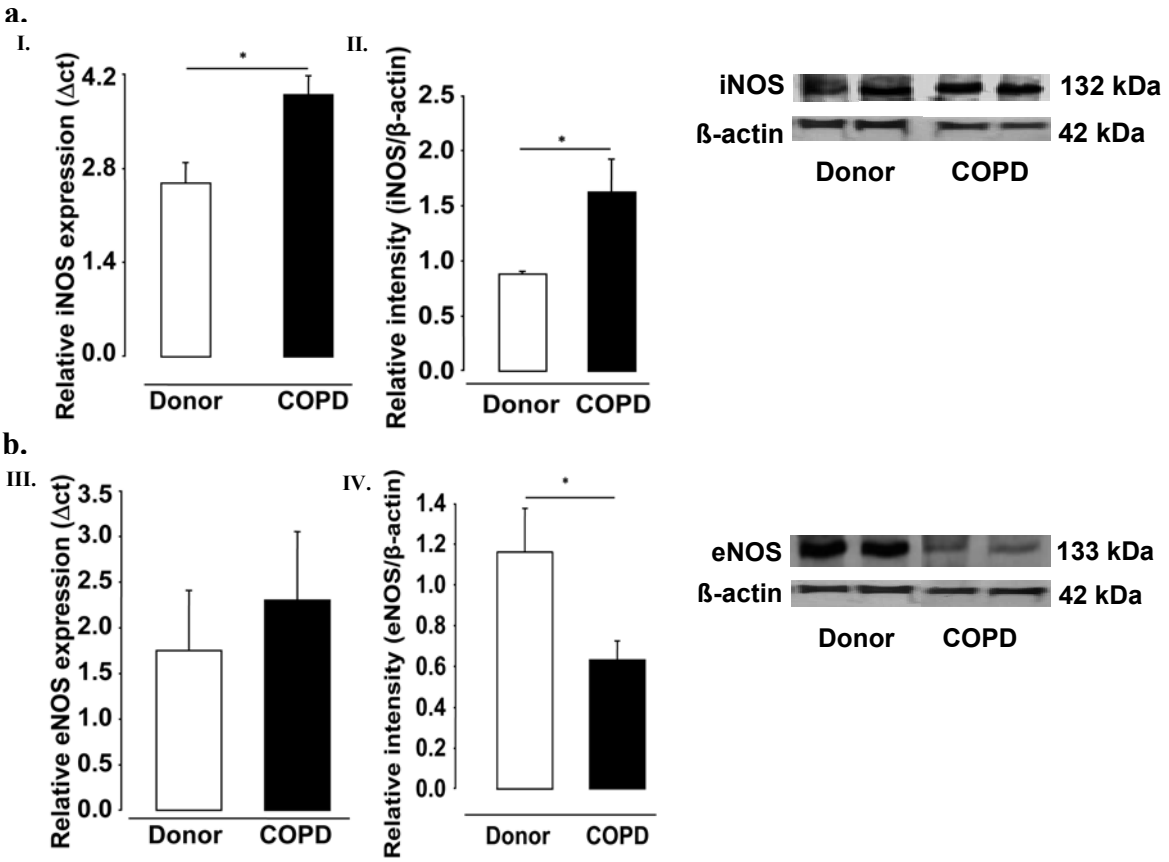

Figure 27. Alterations in inducible nitric oxide synthase (iNOS) and endothelial nitric oxide synthase (eNOS) in lungs from human patients with severe chronic obstructive pulmonary disease (COPD) and healthy donors.

Expression of (**a**) iNOS mRNA (**I**), iNOS protein (**II**), (**b**) eNOS mRNA (**III**), eNOS Protein (**IV**) in GOLD stage IV COPD lungs and healthy donor controls. mRNA data are derived from microdissected vessels (diameter 50–100 μm); protein data are derived from homogenized lung tissue. mRNA data were normalized to porphobilinogen deaminase, and protein data were normalized to α-actin. Representative blots are given on the right and densitometry is given on the left. Data are derived from n = 5 lungs each. ∗significant difference (P<0.05) compared with healthy donor controls.

5.15 Comparison of the localization and expression of nitrotyrosine in lungs tissue from human COPD and in lungs from the mouse model of tobacco smoke induced COPD

5.15.1 Lung tissue of human end stage COPD

Western blotting and immunohistochemical staining revealed increased level of nitrotyrosine in the pulmonary vasculature and alveolar septae from human COPD lungs compared with lung from healthy donor controls (**Fig. 28 a, b**).

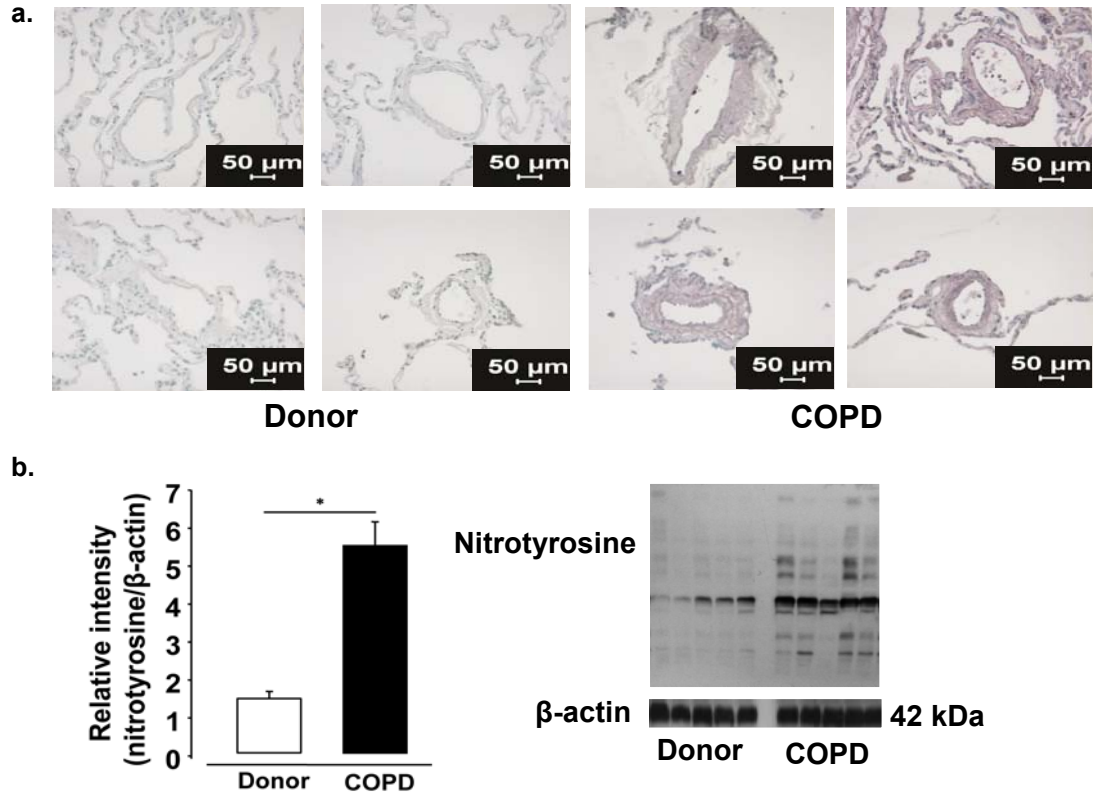

Figure 28. Nitrotyrosine expression in lungs from patients with severe chronic obstructive pulmonary disorder (COPD) and healthy human donors.

(**a**) localization of nitrotyrosine in lung tissue from human GOLD stage IV COPD patients and healthy donor control lungs. The reddish color is the anti-nitrotyrosine staining. In the negative control, the primary antibody was omitted. (**b**) Western blot analysis of nitrotyrosine from homogenized lung tissue from GOLD stage IV COPD lungs and healthy donor controls. Data were normalized to α-actin and are given for n = 5 lungs each. Densitometric data are given on the left and the original blot is given on the right. ∗significant difference (P<0.05) compared with healthy donor controls.

5.15.2 Nitrotyrosine localization and expression in mouse lungs after tobacco smoke exposure

The nitrotyrosine findings in lungs from human COPD patients were compared to investigations of mice lung exposed for 8 months to tobacco smoke. These WT mice had increased nitrotyrosine levels in the pulmonary vasculature and alveolar septae (**Fig. 29 a, b**). Further eNOS$^{-/-}$ mice did show a similar upregulation in nitrotyrosine after smoke exposure. In contrast, iNOS$^{-/-}$ mice did not show upregulation of nitrotyrosine. The L-NIL treated WT

mice did not also show any change in nitrotyrosine regulation with regards to both localization and expression (**Fig. 29 a, b**).

a.

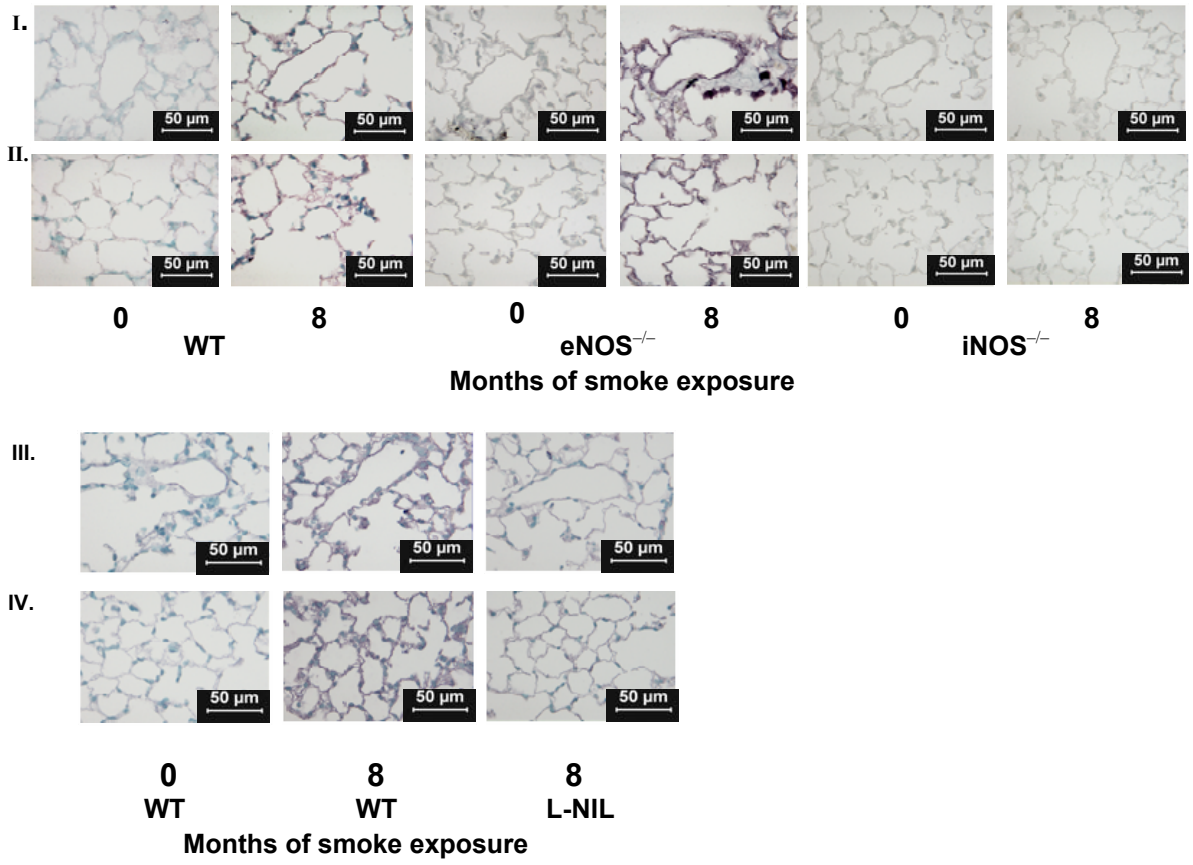

b.

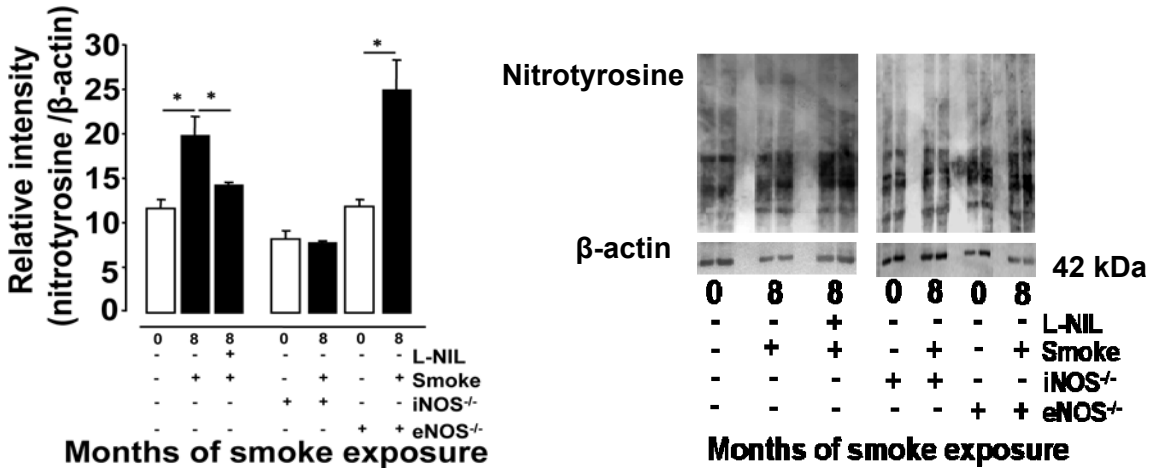

Figure 29. Nitrotyrosine expression in lungs from wild-type mice, inducible nitric oxide synthase-deficient (iNOS$^{-/-}$), endothelial nitric oxide synthase-deficient (eNOS$^{-/-}$), and L-NIL-treated WT mice.
(**a**) nitrotyrosine staining in untreated WT and L-NIL-treated WT mice. Representative vessels (**I, III**) and alveolar structures (**II, IV**) are depicted. Data are given for mice with 8 months of smoke exposure and unexposed controls. (**b**) Western blot analysis of nitrotyrosine from homogenized lungs in WT, iNOS$^{-/-}$, eNOS$^{-/-}$, and L-NIL-treated WT mice. Data were normalized to α-actin and are given for n = 5 lungs each. *significant difference (P<0.05) compared with the respective exposed/ unexposed controls (0 and 8 months of exposure).

6. DISCUSSION

It has been known that pulmonary hypertension can be a complication of chronic obstructive pulmonary disease. However, the prevalence of pulmonary hypertension is not known, because of a lack of systematic screening using right heart catheterization in large numbers of COPD patients. Earlier COPD research was also less prioritized to study alterations to the pulmonary vascular bed. All prior studies were dealing only with the alveolar compartment and thereby revealing less evidence about the association of pulmonary hypertension with COPD human patients as well as in animal models[51, 52]. However, it has been shown that the progression of pulmonary hypertension in COPD over time and its severity correlate with the degree of airflow obstruction as well as with the impairment of pulmonary gas exchange[100, 110, 111]. Recent reports have also suggested that pulmonary hypertension may precede lung emphysema development in COPD[2, 110, 111].

It has now been demonstrated in the present study that cigarette smoke induced alterations in lung vascular structure and function precede airway remodeling and the development of emphysema formation. Furthermore, the present study provided evidence that iNOS is a key molecular player in the development of COPD. Inhibition or deletion of iNOS resulted in full prevention of both pulmonary hypertension and emphysema induced by tobacco smoke in mice. Finally, similar changes regarding iNOS and eNOS expression, nitrotyrosine formation, alveolar/vascular morphology as found in the chronic mouse model were also detected in explanted lungs from COPD patients that underwent transplantation compared to healthy human donor lungs.

6.1 Structural and functional alteration in mouse lungs after tobacco smoke exposure

The structural and functional alterations occurring after chronic tobacco smoke exposure in the alveolar compartment has been well characterized in mouse models. The approach used in this thesis to induce lung emphysema has also been utilized previously as chronic tobacco smoke exposure which is regarded as the major cause of the disease[19, 20, 120]. Another important trigger for COPD is air pollution which explains a stead increase in the incidence of COPD worldwide, although the incident of cigarette smoking has decreased[121, 122]. Long-term exposure of mice to cigarette smoke in this current model enables a through analysis of the sequential changes to

structure and function in both the pulmonary vasculature as well as in the airway and alveolar levels. Changes in the alveolar structure to determine the degree of emphysema formation have been quantified by means of an increase in the mean linear intercept and air space as well as a decrease in the septal wall thickness[123-125].

It has been shown that the development of lung emphysema, the end stage of lung destruction, of this currently used model is well inline with previous reports investigating mice after tobacco smoke exposure[123, 126]. The investigations of this thesis have demonstrated the increased alveoli/vessel ratio, which were evident earlier (after third month of smoke exposure) and can be compared to the acute effect of tobacco smoke exposure in the mouse lung from other studies. This acute effect might be caused by a significant decrease in total antioxidant capacity with changes in oxidized glutathione, ascorbic acid, protein thiols and prostaglandin (PGF-2α) in bronchoalveolar lavage fluid. Moreover, the reduction in antitrypsin activity and an increase in metalloelastase activity of neutrophil and macrophage (MME/MMP-12) as well the increase levels of desmosine (marker of elastin breakdown) and hydroxyproline (a marker of collagen breakdown) in BALF may cause further breakdown of connective tissue in early stage of exposure[127, 128]. Thereafter, the later stage of emphysema in the mouse model might be caused by the increased activity of these proteases (serine elastases and MMPs) and the influx of inflammatory cells with their mediators to increase oxidative/nitrosative stress that ultimately leads the degradation of the lung matrix[120, 129]. It is known that the occurrence of this inflammatory cascade is initiated after the activation of macrophages and the epithelial cells by tobacco smoke that release chemokines and cytokines to recruit different monocytes, neutrophils and T and B-lymphocytes cells in the pulmonary circulation as well as into the alveolar compartment. These chemotactic mediators, proteases, and oxidants induce structural changes by degrading connective tissue. This chronic continuous insult of tobacco smoke may lead further destruction of lung parenchyma as well the loss of number of alveoli/vessel and thinning of septal wall to produce lung emphysema[52].

Structural changes in the lung parenchyma were also accompanied by alterations in lung functional parameters such as increased lung compliance, increased tidal volume and decreased airway resistance. It has been shown that the loss of elastic recoil or tissue elasticity arises from the destruction of elastic fiber network with degradation of extracellular matrix in lung

parenchyma so that the lung cannot deflate back to its original position in expiration after being stretched by inspiration[23, 24]. Thus, the degradation of matrix elements and the loss of alveolar surface reduce lung elastic recoil which is typical for emphysema. Moreover, it has been shown that destroyed alveolar walls and enlarged alveolar spaces can increase the total lung capacity[22], which explain the increase in the tidal volume found in the experiments of this thesis in the mouse model after smoke exposure. Interestingly, the mouse model was characterized by decreased airway resistance[120] upon smoke exposure, whereas COPD patients have an increased airway resistance. This discrepancy, however, can be explained by the differences in the airway anatomy in combination with a less pronounced end-expiratory closure of terminal airways, as shown previously[23, 24].

6.2 Development of pulmonary hypertension precedes emphysema development in wild-type mice exposed to tobacco smoke

The exact temporal relation of possible vascular structural and functional alterations to alveolar destruction in tobacco smoke induced emphysema has not been investigated yet in detail. In this regard, the current investigation found that the chronic tobacco smoke inhalation caused an inward vascular remodeling with an increase in the degree of muscularization, and the development of pulmonary hypertension, quantified by an increase in right ventricular systolic pressure and subsequent development of *cor pulmonale*. Also, evidence of endothelial dysfunction and perturbed vascular reactivity was provided. Most interestingly, vascular remodeling and pulmonary hypertension including a loss of vessels was detected before a significant alveolar structural and functional deterioration in terms of emphysema during tobacco smoke exposure.

Moreover, these data suggest that a degree of pulmonary hypertension is caused by a loss of vascular lumen area not only due to inward vascular remodeling but also due to a loss of vessels by destruction of the lung. However, as the ratio of the number of alveoli to the number of vessels increases again supports the notion that the loss of vessels occurs prior to a loss of the alveolar structure. These findings suggest that vascular structural and functional alterations may be the driving force for emphysema development.

This concept challenges the classical explanation for pulmonary vascular alterations which suggest that alveolar hypoxia, vascular pruning and increased intrathoracic pressures in association with the emphysema drive the pulmonary vascular changes[130, 110]. Instead, they are consistent with a direct impact of cigarette smoke on the pulmonary vasculature[110-112]. The likely reason may be the close proximity of alveolar and vascular structures in the lung that may explain a potential direct effect of inhaled noxious agents on pulmonary resistance vessels[131]. Also, the increased numbers of inflammatory cells in the adventitia of pulmonary muscular arteries produce an inflammatory reaction by activated T lymphocytes, predominantly $CD8^+$ T-cells, leading to impaired endothelium-dependent vascular relaxation and the thickening of the intimal layer. Thereby, increased $CD8^+$ T-cell infiltration of pulmonary arteries of smokers without airflow obstruction supports the hypothesis that an inflammatory mechanism related to tobacco smoking may contribute to the development of the structural and functional alterations to the pulmonary circulation in the early stages of COPD[112]. In addition, increased pulmonary blood flow is associated with the increase in the pulmonary artery pressure due to the loss of vascular distensibility and the inability to recruit unused vasculature[100, 112, 132] as evident with the increased right ventricular systolic pressure by tobacco smoke.

It has been suggested that a variety of vascular growth factors contribute to the evolution of the chronically hypertensive pulmonary vascular bed in COPD. These growth factors may promote endothelial and smooth muscle proliferation and the extension of smooth muscle cells into the smaller, peripheral vessels, which may be a cause for the observed narrowing of the vascular lumen and thus, elevations in pulmonary artery pressure and pulmonary vascular resistance[132]. The subsequent increase in the right ventricular after load than leads to right heart hypertrophy[100,110-112].

Moreover, the muscular pulmonary arteries constrict in response to a variety of stimuli in COPD, including hypoxia; the most potent and frequent stimulus for pulmonary vasoconstriction. This vasoconstriction is unique to pulmonary artery smooth muscle cells and in this regard, it has been shown that the observed changes to the vascular structure were paralleled by alterations in vascular function[100]. The exaggerated responsiveness to alveolar hypoxia and phenylephrine and the loss of vasodilatory capacity to acetylcholine and NO found in present study indicates endothelial and smooth muscle cell dysfunction, and are well inline with previous findings from

studies in human COPD[133, 134, 135, 111, 136, 137]. Moreover, the studies reported in this thesis have shown that the current model is feasible for the analysis of structural and functional changes in the pulmonary vasculature, airways and alveolar structures upon smoke exposure.

6.3 iNOS upregulation and eNOS downregulation in the pulmonary vasculature - a major driving force for the development of emphysema and pulmonary hypertension induced by tobacco smoke exposure

It has previously been shown that cigarette smoke exposure induces rapid changes in gene expression of VEGF, VEGF receptor-1, ET-1, inducible NOS and other mediators that control vascular cell growth and vessel contraction, and thus are candidates which may be involved in the pathogenesis of pulmonary vascular changes of COPD[100, 110, 112, 136]. Earlier studies have also shown that active and passive exposure of both coronary and systemic arteries to tobacco smoke can result in endothelial dysfunction[43, 54, 135, 138]. Moreover, the exposure of pulmonary artery endothelial cells to cigarette smoke caused an irreversible inhibition of eNOS activity by diminishing eNOS protein and mRNA[54, 112, 139]. Such disturbances to vascular function have long since been attributed to the increased oxidative and nitrosative stress via inflammation through nitrotyrosine formation[140]. In this regard, dysregulation of iNOS and nitrotyrosine formation have been proposed as underlying mechanisms of COPD [92, 129, 141-143]. Against this background, the regulation and localization of eNOS, iNOS, and nitrotyrosine was investigated in this own study.

The iNOS was found to be permanently upregulated in the smoke-exposed mouse lung with predominant expression in the pulmonary vasculature. In contrast, the eNOS protein was transiently increased but then downregulated. The iNOS was predominantly expressed in α-smooth muscle actin positive lung cells after eight months of exposure to cigarette smoke, whereas eNOS was not. Against this background, it can be speculated that some uncoupling of eNOS contributes to the oxidative stress in COPD, whereas iNOS is responsible for increased NO generation and this concept is inline with previous findings of uncoupled eNOS and oxidative stress as well as nitrotyrosine formation[140, 141, 143-145]. This interpretation is further supported by our own findings of increased nitrotyrosine levels in WT mice upon smoke exposure.

Along these lines, it has been shown that nitrotyrosine can induce apoptosis[146] a mechanism important for the development of lung emphysema. In this regard, the RNS have previously been

causally linked to the development of lung emphysema through the activation of proteases[147]. Further, the upregulation of iNOS and nitrotyrosine as well as peroxynitrite has been shown to cause nitration of proteins and to alter protein functions[129, 144]. Furthermore, RNS alter lipid oxidation can cause DNA damage and inhibit mitochondrial respiration also leading to apoptosis and necrosis that can be active in emphysema formation[129, 144]. Also the mitogen-activated protein kinases (MAPK) may mediate signal transduction pathways induced by reactive nitrogen species in lung epithelial cells leading to cell death[148]. Moreover, peroxynitrite can inactivate surfactant and inhibits protein phosphorylation by tyrosine kinases, thus interfering again with signal transduction mechanisms that can contribute emphysema development[129, 149].

The protective anti-remodeling effects of iNOS inhibition in other vascular beds (e.g. coronary arteries) are related to suppress metalloproteinase-9 activity and thus restoration of the balance between proteases and anti-proteases[150]. Peroxynitrite may activate matrix metalloproteinase (MMP) which in turn can inactivate α_1-antiproteinase. It can also enhance the production of the potent neutrophil chemoattractant IL-8 to perpetuate inflammatory process[75, 78]. Furthermore, peroxynitrite has been shown to strongly inhibit the activity of Akt and to increase 5′-AMP-activated kinase-dependent phosphorylation of eNOS, resulting in enhanced $O_2^{\cdot-}$ release and inhibition of NO release, further, contributing to oxidative stress production.

All of these factors may participate in the progression of COPD in the smoke-exposed mice of this own investigation due to airway inflammatory mechanisms, protease-antiprotease imbalance, and apoptotic mechanism through oxidative stress via the production of nitrotyrosine[87, 129].

6.4 iNOS inhibition by genetic deletion or application of the iNOS inhibitor L-NIL protects mice from pulmonary hypertension, emphysema and functional alterations induced by tobacco smoke exposure.

The role of eNOS or iNOS was further investigated by determination of the development of vascular and alveolar structural and functional alterations in $eNOS^{-/-}$ and $iNOS^{-/-}$ mice upon long-term tobacco smoke exposure. These investigations demonstrated that $iNOS^{-/-}$ mice were completely protected against the vascular and alveolar alterations caused by tobacco smoke inhalation, including vascular and lung dysfunction, whereas the smoke-induced changes in $eNOS^{-/-}$ mice were similar to those of WT mice. Along these lines, vasoreactivity measurement

also showed resistance towards the smoke-induced changes on hypoxic and phenylnephrine induced vasoconstriction as well as the nitric oxide and acetylcholine induced vasodilatation in $iNOS^{-/-}$ but not with $eNOS^{-/-}$ mice. It is known that nitric oxide is synthesized in vascular endothelial cells from L-arginine by eNOS after stimulation of muscarinic acetylcholine receptors and this NO stimulate soluble guanylate cyclase activity to increase intracellular cGMP concentration for vasorelxation[151]. Furthermore, this muscarnic acetylcholine receptor can be induced by acetylcholine and the investigations in this study have also shown an impaired relaxation response in pulmonary arterial vessels in lungs to tobacco smoke induced WT mice but not in $iNOS^{-/-}$ mice compared to non-smoke exposed controls. Furthermore, this impaired receptor activity to induce eNOS for the production of NO indicates the dysfunction of endothelial cell. Endothelial dysfunction may be caused by nitrotyrosine-dependent mechanism as the lower amounts of nitrotyrosine were seen in $iNOS^{-/-}$ but not with $eNOS^{-/-}$ and WT mice.

In an independent approach, the current thesis examined the effect of an oral treatment with L-NIL in WT mice during tobacco smoke exposure. As found for $iNOS^{-/-}$ mice, this approach completely prevented the development of pulmonary hypertension and emphysema as determined by morphometry and assessment of functional parameters. Even in this approach, a reduction in nitrotyrosine level was seen, further supporting the concept that nitrotyrosine plays a major role for the occurrence of COPD involving both alveolar and vascular compartment for structural and functional changes. Besides the more likely explanation of an impaired left-ventricular function due to pulmonary hypertension induced reduction in left heart pre-load, systemic effects of tobacco smoke could explain systemic hypotension. Consistent with the effects on the lung in $iNOS^{-/-}$ mice and after L-NIL-treatment, mice were protected from smoke-induced systemic hypotension. These findings are reminiscent of the effects of selective iNOS inhibition in short term models of COPD, also focusing on systemic effects[152].

6.5 Comparing human COPD Gold stage IV to the COPD mouse model of tobacco smoke induced emphysema

To demonstrate the relevance of these findings to human disease, lung tissue from five severe COPD (GOLD IV) patients who had undergone lung transplants was examined. Interestingly, similar alveolar and vascular structural alterations as for the mouse model were found in human COPD patient lungs. The ratio of the number of alveoli/ number of vessels was also increased and

a similar upregulation of iNOS and downregulation of the eNOS expression as well as their localization in the pulmonary vascultaure was found. This is in line with the previous suggestion that an activation of iNOS might be important for the occurrence of COPD in humans[153]. The increase in nitrotyrosine levels in lungs of human COPD patients as well as the mouse model further support the concept of nitrosative stress being a key player in COPD development[154].

In this regard, it is important to mention that the progressive impairment of lung function and airflow obstruction via amplification of nitrosative stress-mediated inflammatory process ultimately can cause degradation of extracellular matrix, resulting in alveolar wall destruction and small airways collapse as well responsible for the observed pulmonary vascular abnormalities and endothelial dysfunction. This concept of nitrosative/oxidative stress can be supported by the decreased level of nitrotyrosine in $iNOS^{-/-}$ compared to $eNOS^{-/-}$ and WT mouse lung as well as after L-NIL treatment of WT mice.

In conclusion, this study demonstrated and deciphered in detail that COPD is not only an alveolar but also a vascular disease characterized by alterations to the structure and function of the pulmonary vasculature, suggesting that these alteration are the driving force for emphysema development. Moreover, the current experiments suggest that an upregulation of the inducible nitric oxide synthese might play a key role for the disease induction. As 1) genetic deletion as well as iNOS inhibition prevented the vascular and alveolar alteration in the mouse model, selective iNOS inhibition could offer a potential as a preventive treatment of COPD and 2) similar alteration as in the mouse model were found in human COPD lungs.

7. APPENDICES

Appendix I Protocols for HE staining

SN	Time	Reagent	Remarks
1	20'	Heating slide with paraffin section	60°C
2	10'	Rothistol	
3	10'	Rothistol	
4	10'	Rothistol	
5	5'	Ethanol absolute 99.6%	
6	5'	Ethanol absolute 99.6%	
7	5'	Ethanol 96%	
8	5'	Ethanol 70%	
9	2'	Aqua dest.	
10	20'	Hematoxylin nack Mayer	
11	5'	H_2O (Flow tap water)	
12	1'	Ethanol 96%	
13	4'	Eosin solution	
14	Flow water	Ethanol 96%	
15	2'	Ethanol 96%	
16	5'	Ethanol absolute 99.6%	
17	5'	Isopropyl alcohol	
18	5'	Rothihistol	
19	5'	Rothihistol	
20	5'	Xylol	
21		Coverslip with pertex	

Appendix II Protocols for double antibody immunostaining for α–actin and VWF factor

SN	Time	Reagent	Remarks
1	20'	Heating slide with parrafin section	60°C
2	10'	Rothistol	
3	10'	Rothistol	
4	10'	Rothistol	
5	5'	Ethanol absolut 99.6%	
6	5'	Ethanol absolut 99.6%	
7	5'	Ethanol 96%	
8	5'	Ethanol 96%	
9	15'	H_2O_2 (180ml) + methanol (20 ml)	
10	5'	Aqua dest	
11	5'	Phosphate buffered saline	
12	15'	Trypsin (37^0)	(Trypsin 0.5 ml+ diluent 1.5ml)
13	5'	Phosphate buffered saline	
14	15'	Avidin blocking	
15	5'	Phosphate buffered saline	
16	15'	Biotin blocking	
17	5'	Phosphate buffered saline	
18	15'	10% Bovine serum albumin	
19	5'	Phosphate buffered saline	
20	60'	Mouse IgG blocking reagent (MOM kit)	2 µl IgG blocking reagent + 2.5ml PBS
21	5'	Phosphate buffered saline	
22	5'	MOM diluent/ protein blocking (MOM kit)	7.5ml PBS+ 600µl protein concentrate
23	30'	Primary antibody (alpha actin) mouse	1:900 dilution with 10% BSA
24	5'	Phosphate buffered saline	
25	10'	MOM biotinylated IgG reagent (MOM kit)	10µl reagent 3+ 2.5 ml MOM diluent
26	5'	Phosphate buffered saline	
27	5'	Vector MOM Kit ABC reagent (MOM kit)	2.5 ml PBS+ 2 drop reagent A + 2 µl reagent B
28	5'	Phosphate buffered saline	
29	3' to 4'	Vector VIP substrat kit	5ml PBS +3 µl reagent 1+3 µl reagent 2 +3 µl reagent 3 +3 µl reagent 4

30	5'	H_2O (Tap water)	
31	5'	Phosphate buffered saline	
32	15'	Avidin blocking	
33	5'	Phosphate buffered saline	
34	15'	Biotin blocking	
35	5'	Phosphate buffered saline	
36	15'	10% Bovine serum albumin	
37	5'	Phosphate buffered saline	
38	30'	Blocking serum	1ml goat serum+ 9 ml Phosphate buffered salineer
39	30'	Primary antibody (vWF) rabbit (37^0)	1:900 dilution with 10% bovine serum albumin
40	5'	Phosphate buffered saline	
41	30'	Biotinylated secondary antibody (anti rabbit kit)	10 ml PBS+ 3 drop goat serum+ 1 µl rabbit serum
42	5'	Phosphate buffered saline	
43	30'	ABC reagent (anti rabbit kit)	2.5 ml PBS+ 1 µl reagent A + 1 µl reagent B
44	5'	Phosphate buffered saline	
45	20"	DAB substrat Kit	5 ml aqua dest +2 µl reagent 1+2 µl reagent 2 +2 µl reagent 3 +2 µl reagent 4
46	5'	H_2O (Tap water)	
47	3'	Counter stain with methyl green	under 61^o C in heating plate
48	5'	Aqua dest	
49	2'	Ethanol 96%	
50	2'	Ethanol 96%	
51	5'	Isopropyl alkohol	
52	5'	Isopropyl alkohol	
53	5'	Rothistol	
54	5'	Rothistol	
55	5'	Xylol	
56		Coverslip fixation with pertex (glass covering)	

Appendix III Staining protocol for elastica *van* giesson staining

SN	Time	Reagent	Remarks
1	20'	Heating slide with parrafin section	60^0C
2	10'	Rothistol	
3	10'	Rothistol	
4	10'	Rothistol	
5	5'	Ethanol absolut 99.6%	
6	5'	Ethanol absolut 99.6%	
7	5'	Ethanol 96%	
8	5'	Ethanol 70%	
9	Overnight	Resorcin- Fuchsin	
10	Immesrsion	Aqua dest	
11	5’	Fe-hemtoxylin with Weigert solution A and B (1:1)	100ml solution. A +100ml Solution B
12	Immersion	Aqua dest	
13	15’	Flow tap water	
14	Immersion	Aqua dest	
15	10’	Elastica van giesson reagent	
16	Very short	Aqua dest	
17	2’	Ethanol 96%	
18	2'	Ethanol 96%	
19	5'	Ethanol absolut 99.6%	
20	5'	Isopropyal alcohol	
21	5'	Rothistol	
22	5'	Rothistol	
23	5'	Xylol	
24		Coverslip with pertex	

8. SUMMARY

Chronic obstructive pulmonary disease is a major cause of high morbidity and mortality with a high socioeconomic burden worldwide. The contribution of vascular alterations to the pathogenesis of the disease remains controversial and there is still ongoing debate about the possible development of pulmonary hypertension in COPD. Against this background, the current thesis aimed to decipher the time course for the development of lung emphysema as well as vascular alterations to the pulmonary circulation by use of a mouse model of tobacco smoke-induced COPD. For this purpose, WT mice were exposed for up to eight months to tobacco smoke (6 h/day, 5 days/week). It was demonstrated that both vascular structural and functional alterations occurred, including loss of pulmonary vessels, narrowing of vascular lumen, an increased degree of muscularization, pulmonary hypertension as well as endothelial dysfunction. Against the background, it was hypothesized that oxidative as well nitrosative stress plays a major role to the development of COPD by the regulation of inducible as well as the endothelial NO synthases. An upregulation of the inducible nitric oxide synthase (iNOS) was found in the pulmonary vasculature concomitant with increased nitrotyrosine levels. Comparing the development of vascular alteration and emphysema in WT, $iNOS^{-/-}$, and $eNOS^{-/-}$ mice, this study found that $iNOS^{-/-}$ were completely protected from these structural and functional changes. Moreover, the same effect was observed by the treatment of wild-type mice with the iNOS inhibitor L-NIL. Similar regulatory processes and structural alterations as for tobacco smoke exposed mice were found in GOLD stage IV for explanted COPD patient lungs. Thus, iNOS inhibition may be a strategy for prevention of COPD in the future.

9. ZUSAMMENFASUNG

COPD ist weltweit eine der wichtigsten Ursachen für hohe Morbidität und Mortalität mit hoher sozioökonomischer Bedeutung. Der Beitrag von vaskulären Veränderungen zur Pathogenese der COPD ist derzeit umstritten und es besteht eine laufende Debatte über die mögliche Entwicklung und Bedeutung der pulmonalen Hypertonie in der COPD. Vor diesem Hintergrund, war das Ziel der vorliegenden Arbeit, den zeitlichen Verlauf der Emphysementwicklung und der vaskulären Veränderungen anhand des Mausmodells der Tabakrauch induzierten COPD zu entschlüsseln. Für diesen Zweck wurden Wildtyp-Mäuse für acht Monate Tabak-Rauch für 6 Stunden/Tag und 5 Tage/Woche ausgesetzt. Es konnte gezeigt werden, dass sowohl strukturelle als auch funktionelle Gefäßveränderungen stattfinden, einschließlich des Verlusts der Lungengefäße, der Verengung des Gefäßlumens, des erhöhten Muskularisierungsgrades von Gefäßen, pulmonaler Hypertonie und endothelialer Dysfunktion. Basierend auf diesen Beobachtungen, wurde die Hypothese aufgestellt, dass oxidativer so wie nitrosativer Stress eine wichtige Rolle bei der Entwicklung von COPD spielen, indem es zu einer Regulation von induzierbaren und endothelialen NO-Synthasen kommt. Tatsächlich konnte in der vorliegenden Arbeit im pulmonalen Gefäßsystem eine Hochregulierung der induzierbaren NO Synthase (iNOS) nachgewiesen werden, einhergehend mit erhöhtem Vorkommen von Nitrotyrosin. Durch den Vergleich der Entwicklung von Gefäßveränderungen und der Emphysementwicklung in Wildtyp-, $iNOS^{-/-}$- und $eNOS^{-/-}$- Mäusen, konnte diese Studie zeigen, dass $iNOS^{-/-}$ -Mäuse vor den genannten strukturellen und funktionellen Änderungen komplett geschützt waren. Darüber hinaus, konnte der gleiche Effekt nach Behandlung von Wildtyp-Mäusen mit dem iNOS Inhibitor L-NIL beobachtet werden. Ähnliche regulatorische Prozesse und strukturelle Veränderungen wie in den Wildtyp-Mauslungen nach Rauchexposition wurden in Resektaten von Lungen von Patienten mit COPD (GOLD stage IV) nachgewiesen. Demnach könnte die Inhibierung von iNOS in Zukunft eine Strategie zur COPD Prävention darstellen.

10. REFERENCES

1. Chronic obstructive pulmonary disease. National clinical guideline on management of chronic obstructive pulmonary disease in adults in primary and secondary care. Thorax 59 Suppl 1, 1-232 (2004).

2. Hogg,J.C. Chronic obstructive pulmonary disease: an overview of pathology and pathogenesis. Novartis. Found. Symp. 234, 4-19 (2001).

3. Hogg,J.C. & Senior,R.M. Chronic obstructive pulmonary disease - part 2: pathology and biochemistry of emphysema. Thorax 57, 830-834 (2002).

4. Mannino,D.M. Chronic obstructive pulmonary disease: definition and epidemiology. Respir. Care 48, 1185-1191 (2003).

5. Viegi,G. et al. Definition, epidemiology and natural history of COPD. Eur. Respir. J. 30, 993-1013 (2007).

6. Siafakas,N.M. et al. Optimal assessment and management of chronic obstructive pulmonary disease (COPD). The European Respiratory Society Task Force. Eur. Respir. J. 8, 1398-1420 (1995).

7. Standards for the diagnosis and care of patients with chronic obstructive pulmonary disease (COPD) and asthma. This official statement of the American Thoracic Society was adopted by the ATS Board of Directors, November 1986. Am. Rev. Respir. Dis. 136, 225-244 (1987).

8. BTS guidelines for the management of chronic obstructive pulmonary disease. The COPD Guidelines Group of the Standards of Care Committee of the BTS. Thorax 52 Suppl 5, S1-28 (1997).

9. Pauwels,R. Global initiative for chronic obstructive lung diseases (GOLD): time to act. Eur. Respir. J. 18, 901-902 (2001).

10. Celli,B.R. & MacNee,W. Standards for the diagnosis and treatment of patients with COPD: a summary of the ATS/ERS position paper. Eur. Respir. J. 23, 932-946 (2004).

11. Pauwels,R.A., Buist,A.S., Calverley,P.M., Jenkins,C.R., & Hurd,S.S. Global strategy for the diagnosis, management, and prevention of chronic obstructive pulmonary disease. NHLBI/WHO Global Initiative for Chronic Obstructive Lung Disease (GOLD) Workshop summary. Am. J. Respir. Crit Care Med. 163, 1256-1276 (2001).

12. Mannino,D.M. & Buist,A.S. Global burden of COPD: risk factors, prevalence, and future trends. Lancet 370, 765-773 (2007).

13. Higgins,M.W. et al. Risk of chronic obstructive pulmonary disease. Collaborative assessment of the validity of the Tecumseh index of risk. Am. Rev. Respir. Dis. 130, 380-385 (1984).

14. Barnes,P.J. Genetics and pulmonary medicine. 9. Molecular genetics of chronic obstructive pulmonary disease. Thorax 54, 245-252 (1999).

15. Sandford,A.J. & Pare,P.D. Genetic risk factors for chronic obstructive pulmonary disease. Clin. Chest Med. 21, 633-643 (2000).

16. Silverman,E.K. & Speizer,F.E. Risk factors for the development of chronic obstructive pulmonary disease. Med. Clin. North Am. 80, 501-522 (1996).

17. Agusti,A.G. et al. Systemic effects of chronic obstructive pulmonary disease. Eur. Respir. J. 21, 347-360 (2003).

18. Churg,A., Cosio,M., & Wright,J.L. Mechanisms of cigarette smoke-induced COPD: insights from animal models. Am. J. Physiol Lung Cell Mol. Physiol 294, L612-L631 (2008).

19. Mahadeva,R. & Shapiro,S.D. Animal models of pulmonary emphysema. Curr. Drug Targets. Inflamm. Allergy 4, 665-673 (2005).

20. Wright,J.L., Cosio,M., & Churg,A. Animal models of chronic obstructive pulmonary disease. Am. J. Physiol Lung Cell Mol. Physiol 295, L1-15 (2008).

21. Franssen,F.M., O'Donnell,D.E., Goossens,G.H., Blaak,E.E., & Schols,A.M. Obesity and the lung: 5. Obesity and COPD. Thorax 63, 1110-1117 (2008).

22. Taraseviciene-Stewart,L. & Voelkel,N.F. Molecular pathogenesis of emphysema. J. Clin. Invest 118, 394-402 (2008).

23. Hogg,J.C. et al. Lung structure and function in cigarette smokers. Thorax 49, 473-478 (1994).

24. Hogg,J.C. Lung structure and function in COPD. Int. J. Tuberc. Lung Dis. 12, 467-479 (2008).

25. Pryor,W.A. & Stone,K. Oxidants in cigarette smoke. Radicals, hydrogen peroxide, peroxynitrate, and peroxynitrite. Ann. N. Y. Acad. Sci. 686, 12-27 (1993).

26. Chow,C.K. Cigarette smoking and oxidative damage in the lung. Ann. N. Y. Acad. Sci. 686, 289-298 (1993).

27. Di,S.A. et al. Cellular and molecular mechanisms in chronic obstructive pulmonary disease: an overview. Clin. Exp. Allergy 34, 1156-1167 (2004).

28. Bowler,R.P., Barnes,P.J., & Crapo,J.D. The role of oxidative stress in chronic obstructive pulmonary disease. COPD. 1, 255-277 (2004).

29. Davies,K.J. Oxidative stress: the paradox of aerobic life. Biochem. Soc. Symp. 61, 1-31 (1995).

30. Halliwell,B. Biochemistry of oxidative stress. Biochem. Soc. Trans. 35, 1147-1150 (2007).

31. Beckman,J.S. & Koppenol,W.H. Nitric oxide, superoxide, and peroxynitrite: the good, the bad, and ugly. Am. J. Physiol 271, C1424-C1437 (1996).

32. Wink,D.A. et al. Chemical biology of nitric oxide: regulation and protective and toxic mechanisms. Curr. Top. Cell Regul. 34, 159-187 (1996).

33. Langen,R.C., Korn,S.H., & Wouters,E.F. ROS in the local and systemic pathogenesis of COPD. Free Radic. Biol. Med. 35, 226-235 (2003).

34. Rahman,I. & MacNee,W. Role of oxidants/antioxidants in smoking-induced lung diseases. Free Radic. Biol. Med. 21, 669-681 (1996).

35. Schaberg,T., Klein,U., Rau,M., Eller,J., & Lode,H. Subpopulations of alveolar macrophages in smokers and nonsmokers: relation to the expression of CD11/CD18 molecules and superoxide anion production. Am. J. Respir. Crit Care Med. 151, 1551-1558 (1995).

36. Schaberg,T. et al. Superoxide anion release induced by platelet-activating factor is increased in human alveolar macrophages from smokers. Eur. Respir. J. 5, 387-393 (1992).

37. Mateos,F., Brock,J.H., & Perez-Arellano,J.L. Iron metabolism in the lower respiratory tract. Thorax 53, 594-600 (1998).

38. Wesselius,L.J., Nelson,M.E., & Skikne,B.S. Increased release of ferritin and iron by iron-loaded alveolar macrophages in cigarette smokers. Am. J. Respir. Crit Care Med. 150, 690-695 (1994).

39. Wallaert,B. et al. Inactivation of alpha 1-proteinase inhibitor by alveolar inflammatory cells from smoking patients with or without emphysema. Am. Rev. Respir. Dis. 147, 1537-1543 (1993).

40. Rochelle,L.G., Fischer,B.M., & Adler,K.B. Concurrent production of reactive oxygen and nitrogen species by airway epithelial cells in vitro. Free Radic. Biol. Med. 24, 863-868 (1998).

41. Kobzik,L. et al. Nitric oxide synthase in human and rat lung: immunocytochemical and histochemical localization. Am. J. Respir. Cell Mol. Biol. 9, 371-377 (1993).

42. Pinamonti,S. et al. Xanthine oxidase activity in bronchoalveolar lavage fluid from patients with chronic obstructive pulmonary disease. Free Radic. Biol. Med. 21, 147-155 (1996).

43. Reinders,M.E. et al. Proinflammatory functions of vascular endothelial growth factor in alloimmunity. J. Clin. Invest 112, 1655-1665 (2003).

44. Montuschi,P., Kharitonov,S.A., & Barnes,P.J. Exhaled carbon monoxide and nitric oxide in COPD. Chest 120, 496-501 (2001).

45. Nowak,D., Kasielski,M., Antczak,A., Pietras,T., & Bialasiewicz,P. Increased content of thiobarbituric acid-reactive substances and hydrogen peroxide in the expired breath condensate of patients with stable chronic obstructive pulmonary disease: no significant effect of cigarette smoking. Respir. Med. 93, 389-396 (1999).

46. Corradi,M. et al. Aldehydes in exhaled breath condensate of patients with chronic obstructive pulmonary disease. Am. J. Respir. Crit Care Med. 167, 1380-1386 (2003).

47. Petruzzelli,S. et al. Plasma 3-nitrotyrosine in cigarette smokers. Am. J. Respir. Crit Care Med. 156, 1902-1907 (1997).

48. Tuder,R.M. et al. Oxidative stress and apoptosis interact and cause emphysema due to vascular endothelial growth factor receptor blockade. Am. J. Respir. Cell Mol. Biol. 29, 88-97 (2003).

49. Kinnula,V.L. & Crapo,J.D. Superoxide dismutases in the lung and human lung diseases. Am. J. Respir. Crit Care Med. 167, 1600-1619 (2003).

50. Arner,E.S. & Holmgren,A. Physiological functions of thioredoxin and thioredoxin reductase. Eur. J. Biochem. 267, 6102-6109 (2000).

51. Barnes,P.J., Shapiro,S.D., & Pauwels,R.A. Chronic obstructive pulmonary disease: molecular and cellular mechanisms. Eur. Respir. J. 22, 672-688 (2003).

52. Barnes,P.J. Mediators of chronic obstructive pulmonary disease. Pharmacol. Rev. 56, 515-548 (2004).

53. Finkelstein,R., Fraser,R.S., Ghezzo,H., & Cosio,M.G. Alveolar inflammation and its relation to emphysema in smokers. Am. J. Respir. Crit Care Med. 152, 1666-1672 (1995).

54. Hogg,J.C. Pathophysiology of airflow limitation in chronic obstructive pulmonary disease. Lancet 364, 709-721 (2004).

55. Evans,M.D. & Pryor,W.A. Damage to human alpha-1-proteinase inhibitor by aqueous cigarette tar extracts and the formation of methionine sulfoxide. Chem. Res. Toxicol. 5, 654-660 (1992).

56. Bieth,J.G. The antielastase screen of the lower respiratory tract. Eur. J. Respir. Dis. Suppl 139, 57-61 (1985).

57. Aoshiba,K., Yasuda,K., Yasui,S., Tamaoki,J., & Nagai,A. Serine proteases increase oxidative stress in lung cells. Am. J. Physiol Lung Cell Mol. Physiol 281, L556-L564 (2001).

58. Kilburn,K.H. & McKenzie,W. Leukocyte recruitment to airways by cigarette smoke and particle phase in contrast to cytotoxicity of vapor. Science 189, 634-637 (1975).

59. Selby,C., Drost,E., Wraith,P.K., & MacNee,W. In vivo neutrophil sequestration within lungs of humans is determined by in vitro "filterability". J. Appl. Physiol 71, 1996-2003 (1991).

60. Drost,E.M., Selby,C., Lannan,S., Lowe,G.D., & MacNee,W. Changes in neutrophil deformability following in vitro smoke exposure: mechanism and protection. Am. J. Respir. Cell Mol. Biol. 6, 287-295 (1992).

61. Drost,E.M., Selby,C., Bridgeman,M.M., & MacNee,W. Decreased leukocyte deformability after acute cigarette smoking in humans. Am. Rev. Respir. Dis. 148, 1277-1283 (1993).

62. Lehr,H.A. et al. Cigarette smoke elicits leukocyte adhesion to endothelium in hamsters: inhibition by CuZn-SOD. Free Radic. Biol. Med. 14, 573-581 (1993).

63. Klut,M.E., Doerschuk,C.M., van Eeden,S.F., Burns,A.R., & Hogg,J.C. Activation of neutrophils within pulmonary microvessels of rabbits exposed to cigarette smoke. Am. J. Respir. Cell Mol. Biol. 9, 82-89 (1993).

64. Bosken,C.H., Doerschuk,C.M., English,D., & Hogg,J.C. Neutrophil kinetics during active cigarette smoking in rabbits. J. Appl. Physiol 71, 630-637 (1991).

65. Brown,D.M., Drost,E., Donaldson,K., & MacNee,W. Deformability and CD11/CD18 expression of sequestered neutrophils in normal and inflamed lungs. Am. J. Respir. Cell Mol. Biol. 13, 531-539 (1995).

66. Barnes,P.J. The cytokine network in asthma and chronic obstructive pulmonary disease. J. Clin. Invest 118, 3546-3556 (2008).

67. Takizawa,H. et al. Increased expression of inflammatory mediators in small-airway epithelium from tobacco smokers. Am. J. Physiol Lung Cell Mol. Physiol 278, L906-L913 (2000).

68. Profita,M. et al. Effect of cilomilast (Ariflo) on TNF-alpha, IL-8, and GM-CSF release by airway cells of patients with COPD. Thorax 58, 573-579 (2003).

69. Gilmour,P.S., Rahman,I., Donaldson,K., & MacNee,W. Histone acetylation regulates epithelial IL-8 release mediated by oxidative stress from environmental particles. Am. J. Physiol Lung Cell Mol. Physiol 284, L533-L540 (2003).

70. Scholz,H. et al. 8-isoprostane increases expression of interleukin-8 in human macrophages through activation of mitogen-activated protein kinases. Cardiovasc. Res. 59, 945-954 (2003).

71. Leonarduzzi,G. et al. The lipid peroxidation end product 4-hydroxy-2,3-nonenal up-regulates transforming growth factor beta1 expression in the macrophage lineage: a link between oxidative injury and fibrosclerosis. FASEB J. 11, 851-857 (1997).

72. Arsalane,K. et al. Transforming growth factor-beta1 is a potent inhibitor of glutathione synthesis in the lung epithelial cell line A549: transcriptional effect on the GSH rate-limiting enzyme gamma-glutamylcysteine synthetase. Am. J. Respir. Cell Mol. Biol. 17, 599-607 (1997).

73. Rahman,I. & MacNee,W. Role of transcription factors in inflammatory lung diseases. Thorax 53, 601-612 (1998).

74. MacNee,W. & Rahman,I. Is oxidative stress central to the pathogenesis of chronic obstructive pulmonary disease? Trends Mol. Med. 7, 55-62 (2001).

75. Tomita,K., Barnes,P.J., & Adcock,I.M. The effect of oxidative stress on histone acetylation and IL-8 release. Biochem. Biophys. Res. Commun. 301, 572-577 (2003).

76. Ito,K. et al. A molecular mechanism of action of theophylline: Induction of histone deacetylase activity to decrease inflammatory gene expression. Proc. Natl. Acad. Sci. U. S. A 99, 8921-8926 (2002).

77. Marwick,J.A. et al. Cigarette smoke-induced oxidative stress and TGF-beta1 increase p21waf1/cip1 expression in alveolar epithelial cells. Ann. N. Y. Acad. Sci. 973, 278-283 (2002).

78. Ito,K., Hanazawa,T., Tomita,K., Barnes,P.J., & Adcock,I.M. Oxidative stress reduces histone deacetylase 2 activity and enhances IL-8 gene expression: role of tyrosine nitration. Biochem. Biophys. Res. Commun. 315, 240-245 (2004).

79. Ito,K. et al. Decreased histone deacetylase activity in chronic obstructive pulmonary disease. N. Engl. J. Med. 352, 1967-1976 (2005).

80. Tuder,R.M., Petrache,I., Elias,J.A., Voelkel,N.F., & Henson,P.M. Apoptosis and emphysema: the missing link. Am. J. Respir. Cell Mol. Biol. 28, 551-554 (2003).

81. Kasahara,Y. et al. Endothelial cell death and decreased expression of vascular endothelial growth factor and vascular endothelial growth factor receptor 2 in emphysema. Am. J. Respir. Crit Care Med. 163, 737-744 (2001).

82. Hodge,S.J., Hodge,G.L., Reynolds,P.N., Scicchitano,R., & Holmes,M. Increased production of TGF-beta and apoptosis of T lymphocytes isolated from peripheral blood in COPD. Am. J. Physiol Lung Cell Mol. Physiol 285, L492-L499 (2003).

83. Langen,R.C., Korn,S.H., & Wouters,E.F. ROS in the local and systemic pathogenesis of COPD. Free Radic. Biol. Med. 35, 226-235 (2003).

84. Andrade,F.H., Reid,M.B., Allen,D.G., & Westerblad,H. Effect of hydrogen peroxide and dithiothreitol on contractile function of single skeletal muscle fibres from the mouse. J. Physiol 509 (Pt 2), 565-575 (1998).

85. Langen,R.C. et al. Tumor necrosis factor-alpha inhibits myogenic differentiation through MyoD protein destabilization. FASEB J. 18, 227-237 (2004).

86. Stangel,M. et al. H2O2 and nitric oxide-mediated oxidative stress induce apoptosis in rat skeletal muscle myoblasts. J. Neuropathol. Exp. Neurol. 55, 36-43 (1996).

87. Ricciardolo,F.L., Di,S.A., Sabatini,F., & Folkerts,G. Reactive nitrogen species in the respiratory tract. Eur. J. Pharmacol. 533, 240-252 (2006).

88. Folkerts,G., Kloek,J., Muijsers,R.B., & Nijkamp,F.P. Reactive nitrogen and oxygen species in airway inflammation. Eur. J. Pharmacol. 429, 251-262 (2001).

89. Montuschi,P., Kharitonov,S.A., Ciabattoni,G., & Barnes,P.J. Exhaled leukotrienes and prostaglandins in COPD. Thorax 58, 585-588 (2003).

90. Agusti,A.G., Villaverde,J.M., Togores,B., & Bosch,M. Serial measurements of exhaled nitric oxide during exacerbations of chronic obstructive pulmonary disease. Eur. Respir. J. 14, 523-528 (1999).

91. Ricciardolo,F.L. et al. Nitrosative stress in the bronchial mucosa of severe chronic obstructive pulmonary disease. J. Allergy Clin. Immunol. 116, 1028-1035 (2005).

92. Ichinose,M., Sugiura,H., Yamagata,S., Koarai,A., & Shirato,K. Increase in reactive nitrogen species production in chronic obstructive pulmonary disease airways. Am. J. Respir. Crit Care Med. 162, 701-706 (2000).

93. Corradi,M. et al. Increased nitrosothiols in exhaled breath condensate in inflammatory airway diseases. Am. J. Respir. Crit Care Med. 163, 854-858 (2001).

94. Sadeghi-Hashjin,G. et al. Peroxynitrite induces airway hyperresponsiveness in guinea pigs in vitro and in vivo. Am. J. Respir. Crit Care Med. 153, 1697-1701 (1996).

95. Okamoto,T. et al. Activation of human neutrophil procollagenase by nitrogen dioxide and peroxynitrite: a novel mechanism for procollagenase activation involving nitric oxide. Arch. Biochem. Biophys. 342, 261-274 (1997).

96. Whiteman,M., Szabo,C., & Halliwell,B. Modulation of peroxynitrite- and hypochlorous acid-induced inactivation of alpha1-antiproteinase by mercaptoethylguanidine. Br. J. Pharmacol. 126, 1646-1652 (1999).

97. Filep,J.G., Beauchamp,M., Baron,C., & Paquette,Y. Peroxynitrite mediates IL-8 gene expression and production in lipopolysaccharide-stimulated human whole blood. J. Immunol. 161, 5656-5662 (1998).

98. Tuder,R.M., Yun,J.H., Bhunia,A., & Fijalkowska,I. Hypoxia and chronic lung disease. J. Mol. Med. 85, 1317-1324 (2007).

99. Tuder,R.M., Yoshida,T., Fijalkowka,I., Biswal,S., & Petrache,I. Role of lung maintenance program in the heterogeneity of lung destruction in emphysema. Proc. Am. Thorac. Soc. 3, 673-679 (2006).

100. Voelkel,N.F. & Cool,C.D. Pulmonary vascular involvement in chronic obstructive pulmonary disease. Eur. Respir. J. Suppl 46, 28s-32s (2003).

101. Nikula,K.J. & Green,F.H. Animal models of chronic bronchitis and their relevance to studies of particle-induced disease. Inhal. Toxicol. 12 Suppl 4, 123-153 (2000).

102. Groneberg,D.A. & Chung,K.F. Models of chronic obstructive pulmonary disease. Respir. Res. 5, 18 (2004).

103. Shapiro,S.D. Animal models for chronic obstructive pulmonary disease: age of klotho and marlboro mice. Am. J. Respir. Cell Mol. Biol. 22, 4-7 (2000).

104. Kodavanti,U.P. & Costa,D.L. Rodent models of susceptibility: what is their place in inhalation toxicology? Respir. Physiol 128, 57-70 (2001).

105. Kodavanti,U.P. & Costa,D.L. Rodent models of susceptibility: what is their place in inhalation toxicology? Respir. Physiol 128, 57-70 (2001).

106. Aoshiba,K., Yokohori,N., & Nagai,A. Alveolar wall apoptosis causes lung destruction and emphysematous changes. Am. J. Respir. Cell Mol. Biol. 28, 555-562 (2003).

107. Tuder,R.M., Petrache,I., Elias,J.A., Voelkel,N.F., & Henson,P.M. Apoptosis and emphysema: the missing link. Am. J. Respir. Cell Mol. Biol. 28, 551-554 (2003).

108. Wright,J.L. & Churg,A. Cigarette smoke causes physiologic and morphologic changes of emphysema in the guinea pig. Am. Rev. Respir. Dis. 142, 1422-1428 (1990).

109. Taraseviciene-Stewart,L. & Voelkel,N.F. Molecular pathogenesis of emphysema. J. Clin. Invest 118, 394-402 (2008).

110.Wright,J.L., Levy,R.D., & Churg,A. Pulmonary hypertension in chronic obstructive pulmonary disease: current theories of pathogenesis and their implications for treatment. Thorax 60, 605-609 (2005).

111. Barbera,J.A., Peinado,V.I., & Santos,S. Pulmonary hypertension in chronic obstructive pulmonary disease. Eur. Respir. J. 21, 892-905 (2003).

112. Peinado,V.I., Pizarro,S., & Barbera,J.A. Pulmonary vascular involvement in COPD. Chest 134, 808-814 (2008).

113. Woyda,K. et al. Inhibition of phosphodiesterase 4 enhances lung alveolarisation in neonatal mice exposed to hyperoxia. Eur. Respir. J. 33, 861-870 (2009).

114. Dumitrascu,R. et al. Activation of soluble guanylate cyclase reverses experimental pulmonary hypertension and vascular remodeling. Circulation 113, 286-295 (2006).

115. Schermuly,R.T. et al. Reversal of experimental pulmonary hypertension by PDGF inhibition. J. Clin. Invest 115, 2811-2821 (2005).

116. Weissmann,N. et al. Classical transient receptor potential channel 6 (TRPC6) is essential for hypoxic pulmonary vasoconstriction and alveolar gas exchange. Proc. Natl. Acad. Sci. U. S. A 103, 19093-19098 (2006).

117. Weissmann,N. et al. Basic features of hypoxic pulmonary vasoconstriction in mice. Respir. Physiol Neurobiol. 139, 191-202 (2004).

118. Mittal,M. et al. Hypoxia-dependent regulation of nonphagocytic NADPH oxidase subunit NOX4 in the pulmonary vasculature. Circ. Res. 101, 258-267 (2007).

119. Fink,L. et al. Real-time quantitative RT-PCR after laser-assisted cell picking. Nat. Med. 4, 1329-1333 (1998).

120. March,T.H. et al. Modulators of cigarette smoke-induced pulmonary emphysema in A/J mice. Toxicol. Sci. 92, 545-559 (2006).

121. Mannino,D.M. & Buist,A.S. Global burden of COPD: risk factors, prevalence, and future trends. Lancet 370, 765-773 (2007).

122. Yoshida,T. & Tuder,R.M. Pathobiology of cigarette smoke-induced chronic obstructive pulmonary disease. Physiol Rev. 87, 1047-1082 (2007).

123. Maeno,T. et al. CD8+ T Cells are required for inflammation and destruction in cigarette smoke-induced emphysema in mice. J. Immunol. 178, 8090-8096 (2007).

124. Bracke,K.R. et al. Cigarette smoke-induced pulmonary inflammation and emphysema are attenuated in CCR6-deficient mice. J. Immunol. 177, 4350-4359 (2006).

125. Wright,J.L., Cosio,M., & Churg,A. Animal models of chronic obstructive pulmonary disease. Am. J. Physiol Lung Cell Mol. Physiol 295, L1-15 (2008).

126. Bracke,K.R. et al. Cigarette smoke-induced pulmonary inflammation and emphysema are attenuated in CCR6-deficient mice. J. Immunol. 177, 4350-4359 (2006).

127. Ruta,A., Mark,B., Edward,B., Jawaharlal,P., & Jianliang,Z. Nuclear localization of active matrix metalloproteinase-2 in cigarette smoke-exposed apoptotic endothelial cells. Exp. Lung Res. 35, 59-75 (2009).

128. Morris,A. et al. Comparison of cigarette smoke-induced acute inflammation in multiple strains of mice and the effect of a matrix metalloproteinase inhibitor on these responses. J. Pharmacol. Exp. Ther. 327, 851-862 (2008).

129. Ricciardolo,F.L., Sterk,P.J., Gaston,B., & Folkerts,G. Nitric oxide in health and disease of the respiratory system. Physiol Rev. 84, 731-765 (2004).

130. Wright,J.L., Levy,R.D., & Churg,A. Pulmonary hypertension in chronic obstructive pulmonary disease: current theories of pathogenesis and their implications for treatment. Thorax 60, 605-609 (2005).

131. Staub,N.C. Site of hypoxic pulmonary vasoconstriction. Chest 88, 240S-245S (1985).

132. Kanazawa,H. Role of vascular endothelial growth factor in the pathogenesis of chronic obstructive pulmonary disease. Med. Sci. Monit. 13, RA189-RA195 (2007).

133. nh-Xuan,A.T., Pepke-Zaba,J., Butt,A.Y., Cremona,G., & Higenbottam,T.W. Impairment of pulmonary-artery endothelium-dependent relaxation in chronic obstructive lung disease is not due to dysfunction of endothelial cell membrane receptors nor to L-arginine deficiency. Br. J. Pharmacol. 109, 587-591 (1993).

134. Dinh-Xuan,A.T., Pepke-Zaba,J., Butt,A.Y., Cremona,G., & Higenbottam,T.W. Impairment of pulmonary-artery endothelium-dependent relaxation in chronic obstructive lung disease is not due to dysfunction of endothelial cell membrane receptors nor to L-arginine deficiency. Br. J. Pharmacol. 109, 587-591 (1993).

135.Wright,J.L. & Churg,A. Short-term exposure to cigarette smoke induces endothelial dysfunction in small intrapulmonary arteries: analysis using guinea pig precision cut lung slices. J. Appl. Physiol 104, 1462-1469 (2008).

136. Wright,J.L., Tai,H., & Churg,A. Vasoactive mediators and pulmonary hypertension after cigarette smoke exposure in the guinea pig. J. Appl. Physiol 100, 672-678 (2006).

137. Wright,J.L., Tai,H., & Churg,A. Cigarette smoke induces persisting increases of vasoactive mediators in pulmonary arteries. Am. J. Respir. Cell Mol. Biol. 31, 501-509 (2004).

138. Celermajer,D.S. et al. Passive smoking and impaired endothelium-dependent arterial dilatation in healthy young adults. N. Engl. J. Med. 334, 150-154 (1996).

139. Su,Y., Cao,W., Han,Z., & Block,E.R. Cigarette smoke extract inhibits angiogenesis of pulmonary artery endothelial cells: the role of calpain. Am. J. Physiol Lung Cell Mol. Physiol 287, L794-L800 (2004).

140. Forstermann,U. Oxidative stress in vascular disease: causes, defense mechanisms and potential therapies. Nat. Clin. Pract. Cardiovasc. Med. 5, 338-349 (2008).

141. Brindicci,C., Ito,K., Torre,O., Barnes,P.J., & Kharitonov,S.A. Effects of aminoguanidine, an inhibitor of inducible nitric oxide synthase, on nitric oxide production and its metabolites in healthy controls, healthy smokers and COPD patients. Chest(2008).

142. Maestrelli,P. et al. Decreased haem oxygenase-1 and increased inducible nitric oxide synthase in the lung of severe COPD patients. Eur. Respir. J. 21, 971-976 (2003).

143. Kharitonov,S.A. NOS:molecular mechanisms, clinical aspects, therapeutic and monitoring approaches. Curr. Drug Targets. Inflamm. Allergy 4, 141-149 (2005).

144. Kharitonov,S.A. & Barnes,P.J. Nitric oxide, nitrotyrosine, and nitric oxide modulators in asthma and chronic obstructive pulmonary disease. Curr. Allergy Asthma Rep. 3, 121-129 (2003).

145. Arif,E. et al. Endothelial nitric oxide synthase gene variants contribute to oxidative stress in COPD. Biochem. Biophys. Res. Commun. 361, 182-188 (2007).

146. Kim,K.M. et al. Regulation of apoptosis by nitrosative stress. J. Biochem. Mol. Biol. 35, 127-133 (2002).

147. Owen,C.A. Proteinases and oxidants as targets in the treatment of chronic obstructive pulmonary disease. Proc. Am. Thorac. Soc. 2, 373-385 (2005).

148. Kanazawa,H., Shiraishi,S., Hirata,K., & Yoshikawa,J. Imbalance between levels of nitrogen oxides and peroxynitrite inhibitory activity in chronic obstructive pulmonary disease. Thorax 58, 106-109 (2003).

149. Medicherla,S. et al. p38alpha-selective mitogen-activated protein kinase inhibitor SD-282 reduces inflammation in a subchronic model of tobacco smoke-induced airway inflammation. J. Pharmacol. Exp. Ther. 324, 921-929 (2008).

150. Egi,K. et al. Inhibition of inducible nitric oxide synthase and superoxide production reduces matrix metalloproteinase-9 activity and restores coronary vasomotor function in rat cardiac allografts. Eur. J. Cardiothorac. Surg. 26, 262-269 (2004).

151. Peinado,V.I. et al. Endothelial dysfunction in pulmonary arteries of patients with mild COPD. Am. J. Physiol 274, L908-L913 (1998).

152. Anazawa,T. et al. Effect of exposure to cigarette smoke on carotid artery intimal thickening: the role of inducible NO synthase. Arterioscler. Thromb. Vasc. Biol. 24, 1652-1658 (2004).

153. Peinado,V.I., Pizarro,S., & Barbera,J.A. Pulmonary Vascular Involvement in COPD. Chest 134, 808-814 (2008).

154. Ricciardolo,F.L., Di,S.A., Sabatini,F., & Folkerts,G. Reactive nitrogen species in the respiratory tract. Eur. J. Pharmacol. 533, 240-252 (2006).

11. A. ACKNOWLEDGEMENTS

I would like to express my gratitude and thanks to Prof Dr. Werner Seeger, University of Giessen Lung Center for providing me the opportnunity and the support to do my PhD study in the Excellence Cluster of Cardio pulmonary System (ECCP), University of Giessen Lung Research Center, Germany.

I would like to express with deep sense of full respect and gratitude to my supervisor Prof. Norbert Weissmann forever and ever for his continuous support, extreme encouragement, technical and moral support for this research work environment and this thesis. Your team work and patience will be my source of inspiration to keep enthusiasam to move forward my carrer in research. My sincere thanks also go to Prof. R.T. Schermuly and Prof. A.Ghofrani for providing direct and indirect support for me in this research.

Things will be not complete unless I mentioned and appreciate the help of my friend Dr. B.K. Dahal, Dr. R.B. Dumitrascu, Dr. A. Sydykov, Dr. B. Egemnazarov and M. Seimetz for technical support and suggestion in need. I deeply appreciate your help, expertise and will be always memorable. Further, I like to appreciate Dr. M. Roth, Mr. F. Veit and Mr. M. Mittal for your support during my studies in Giessen. My sincere thanks also go to all lab members who help and support me directly and indirectly. My thanks also go to Dr.W. Kelpetko, Dr. P. Jaksch for providing human lungs sample and Dr. R.E. Morty for linguistics edition.

I would also like to express my thanks to all technical staff namely Ingrid Breitenborn-Müller, S. Gräf-Höchst, A. Hanschke, C. Homberger, K. Quanz, A. Vogt and E. Bieniek for their support.

At the last but not least, my PhD study research would not have been completed without love of my parents C.P. Parajuli and L. Parajuli, parents in law- Prof. L.P. Subedi, M. Subedi, my lovely wife Dr. K. Subedi, brother N. Parajuli, brother in law T.N. Subedi and my host family W. Slot, H. Slot. Sincere thanks to you all.

Thanking you

Der Lebenslauf wurde aus der elektronischen Version der Arbeit entfernt.

The curriculum vitae was removed from the electronic version of the paper.

Professional Experience

1998 - 2001 Faculty and as vet clinician at Tribhuvan University, Nepal

Awards/Certificates

European Respiratory Society COPD travel grant award in 2008 for thematic poster presentation at ERS congress supported by Boehringer Ingelheim, Berlin, Germany

DAAD Fellowship Award in 2004-2005 for research study from German Government Academic Exchange Programme, University of Bonn, Germany.

Monbukagusho Scholarship Award (Monbusho) in 2002-2004 for Master study from Japanese Government, Hiroshima University, Japan.

Netherlands Fellowship Award (NFP) for post graduate diploma study, 2001-2002. Wageninegen University, The Netherlands.

Publications

1. Parajuli, N, et al. Seimetz M, Ghofrani HA, Schermuly RT, Medebach T, Roth M, Klepetko W, Jaksch P, Dumitrascu R, Seeger W, Grimminger F and Weissmann N "COPD – a lung vascular diseases completely dependent on iNOS." Revision in ***Nature*** **(2009)**.

2. Roth M, Rupp M, Hofmann S, Mittal M, Fuchs B, Sommer N, **Parajuli N**, Quanz K, Schubert D, Dony E, Schermuly RT, Ghofrani HA, Sausbier U, Rutschmann K, Wilhelm S, Seeger W, Ruth P, Grimminger F, Sausbier M, Weissmann N., "Heme Oxygenase-2 and Large-conductance Ca2+ activated K+ Channels: Lung Vascular Effects of Hypoxia." ***Am J Respir Crit Care Med.*** (**2009**).

3. Wempe, F., De-Zolt, S., Koli, K., Bangsow, T., **Parajuli, N.**, Dumitrascu, R., Sterner-Kock, A., Weissmann, N., Keski-Oja, J. and von Melchner, H.: The mutational inactivation of the antioxidant protein Sestrin 2 induces TGF-β signaling and partially rescues pulmonary emphysema in a genetic mouse model of pulmonary emphysema. **Dis. Model Mech., (2009**) in press.

4. Gurung YB, **Parajuli N**, Miyazaki Y, Imai S and Kobayashi K published in "Rumen ciliate Faunae of water Buffalo (Bubalus bubalis) and goat (Capra hircus) in Nepal." ***J Vet Med Sci.*** (**2002**).

Conferences: Poster / Oral

1. Seimetz M, **Parajuli N,** Roth M, Schermuly RT, Ghofrani HA, Seeger W, Grimminger F, and Weissmann N (**2009**). "Regulation of NADPH oxidases in a mouse model of tobacco smoke induced COPD." ERS congress Vienna, Austria.

2. Seimetz M, **Parajuli N,** Roth M, Schermuly RT, Ghofrani HA, Seeger W, Grimminger F, and Weissmann N (**2009**). "Regulation of NADPH oxidases in a mouse model of tobacco smoke induced COPD." ECCP retreat, Germany.

3. Parajuli N, Seimetz M, Schermuly RT, Ghofrani HA, Seeger W, Grimminger F, and Weissmann N (**2009**). "A vascular phenotype precedes emphysema dvelopment in a mouse model of chronic tobacco smoke inhalation" ECCP retreat, Germany.

4. Parajuli N, Seimetz M, Schermuly RT, Ghofrani HA, Seeger W, Grimminger F, and Weissmann N (**2009**). "Alveolo-vascular alterations in a mouse model of tobacco-smoke inhalation" ATS conference San Diego, USA

5. Seimetz M, **Parajuli N,** Roth M, Schermuly RT, Ghofrani HA, Seeger W, Grimminger F, and Weissmann N (**2009**). "Regulation of NADPH oxidases in a mouse model of tobacco smoke induced COPD" ATS conference San Diego, USA. **Poster awarded with ITTA Travel Grant Award from American Thoracic Society 2009.**

6. Parajuli N, Seimetz M, Roth M, Fuchs B, Schermuly RT, Ghofrani HA, Schudt C, Hesslinger C, Seeger W, Grimminger F, and Weissmann N **(2008**) "Alveolar changes in a chronic tobacco smoke inhalation mouse model" at **ERS Berlin congress**, October 4-8 Berlin, Germany, Poster awarded with the **COPD Research Travel Award** from Boehringer Ingelheim

7. Parajuli N, Seimetz M, Roth M, Fuchs B, Schermuly RT, Ghofrani HA, Schudt C, Hesslinger C, Seeger W, Grimminger F, and Weissmann N **(2008**) "Altered alveo-vascular changes in a chronic tobacco smoke inhalation mouse model" **COPD conference,** Birmingham, UK.

8. Parajuli N, Seimetz M, Roth M, Fuchs B, Schermuly RT, Ghofrani HA, Schudt C, Hesslinger C, Seeger W, Grimminger F, and Weissmann N **(2008)** "Alveolar remodeling in a mouse model of chronic tobacco smoke inhalation" DGP congress an **oral presentation** Lübeck, Germany.

C. STATEMENT/ERKLÄRUNG AN EIDES STATT

"I declare that I have completed this dissertation single-handedly without the unauthorized help of a second party and only with the assistance acknowledged therein. I have appropriately acknowledged and referenced all text passages that are derived literally from or are based on the content of published or unpublished work of others, and all information that relates to verbal communications. I have abided by the principles of good scientific conduct laid down in the charter of the Justus Liebig University of Giessen in carrying out the investigations described in the dissertation."

"Ich erkläre: Ich habe die vorgelegte Dissertation selbständig, ohne unerlaubte fremde Hilfe und nur mit den Hilfen angefertigt, die ich in der Dissertation angegeben habe. Alle Textstellen, die wörtlich oder sinngemäß aus veröffentlichten oder nicht veröffentlichten Schriften entnommen sind, und alle Angaben, die auf mündlichen Auskünften beruhen, sind als solche kenntlich gemacht. Bei den von mir durchgeführten und in der Dissertation erwähnten Untersuchungen habe ich die Grundsätze guter wissenschaftlicher Praxis, wie sie in der „Satzung der Justus-Liebig-Universität Gießen zur Sicherung guter wissenschaftlicher Praxis" niedergelegt sind, eingehalten."

Nirmal Parajuli

Giessen

Dec 2009